IMPACT OF P-GLYCOPROTEIN ON DRUG ABSORPTION FROM THE AIRWAYS

Michaela Mádlová

Dissertation thesis

Disertační práce

2008

Faculty of Pharmacy in Hradec Králové, Charles University in Prague

King´s College London, University of London

ABSTRACT

The P-glycoprotein (P-gp) efflux pump is known to be present within several major physiological barriers e.g. in the brain, kidney, lung and placenta, however, the exact location and function of P-gp in the airways of the lung is not yet fully understood. Previous studies that have attempted to study P-gp transport using the immortalised Calu-3 respiratory cell line model have reported contradictory findings which has raised questions about the most appropriate *in vitro* model to investigate P-gp activity in the airways of the lung. The purpose of this study was to systematically investigate the location and activity of the P-gp efflux pump in the airways using three commonly employed *in vitro* models in order to determinate if this active transporter could influence to the effectiveness of therapeutic agents administered via the inhalation. P-gp functionality was assessed by monitoring the transport of a known P-gp substrate digoxin in normal human bronchial epithelial (NHBE) cells, Calu-3 and Caco-2 cell lines and in a simple IPL model with and without the presence of two P-gp inhibitors (verapamil and GF120918A). To facilitate both location and functional studies, cell layers were cultured on 1.13 cm^2 Transwell® supports either at an air-interface (Calu-3, NHBE cells) or under submerged conditions (Caco-2 cells). Integrity of the cell monolayers and the IPL epithelia was evaluated by determination of [^{14}C]-mannitol flux through these barriers. The basolateral to apical P_{app} of digoxin was significantly higher ($p < 0.05$) in Calu-3 and Caco-2 cell layers compared to the apical to basolateral transport and this resulted in an efflux ratio of 2.08 and 8.58 on day 21 in culture for the two cell lines, respectively. The Calu-3 and Caco-2 digoxin efflux was reduced by 40.0 % and 50.9 %, respectively, in the presence of GF120918A. In NHBE, the apical to basolateral transport rate was 2.58-fold greater than basolateral to apical, but this was unchanged in the presence of GF120918A. Although the presence of P-gp in IPL was confirmed using confocal laser scanning microscopy, the GF120918A applied directly to the model did not influence the digoxin transport. However, the absorption rate of digoxin was significantly increased ($p < 0.05$) in the presence of verapamil in the perfusion solution, which suggests the presence of an active efflux mechanism in the IPL model. It was hypothesised that the Pg-p pump was more difficult to inhibit compared to the cell line studies, presumably due to the difficulties in localising the inhibitor at the barrier for a significant period of time.

Prohlašuji, že tato práce je mým původním autorským dílem, které jsem vypracovala samostatně. Veškerá literatura a další zdroje, z nichž jsem při zpracování čerpala, jsou uvedeny v seznamu použité literatury a v práci řádně citovány.

ACKNOWLEDGEMENTS

I am very grateful to my primary supervisor Doc. Pavel Doležal, CSc. (Charles University in Prague) for his support during the PhD. Many thanks to my supervisor Dr. Ben Forbes (King´s College London) for allowing me to work at King´s College London. I am very grateful to the Galenos Network for providing me with Marie Curie Fellowship that funded my work at King´s College London. I would like to thank Dr. Cynthia Bosquillon (Universtity of Nottingham) for the advice on the experimental design. I am very grateful to GlaxoSmithKline for providing me with the inhibitor GF120918A and Dr. Anthony Brain (King´s College London) for the assistance with SEM and TEM photos. Many thanks to Dr. Lea Anne Dailey (King´s College London) for the help with confocal scanning microscopy. Finally I would like to thank to my family for their continued support and encouragement throughout the course of PhD.

CONTENTS

LIST OF FIGURES

Figure 32: Confocal microscopy of P-glycoprotein expression in rat lung. Acetone-fixed cryostat sections of (A) alveolar and (B) brochial tissue. Alexa Fluor® 568 goat anti-mouse IgG secondary antibody (red) was used to visualise anti-P-glycoprotein mouse mAb (C219). Nuclei stained with DAPI (blue). (Page 90).

Figure 33: Cumulative percentage of administered [^{3}H]-digoxin (45.8 nM co-administered with [^{14}C] mannitol, 65.6 μM) transferred to the perfusate vs time in presence/absence of P-glycoprotein inhibitors (♦) verapamil in perfusion solution, (■) verapamil co-administered with [^{3}H]-digoxin, (x) GF120918A co-administered with [^{3}H]-digoxin, (▲) no inhibitor. Data are expressed as mean ± SD, n=4. (Page 91).

LIST OF TABLES

LIST OF EQUATIONS

LIST OF ABBREVIATIONS

A-B: apical to basolateral
ABC: ATP binding cassette
ABCB1: P-glycoprotein
ALI: air-liquid interface
ATCC: American Type Cell Culture Collection
ATP: adenosine triphosphate
B-A: basolateral to apical
BEBM: bronchial epithelial cell basal medium
BPE: bovine pituitary extract
BSA: bovine serum albumin
Caco-2: epithelial cell line derived from human bronchial adenocarcinoma
Calu-3: epithelial cell line derived from human colonic carcinoma
CC: cell cytoplasm
CLMS: confocal laser scanning microscopy
CM: cell membrane
COPD: chronic obstructive pulmonary disease
CPM: counts per minute
CsA: cyclosporin A
CYP: cytochrome P450
D: desmosom
DAPI: 4´-6-diamidino-2-phenylindole
DME/F12: Dulbecco´s modified Eagle´s medium/nutrient mixture F12 HAM
DMEM: Dulbecco´s modified Eagle´s medium
DMSO: dimethylsulfoxide
DPPC: dipalmitoylphosphatidylcholine
EDTA: ethylene diamine tetraacetate sodium
FBS: fetal bovine serum
G. I.: gastrointestinal
GF120918A: (HCl salt of GF120918, 9,10-Dihydro-5- methoxy-9-oxo-N-[4-[2-(1,2,3,4-tetrahydro-6,7-dimethoxy-2-isoquinolinyl)ethyl]phenyl]-4-acridine-carboxamide)
HBSS: Hanks balanced buffer solution
HEPES: 4-(2-hydroxyethyl) piperazine-1-ethanesulfonic acid
IPL: isolated perfused rat lung
ka lung: apparent first order absorption rate constant from air-to-blood
LLI: liquid-liquid interface
LRP: lung resistance protein
M: microvilli
MDR: multidrug resistance
MDR1: P-glycoprotein
MRP1; ABCC1: multidrug resistance associated protein 1
MVP: major vault protein
NHBE: normal human bronchial epithelial
OCT: organic cation transport system
P_{app}: apparent permeability coeficient
PBS: phosphate buffer saline
P-gp: P-glycoprotein
R^2: linear correlation coefficient
Rh123: rhodamine-123

RT-PCR: reverse transcription polymerase chain reaction

SD: standard deviation

SEM: scanning electron microscopy

$T_{1/2}$: absorption half-time

TEM: transmission electron microscopy

TER: transepithelial electrical resistance

TJ: tight junction

TMD: transmembrane domain

ZO: zonula occludens

1 INTRODUCTION

1.1 General introduction

The medical benefits of delivering therapeutic agents to the airways of the lung have been acknowledged for several decades, most notably in the treatment of local pulmonary diseases such as asthma, chronic obstructive pulmonary disease (COPD) and cystic fibrosis (Brewis *et al.*, 1995). However, more recently, technological advancements in this field have allowed the delivery of systemically acting substances via the inhaled route e. g. insulin (Vanbever *et al.*, 1999; Patzon *et al.*, 1999). Regardless if the intended outcome is the treatment of local or systemic disorders, the administration of xenobiotics via the airways of the lung posses several advantages compared to more traditional routes of drug delivery. The airways provide a large, easily accessible epithelium, which allows immediate drug uptake and onset (van den Bosch *et al.*, 1993; Lipworth, 1996). In addition, both large and small molecular weight molecules can be delivered via this route (von Wichert *et al.*, 2005). Furthermore, the pH and enzymatic activity in the airways is more favourable for drug delivery compared to the gastrointestinal tract (Sakagami, 2006; Masood and Thomas 1996). As a result, drug delivery via the inhaled route is an area that is receiving ever increasing research interest.

Therapeutic agents are commonly delivered to the airways as an aerosol and there have been numerous previous studies that have documented novel methods to generate and administer drug rich aerosols with excellent deposition efficiencies (Vanbever *et al.*, 1999; Niven 1992). However, the drug delivery efficiency of an inhaled compound is not only dependent upon effective aerosol generation and deposition, because once deposited in the airways of the lung, a drug has to overcome numerous biological barriers to reach the ultimate site of action. The amount of drug absorbed from the airways is limited by processes occurring at the epithelium surface such as mucus excretion, surface binding, removal of the drug by mucociliary clearance (in the upper airways), and metabolism (Hamilton *et al.*, 2001[a]). In order to predict if a drug can be delivered via the inhaled route and/or to maximise drug delivery efficiency, the effect of post deposition processes on drug absorption must be investigated.

Due to the complexity of the *in vivo* environment, numerous models have been developed specifically to study the fate of therapeutic agents in the lung airways. Three main types of models are typically used: 1) immortalised respiratory epithelial cells, 2) primary cultures of epithelial cells and 3) the isolated perfused lung (IPL). Although studies exist showing that cell

lines, primary cells and the IPL model each provide a good representation of the *in vivo* respiratory epithelium, these studies are typically very variable and based on the transport of a selected number of compounds (van der Sandt *et al.*, 2000). Furthermore, a number of studies have previously shown discrepancies between the three *in vitro* models in terms of drug transport (Hamilton *et al.*, 2001[b]; Cavet *et al.*, 1996 and 1997). As the pulmonary route becomes an increasingly attractive site for drug delivery, a greater understanding of the post deposition processes in the lung is required. In order to achieve this a fundamental understanding of the functional differences between the available *in vitro* models is required to facilitate the development of new inhaled medicines.

1.2 Lung anatomy and physiology

The lung is the major organ of external gas exchange. Carbon dioxide and oxygen are exchanged during respiration which provides a vital supply of oxygen to the cells in the body. The structural architecture of the lung is complex, but undoubtedly it is specifically designed to maximise the surface area at which gas exchange can occur. When designing a formulation to deliver a therapeutic agent to the lung for local or systemic effect a clear understanding of the anatomy and physiology of the lung is required to facilitate administration of the compound to the correct lung region and facilitate effective post deposition transport.

1.2.1 Airways

The airways of the lung constitute a series of cylindrical sections, which are dichotomously branched in daughter sections with a smaller diameter and shorter length than the parent branch (Figure 1) (Weibel *et al.*, 1973). The number of branches of the bronchial tree that occur before the region where gas exchange takes place is reached can vary from 6 to 30 which illustrates the diversity of this anatomy in individual patients (Plopper, 1996). The internal diameter of the airway branches decreases from approximately 1.8 cm (generation 0) to about 0.04 cm in the alveolar region which leads to a dramatic increase in surface area as the sections of the lung airways are descended (Hickney and Thompson, 1992). The total surface area of the airways in human has been quoted to range from 70 m^2 (Taylor, 2002) to 140 m^2 (Dalby *et al.*, 1996) and thus this organ provides a very large area of accessible epithelium for drug administration.

Anatomically the airways of the lung are divided into seven regions that are defined according to the diameter of the airway section within the considered region. Three of the most important regions of the airways in terms of drug delivery are the trachea (generation 0), which represents the first region of highly turbulent airflow, the terminal bronchioles (generation 16), which is arguably the optimal deposition of most locally acting compounds and the alveolar region (generation 23), which is the site of systemic absorption (Figure 1).

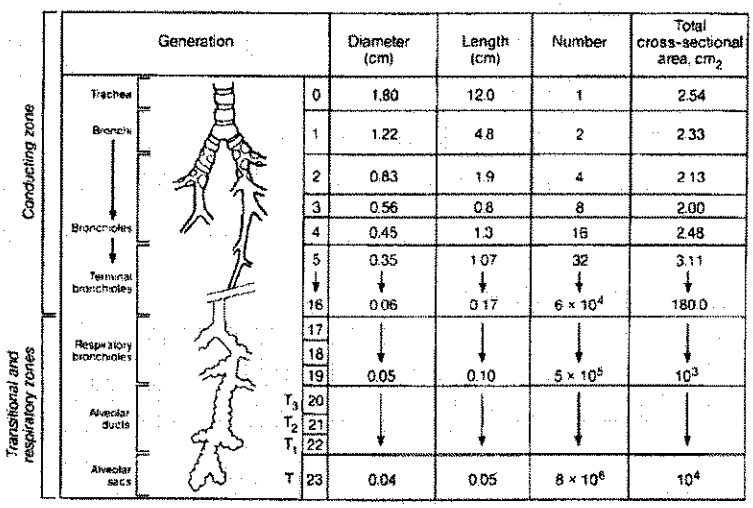

Generation		Diameter (cm)	Length (cm)	Number	Total cross-sectional area, cm_2
0		1.80	12.0	1	2.54
1		1.22	4.8	2	2.33
2		0.83	1.9	4	2.13
3		0.56	0.8	8	2.00
4		0.45	1.3	16	2.48
5 ↓ 16		0.35 ↓ 0.06	1.07 ↓ 0.17	32 ↓ 6×10^4	3.11 ↓ 180.0
17					
18					
19		0.05	0.10	5×10^5	10^3
20	T_3				
21	T_2				
22	T_1				
23	T	0.04	0.05	8×10^6	10^4

Figure 1: *A schematic illustration detailing the structure of the airways according to Weibel's model (1973). Each airway generation is described by the internal diameter, length, number of sections and the sum or the cross section area of the sections in individual generation.*

In terms of function, the regions of the lung can be classified into two distinct sections. The first, the central conducting airways (also known as the conducting zone), consist of the nasopharynx, larynx, trachea, bronchi and bronchioli and are responsible for conducting the inhaled air, filtering and removing foreign particles, humidifying and warming the inhaled air before reaching the terminal alveolar region. The second, the peripheral airways (also known as the transitional zone), composed of respiratory bronchioles, the alveolar ducts and alveolar sacs, enable the rapid gas exchange across the epithelial barrier between the lung lumen and blood stream. In general terms the target deposition region for locally acting drugs is the conducting zone whilst for systemically acting drugs it is the transitional zone.

1.2.2 Blood supply in lung

The anatomy of the airway circulation influences the site of systemic drug absorption, metabolism and clearance in the airways (Chediak *et al.*, 1990). For example, whilst it is known that therapeutic compounds can be systemically absorbed from any region within the airways the extensive vascularisation and large supply of blood in the alveolar region results in this area being the primary target for systemic absorption (Wichert *et al.*, 2004). Conversely, locally acting compounds are targeted to the upper airways specifically to avoid systemic absorption. Despite the wealth of both *in vitro* and *in vivo* studies to investigate the influence of disease state and inter-patient differences upon airway anatomy, very little corresponding work has been performed with respect to blood supply. As a result the influence of blood supply variability upon drug absorption is currently unknown.

Blood is supplied to the lung via the bronchial and the pulmonary circulatory systems (Staub *et al.*, 1991). The bronchial circulatory system originates from the aorta, which delivers approximately 1% of the total cardiac output under high blood pressure to the lung. The main function of the bronchial circulatory system is the supply of the airways with oxygenated blood and nutrients, but it also plays a role in pulmonary and pleural fluid balance (Serikov, 1985). The pulmonary circulatory system on the other hand comprises of an extensive low-pressure vascular bed, which transfers the rest of the cardiac output to facilitate efficient gas and nutrition exchange for the alveolar cells including those that make up the septae (alveolar walls that are composed of capillaries sandwiched between two epithelial monolayers and all held together by numerous extracellular and intracellular fibres; Weibel *et al.*, 1991).

1.2.3 Barriers to drug absorption in the lung

During the inhalation process an aerosol is transported within inspired air. The passage of particles/droplets through the airways of the lung is influenced by numerous factors including speed of air-flow, aerosol size, aerosol density and airway physiology. The particle can potentially deposit at any point within the airway from the mouth to the alveoli and this is dependant upon the susceptibility of individual particle/droplets to impaction, sedimentation and diffusion, which are the three main deposition methods. Once deposited in the airways, irrespective of if the drug is for local or systemic therapy, the molecule must enter the respiratory epithelium. However, in order to reach the epithelial barrier a drug must be released from the formulation before being removed from the lung by mucociliary clearance, avoid

metabolism and penetrate the airways lining fluid (Patton, 1996). To facilitate systemic absorption the agent has to pass further through the epithelial cells, interstitium and endothelium (Figure 2) (Patton *et al.*, 1996). The physiology of each of these barriers is unique and must be fully understood to allow the development of effective *in vitro* models to assess the post-deposition drug transport in the lung. The following sections describe each of the barriers to drug absorption in chronological order after a particle has deposited either in the conducting or respiratory zones of the lung.

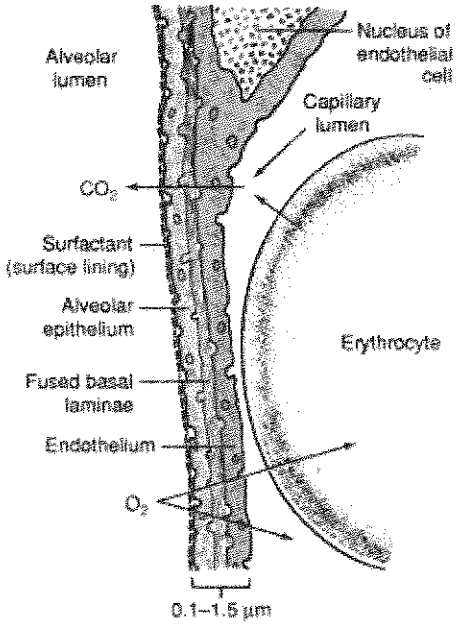

***Figure 2**: A schematic diagram to describe the barriers to drug absorption in the airways of the lung. Taken from Bloodgood (2005).*

1.2.4 Mucocilliary clearance

Mucociliary clearance is one of the most important mechanical host defence mechanisms in the lung (Salathé *et al.*, 1997). During this process the inhaled material trapped in the mucus covering the ciliated epithelium of the airways is moved towards the upper respiratory tract, where it is swallowed or expectorated. The continued migration of mucus from the lower airways of the lung to the trachea against gravity is also commonly known as the mucociliary escalator. The movement is driven by the continual coordinated beating of the cilia on the surface of ciliated respiratory epithelial cells. Material deposited in the airways can be removed by mucociliary clearance in a few minutes but it can also take several hours and this clearance time is influenced mainly by the site of particle deposition (Lansley *et al.*, 1993). Generally, the

movement is faster in trachea than in distal airways as a result of the airway morphology, percentage of ciliated cells and relatively low level of secretory cells in the peripheral airways (Labiris and Dolovich, 2003). The speed and efficiency of the mucociliary clearance mechanism means that the retention of a traditional particulate base drug delivery system in the upper airways form more than a few hours and therefore controlled drug release is impossible. The lower respiratory tract e. g. the respiratory zone, does not have such a clearance mechanism. The alveolar respiratory epithelium is protected by the body's immune system via macrophages. This is a much slower process compared to the mucociliary clearance and therefore the retention of therapeutic agents at the cell surface occurs for a longer period. The contact time of a therapeutic agent with the respiratory cells *in vivo* is important to consider when designing *in vitro* experiments as using non-appropriate times may lead to poor *in vitro-in vivo* correlations.

1.2.5 Airway epithelium lining fluid

Epithelium lining fluid forms one of the first barriers to drug absorption in the airways of the lung. Inhaled particles are required to dissolve in this fluid prior to removal by mucociliary clearance and then pass through it to reach the airway epithelial cell surface. The thickness of the layer ranges from 0.05 to 10 μm depending on the airway region (Patton, 1996). The epithelial lining fluid is produced by mucus glands and goblet cells. It is formed of two layers, an underlying low viscosity periciliary layer close to the cell surface which is covered by a high viscosity gel layer (Patton, 1996). An intercalated phospholipid reduces the surface tension between these two mucus layers (Samet and Cheng, 1994). The airway epithelial lining fluid is composed of water (95%), glycoproteins (mucins) (2%), proteins (1%), inorganic salts (1%), and lipids (1%) (Samet *et al.*, 1994). The main function of the lining fluid is to protect the lung epithelium against mechanical damage that could be caused by inhaled particles (Puchelle *et al.*, 1995). Moreover, the fluid protects the body from microbial attack by the production of several bacteriostatic and bactericidal enzymes e.g. IgA, lactoferrin and lysozyme. Once a compound has dissolved in the airway lining fluid the penetration of this barrier is dependent on molecular charge, solubility, lipophilicity and size (Rubin, 1996). Whilst the airway epithelial lining fluid does not provide a very effective barrier against the absorption of drugs in solution, together with the mucociliary clearance it provides an excellent removal mechanism for particles, therefore it does act to protect the body against entry of potentially harmful substances.

1.2.6 Alveolar lining fluid

Alveolar lining fluid, also commonly known as lung surfactant, is a complex lipoprotein layer produced by type II alveolar cells. Over 90% of the alveolar lining fluid is composed of lipids, around half of which is dipalmitoylphosphatidylcholine (DPPC). Proteins make up the remaining 10% of the fluid, half of which 10% are plasma proteins and the rest mainly apoproteins (SpA, SpB, SpC, and SpD). The majority of proteins and lipids that have been identified in the alveolar lining fluid are amphiphilic and it is the adsorption of these surface active compounds to the air-water interface of the alveoli cells that reduces the surface tension within the distal sections of the airway and prevents the lung from collapsing at the end of expiration. The presence of these surface active compounds in the alveolar fluid also allows a wide range of drugs to dissolve in this fluid, however there is only reported to be between 10 – 20 ml of alveolar lining fluid covering the whole surface area in the lung (Patton, 1996). As a consequence it is a considerable challenge for a therapeutic agent delivered to this site within the airways to dissolve and access the alveolar epithelium prior to clearance by macrophages.

1.2.7 Epithelium

The type, number and co-localisation of epithelial cells present in the airways of the lung constantly changes when moving from the trachea down to the distal regions of the airways. These changes are driven by the function of the different regions of the lung. It is important to consider the subtle differences in epithelia *in vivo* so that appropriate models can be used to model transport *in vitro*. Generally, the epithelium found in the conducting zone of the airways are pseudo-stratified and consist of six major cell types including ciliated cells, mucous goblet cells, Clara cells, serous cells, basal cells and dense core-granulated cells (Tyler *et al.*, 1989; Figure 2). The cell composition of the upper airways can vary between species and with the generation of the lung (Harkema *et al.*, 1991). However, the surface of the epithelium is usually dominated by ciliated epithelial cells responsible for the clearance of deposited material in the airways (Gruenert *et al.*, 1987). Secretory cells, mainly goblet cells, are highly abundant in the upper respiratory tract and are located amongst the ciliated cells. Clara cells both of columnar and cuboidal morphology can be found dispersed amongst the ciliated cells mainly in the lower portion of the conducting zone in the respiratory tract. Basal cells and core-granulated cells can be found in the lower layers of the epithelium whilst migratory cells such as lymphocytes, leukocytes and mast cells are present in the epithelium throughout entire respiratory tract (Evans *et al.*, 2001).

The major function of the conducting airways is to restrict the entry of potentially harmful substances into the body. This is achieved by forming a physical barrier, which is generated by the formation of tight junctions between cells that regulate paracellular diffusion. The tight junctions are composed of proteins and lipids. In order to accurately model permeation of compounds across this barrier it is important that airway cell lines or primary culture models of native epithelia form tight junctions and present a barrier with similar permeability to that found *in vivo*.

The respiratory zone of the lung contains several different types of airway epithelium compared to the conducting zone. The alveolar surface is composed of four major cell types: epithelial type I and II cells, alveolar brush cells (type III) and mobile alveolar macrophages (Ma *et al.*, 1996; Figure 2). The squamous type I cells cover approximately 93-97% of the alveolar surface area (Taylor *et al.*, 2001). As type I cells are relatively thin with an average depth of 0.26 μm a wide range of therapeutic agents can penetrate this barrier rapidly and this is one reason why the distal parts of the airways are considered a favourable site for drug absorption. The more abundant, much smaller type II alveolar cells make up approximately 5% of the lower airway epithelia. The primary role of type II cells is to produce alveolar lining fluid (Mason and Crystal, 1998). The alveolar area is patrolled by macrophages which actively remove inhaled particles. The alveolar macrophages play a critical role in the protection of this highly permeable barrier against the entry of harmful substances into the systemic circulation.

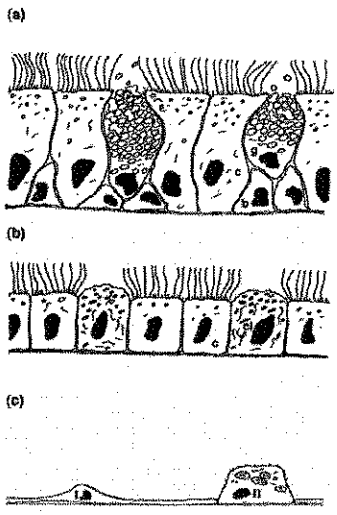

Figure 3: *The major lung epithelia cell types.* ***(a)*** *The bronchial columnar epithelium containing (c) ciliated cells (g) goblet cells (b) basal cells.* ***(b)*** *The bronchiolar cuboidal epithelium containing (c) ciliated cells (cl) Clara cells.* ***(c)*** *The alveolar squamous epithelium (I) type I cell (II) type II cell (Taken from Forbes, 2000).*

1.2.8 Interstitium and lymphatic system

After passing through the epithelial cell barrier a molecule has to pass the interstitium to be absorbed into the systemic circulation (Figure 2). The interstitial compartment is formed mainly by fibroblasts composed of collagen fibres that are embedded in interstitial fluid. The fibroblasts are connected with a basement membrane which provides support for the epithelial cells on the luminal side and the endothelial capillary cells on the external side. Other cells present in the interstitium include myofibroblasts, pericytes, monocytes, lymphocytes and plasma cells (Plopper *et al.*, 1996). The interstitial fluid percolates slowly through the network of fibroblast relatively unhindered and is collected in the lymphatic vessels to prevent the fluid accumulation in the lung (Puchelle *et al.*, 1995).

In terms of drug delivery, the interstitium provides another barrier through which a molecule has to pass to achieve entry into the systemic circulation. However, few, if any systematic studies have been undertaken to demonstrate if the interstitium provides a rate limiting barrier for drug absorption. It has previously shown that micron-sized particles (e.g. lipoproteins, plasma proteins, bacteria, and immune cells) can pass through the lymphatic endothelia into the lymph fluid that is returned to the venous blood circulation at the right jugular and subclavian veins (Patton, 1996). Therefore, it is generally accepted that the interstitium is a minor limiting barrier for drug absorption from the airways of the lung in comparison to the respiratory epithelial barrier that lines the distal air spaces (Gorin *et al.*, 1979; Kim and Malik, 2003).

1.2.9 Endothelium

Up to 40% of the total cellular composition of the lung is thought to be made up of capillary endothelium. This cell type forms such a large part of the lung that it represents the largest capillary endothelial surface in the body (Simionescu *et al.*, 1991). Due to the presence of specialised organel-free domains in the cells, the endothelium is particularly thin (from 200 nm down to 30-35 nm). The endothelial cells are joined by tight junctions in a similar manner to the epithelium but they have fewer parallel arrays of contacts, which renders them leaky when the hydrostatic pressure increases (Plopper *et al.*, 1996; Simionescu *et al.*, 1991). Endothelial cells have a relatively large number of endocytotic vesicles which reduces their barrier capacity (Schnitzer *et al.*, 2001). These features enable rapid gas exchange at the alveolar-capillary interface, but they also result in a very minimal barrier to the passage of therapeutic agents (Simionescu *et al.*, 1991).

1.2.10 Metabolic activity

Generally all metabolising enzymes found in the liver are also present in the lung, but in lower amounts. The cytochrome P450 (CYP) enzyme system in human lung is an essential component in the pulmonary first-pass metabolism of xenobiotics. The level of CYP in lung cells is generally lower than in liver, where the expression is more prevalent. On the other hand, the blood flow normalised for tissue weight is approximately 10-fold lower in the liver than in the lung (Taylor *et al.*, 1990) resulting in higher metabolic clearance of some xenobiotics by the lung than in liver (Roth *et al.*, 1979). It is therefore crucial that when modelling absorption in the airways of the lung that the innate metabolic processes must either be active or accounted for.

Metabolising enzymes are primarily distributed in the Clara cells and the alveolar type II cells. The pattern of CYP expression in alveolar macrophages closely resembles the expression pattern in human lung tissue, while the pattern in lymphocytes is significantly different. The expression of CYP2B6, CYP2C, CYP3A5 and CYP4B1 mRNA in alveolar macrophages has been demonstrated (Hukkanen *et al.*, 2000). The expression of CYP3A in human pulmonary tissue has previously been studied with RT-PCR and immunohistochemistry and both methods established CYP3A5 was highly prevalent, but CYP3A4 was only expressed in only about 20% of the cases (Hukkanen *et al.*, 2000).

The proteolytic activity in the airways of the lung is generally thought to be low. In addition to the CYP enzymes trypsin, chymotrypsin and aminopeptidases are known to be active. However, most of these enzymes are membrane bound and the cellular release of proteases into the epithelial lining fluid only occurs as a consequence host defence mechanism initiation. For example, the release of antiproteases such as α1-antitrypsin is initiated only in response to the damage of the lung tissues (Ma *et al.*, 1996).

1.3 Mechanisms of drug transport in the airways of the lung

Drug transport in the airways of the lung is a complex process influenced by the permeability of a compound through several barriers as described in Section 1.2. In addition, the movement and accumulation of therapeutic agents is dependent upon the ventilation and the perfusion of the lungs and the physicochemical properties of the substance. The intricacy of the situation is increased further in the airways as many of the processes influencing drug transport are often site-dependent due to the different physiologies of the cell types involved (Byron *et al.*, 1986).

As with all complex environments a number of models are usually used to dissect all the processes involved in drug transport. In its simplest form the airways can be considered as a single passive membrane which compounds can cross via either paracellular or transcellular transport. Of course, this does not accurately model the *in vivo* situation, but for drug solutions, which are not influenced by mucociliary clearance, are not extensively metabolised (which in fact does represent a large number of therapeutic agents) this simple inert cell layer barrier model is useful. The complexity of this simple passive model can be enhanced by considering active permeation processes such as vesicle transport and transporter mediated permeation (Figure 3) (Groneberg *et al.*, 2003). It would be expected that *in vitro* models should be able to model the majority, if not all of these transport routes and therefore each of these will be described in detail in the subsequent sections, but to understand transport in the airways of the lung the fundamentals of diffusion must first be discussed.

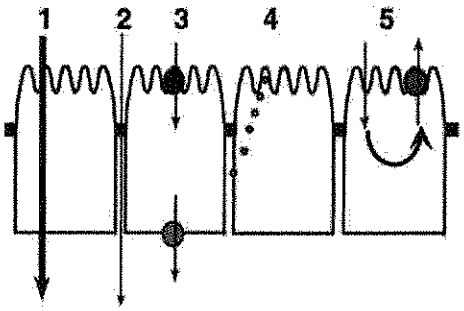

Figure 4: *Epithelial drug transport mechanisms. 1- transcellular passive transport, 2 - paracellular passive transport, 3- active transport, 4 - vesicle mediated transport, 5- transporter mediated efflux.*

1.3.1 Diffusion

Diffusion is a process which involves the random movement of molecules throughout a medium (Flynn *et al.*, 1974). The course of each molecule is erratic due to multiple elastic collisions with like and unlike molecules in its physical path. The basic hypothesis underlying the mathematical theory for isotropic materials is that the transfer rate of differing substances per unit area of sections proportional to the concentration gradient measured normalised to the section through which they must pass. This is expressed as Fick´s first law (Equation 1):

$$J = -D\frac{dC}{dx} \qquad \text{Equation 1}$$

where J is the rate of transfer per unit area of surface (the flux), C is concentration of the diffusing substance, x is the space coordinate measured normal to the section, and D is the diffusion coefficient. The negative sign indicates that flux is in the direction of decreasing concentration. In many situations D is constant, but in more complex materials D depends on concentration. The dimension of flux is $cm^2.s^{-1}$.

Apparent permeability, first described by Walker and co-workers (1964) (Equation 2), is derived from Fick's first law and relates the concepts of concentration, surface area and time to drug transport. This model is routinely employed in the study of drug transport in the airways of the lung.

$$P_{app} = \frac{dQ/dt}{AC_0} \qquad \text{Equation 2}$$

The transport rate dQ/dt ($mol.s^{-1}$) is indicative of the drug concentration increase in the receiver compartment per time interval (s). A is the surface area (cm^2) across which the compound must pass, and C_0 (mol/cm^{-3}) is the initial drug concentration in the donor compartment. The units for apparent permeability (P_{app}) are $cm.s^{-1}$. During a well controlled transport experiment the solute fate can also be determined using a full mass balance, which provides greater confidence in the overall quality of the conducted experiment (Equation 3):

$$MassBalance = \frac{C_c}{C_0} x100\% \qquad \text{Equation 3}$$

where C_0 is the quantity of drug applied to the apical surface of the cell line and C_c is the calculated cumulative concentration at the basolateral side of the cells at the final time point of the permeation experiment.

1.3.2 Passive transport

In 1895 Charles Overton postulated that the entry of any molecule into a cell is governed by its lipid solubility. Overton´s studies led to the hypothesis that cell membranes are composed of lipid domains that mediate the transport of lipophilic molecules, and protein ´pores´ which transport hydrophilic molecules. Studies conducted by Schanker *et al.* (1986) have subsequently demonstrated that most compounds administered to the airways of the lungs are rapidly absorbed by passive diffusion with the rate of absorption increasing as the lipophilic nature of each compound increases (Brown and Schanker, 1983; Schanker and Hemberger, 1983). However, if a drug is highly lipophilic, combined with other physicochemical properties, that favour a strong interaction with the cell, the drug can be retained at the apical membrane surface, resulting in poor bioavailability (Pal *et al.*, 2000; Sawada *et al.*, 1999; Wills *et al.*, 1994a).

Although most of the therapeutic agents are thought to be absorbed by passive transcellular permeation, compounds of small to moderate size (100 - 1000 kDa) can also be transported by the paracellular route. Paracellular transport is the process whereby compounds with a small to intermediate molecular weight permeate epithelia through intercellular junctions (Schneeberger, 1978). This is generally considered to be a passive process, despite having a tendency to be selective for cationic rather than anionic and neutral drugs (Karlsson *et al.*, 1999; Adson *et al.*, 1994). The paracellular pathway has the potential to become saturated rapidly (Lee and Thakker, 1999; Gan *et al.*, 1998; Zhou *et al.*, 1999). In a similar manner to transcellular transport, the rate of paracellular diffusion has been previously found to be inversely proportional to the radius of the diffusing molecules (Effros and Mason, 1983; Schneeberger, 1991).

Passive diffusion has previously been shown to be the major means by which macromolecules with molecular weight less than 40 kDa are transported across the airways of the lung (Matsukawa *et al.*, 1997). The rate of macromolecular transport is inversely related to the molecular mass of the permeating species (Crandall *et al.*, 1991). It has been suggested that macromolecules pass through paracellular pores, regulated by tight junction complexes, in the airway epithelium and it is the passage through these complexes that limits the transport. Various studies have attempted to manipulate the paracellular transport of macromolecules by temporarily opening of the tight junction (Junginger *et al.*, 1998). However, the potential toxicological implications of reducing the airway cell integrity render this approach unacceptable. Based on previous work, which investigated the rate of peptide and protein absorption in lung airways, it has been suggested that pores in both the airway epithelium and vascular endothelium exist that are big enough to allow relatively rapid (5-90 min) absorption of macromolecules with diameters less than 5-6 nm, and relatively slow absorption (hours to days)

of macromolecules with diameters greater than 5-6 nm across the airspace passively (Patton, 1996).

1.3.3 Active transport

Transport proteins embedded in the membrane of airway epithelial cells can actively transport a wide range of chemicals and therefore influence the retention/clearance of the drug from the lung. Active transport is energy-consuming and can be utilised to drive a compound into or out of a cell irrespective of the local concentration gradients. Many nutrients such as sugars, amino acids and peptides can be transported into and across respiratory epithelial cells using active transport. The transporters usually exhibit substrate specificity to restrict the access of potentially harmful xenobiotics into the body. As a result, for a drug to be transported into airway cells via this method it has to share some common chemical structure features with the endogenous substrate in order to utilise the transporter protein binding to increase absorption.

One example of an active transport mechanism that can be used to enhance the delivery of therapeutic agents to the respiratory epithelium is the oligopeptide transportation system. In normal and airway epithelial cells of patients suffering from cystic fibrosis oligopeptide transporters (Groneberg *et al.*, 2002) with broad substrate specificity have previously been detected (Doring *et al.*, 1998). These transporters are known to be distributed in alveolar pneumocytes, bronchial epithelium and endothelium (Gronenberg *et al.*, 2002; Tsuji *et al.*, 1999). Han *et al.* (1998) synthesised a number of compounds specifically to mimic the structure of the endogenous oligopeptide substrates, with a view of increasing their absorption in the lung airways via oligopeptide transporters (Han *et al.*, 1998; Ganapathy *et al.*, 1998). This strategy increased transport of certain agents by up to ten fold. In similar manner, the uptake of cephalosporine antibiotics, cytostatics and angitensin-converting enzyme inhibitors has previously been enhanced by this transport system (Lee *et al.*, 2000).

The organic cation transport system (OCT) is another well characterised active transport process (Shen *et al.*, 1999; Enna *et al.*, 1973; Lin and Schanker, 1981). Two types of OCT systems are known to be prevalent in the airways of the lung. The first is driven by a negative membrane potential difference within the cells (Moseley *et al.*, 1996) as observed in OCT1 (Grundemann *et al.*, 1994), OCT2 (Okuda *et al.*, 1996) and OCT3 subtypes (Kekuda *et al.*, 1998). The second appears to be an energy dependant OC^+/H^+ exchange mechanism that is driven by a proton gradient generated by H^+ efflux through a Na^+/H^+ antiport and/or –ATPase (Ott *et al.*, 1991).

Both systems carry cationic xenobiotics, amino acids (Enna *et al.*, 1973; Lin *et al.*, 1981) and endogenous amines (e.g. epinephrine, choline, dopamine, and guanidine).

1.3.4 Vesicle mediated transport

The transport of chemicals across cell membrane in the airways of the lung can be mediated by vesicles and vacuoles that use energy to take up an agent, fuse with the cell membrane and induce subsequent release of the drug within the cell. Gumbleton *et al.* (2001) and Cambell *et al.* (1999) have reported a high number of vesicles (caveolae) in alveolar endothelial cells and epithelial type I cells. The precise function and potential capacity of the caveolae is the subject of debate (Schnitzer *et al.*, 2001; Predescu *et al.*, 1997; Frokjaer-Jensen, 1991; Bundgaard *et al.*, 1979; Anderson *et al.*, 1992). Caveolae have previously been reported to be involved in the process of potocytosis (Anderson *et al.*, 1992), the mediation of macromolecule endocytosis, transcytosis and intracellular trafficking (Schnitzer *et al.*, 1994; Fielding and Fielding, 1997). In addition, they are thought to serve as a localising domain for a broad range of signal transducing molecules (Shaul and Anderson, 1998; Lisanti, 1994).

The potential of vesicle mediated transport of macromolecules across the lung epithelium is of growing interest, however this field is in its infancy and the process requires further investigation to understand the epithelial cellular routing and targeting before it can be established as suitable method of drug delivery via the airways of the lungs. The current general view is that alveolar vesicle-mediated trafficking across the air-blood barrier functions is a minor pathway in protein absorption (Gumbleton *et al.*, 2001; Patton, 1996).

1.3.5 Transport mediated efflux

Proteins responsible for the efflux of chemicals out of the cell cytoplasm via active transport mediated efflux (except for the major vault protein, MVP) are classified into seven subfamilies (ABCA, ABCB, ABCC, ABCD, ABCE, ABCF, ABCG) of the ATP binding cassette (ABC) transporter family (Higgins, 1993). ABC transporters are found in most organisms, from bacteria to humans (Ambudkar *et al.*, 2003). So far, about 48 human ABC transporters have been described (Dean *et al.*, 2001). However, the most important ABC transporter found in the airways of the lung are commonly considered to be multidrug resistance P-glycoprotein (MDR1;

P-gp; ABCB1), multidrug resistance associated protein 1 (MRP1; ABCC1) and major vault protein (MVP or LRP) (Scheffer *et al.*, 2002; Sugawara *et al.*, 1997).

Efflux transporter proteins are thought to be involved in protecting the lungs against inhaled toxic pollutants by actively decreasing intracellular concentrations of these agents (Higgins *et al.*, 1993). However, therapeutic agents have also been selectively removed via a selective efflux mechanism (Ambudkar *et al.*, 2003; Leonard *et al.*, 2003; Tian *et al.*, 2005; Staud and Pavek, 2005). This type of active transport system was originally identified as a major cause of the multidrug resistance (MDR) exhibited by tumour cells (Moscow *et al.*, 1997). An increase in expression of efflux transporter molecules in a tumour cell has been shown to render it resistant to structurally and functionally unrelated cytotoxic drugs. The involvement of different MDR transporters in the efflux of a single agent is a complex process because of the overlapping spectra of transporter substrates. For example, even though P-gp and MRP1 have similar transport specificity for a wide range of compounds, P-gp only transports neutral and cationic compounds, whilst MRP1 prefers to translocate anionic compounds, this suggests that they are both active in the permeation of certain compounds (Borst *et al.*, 1999).

Whereas the activity of P-gp at several biological barriers has already been well characterised and described in literature, the exact role of this transporter in airways of the lung is not fully understood. As the current study is focused on investigating the impact of P-gp on pulmonary drug absorption, the subsequent sections will specifically review the published details of the location and function of P-gp.

1.4 P-glycoprotein

P-gp is a 170 kDa membrane bound protein that acts as an ATP-dependent efflux pump transporter capable of removing a wide range of physicochemically different substrates from the cell cytoplasm. P-gp was originally discovered in Chinese hamster ovarian cells that were resistant to colchicine in the 1970s. These cells also showed resistance to a wide range of natural substances such as actinomycin D, methotrexate and daunorubicin (Juliano and Ling, 1976). The over expression of P-gp has subsequently been shown in a variety of tumours and P-gp is now considered to be one of the most important amongst the ATP-dependent efflux transporters that confer multidrug resistance in tumour cells (Burger *et al.*, 2003; Materna *et al.*, 2004; Stravrovskaya, 2000; Choi, 2005; Endicott *et al.*, 1997; Ling 1995; Chu *et al.*, 1994).

1.4.1 P-glycoprotein structure

The P-gp molecule contains approximately 1280 amino acids and it is divided into two similar halves. Each half consists of a transmembrane domain (TMD) with 6 membrane-spanning α-helices and an intracellular hydrophilic region with an ATP binding domain (Figure 5).

1.4.2 P-glycoprotein mechanism of action

Speculation on the manner in which P-gp is able to remove xenobiotics from multidrug resistant cells has been ongoing for the past decade. The four prevalent models; the ´altered partitioning´ model, the pore model, the flippase model (Lee *et al.*, 2002; Hunter and Hirst, 1997) and the "hydrophobic vacuum cleaner" model, all attempt to explain the diversity of substrate removal attributed to P-gp's efflux mechanism (Figure 6).

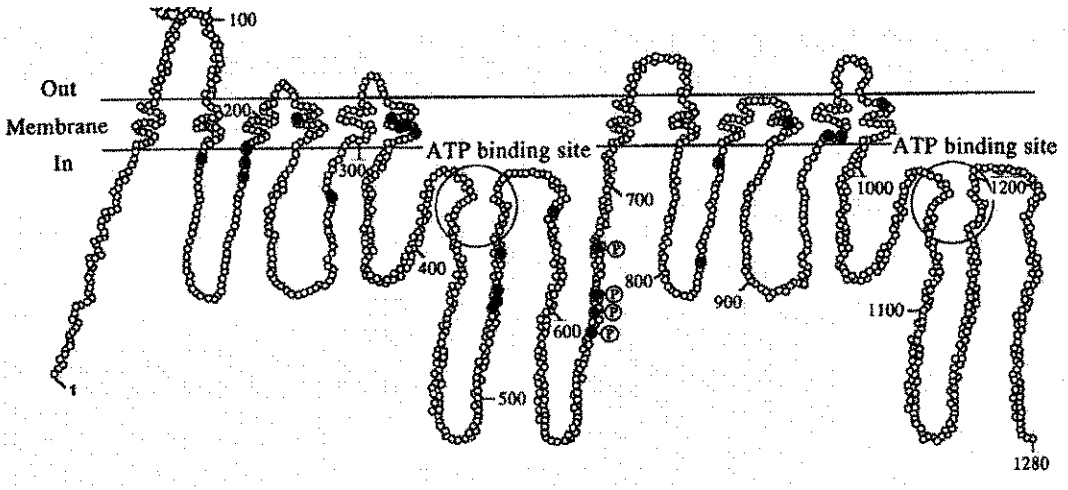

Figure 5: *A diagram showing the structure of P-glycoprotein, when associated with a cell membrane with 12 transmembrane (TM) domains and two ATP sites. In and Out represent the internal and external regions of the cell. Each circle represents an amino acid residue (numbered) with the filled black circles representing the positions of mutations that alter substrate specificity. ATP is adenosine triphosphate. P sites of phosphorylation (adapted from German et al., 1996).*

The most obscure of the proposed P-gp models is the ´altered partitioning´ model, which was first suggested by Roepe (1995). This model suggests that the over expression of P-gp results in an alteration of the cells´ electrical membrane potential and/or an elevated intracellular pH. It was proposed that these disturbances within the cell alter the partitioning of the P-gp substrate and as a consequence this model assumes that P-gp indirectly promotes decreased intracellular drug accumulation.

The bulk of the literature favours the "hydrophobic vacuum cleaner" model, where the mechanism of P-gp action involves the drug being detected and expelled as it enters the plasma membrane in a similar fashion to a "vacuum cleaner" (Higgins and Gottesman, 1992). The hydrophobic vacuum cleaner" model requires energy from ATP hydrolysis by P-gp to remove drugs from cell membranes and cytoplasm. This process is analogous to ion-translocation pumps where the pump recognises substrates directly through a complex substrate recognition region(s) or through use of molecular cues.

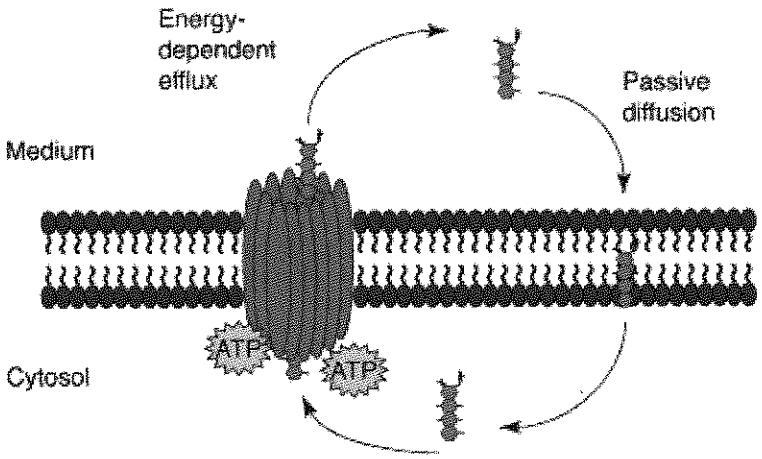

Figure 6: *General mechanism of P-glycoprotein (P-gp) action. Passive diffusion of the drug represented by the four solid circles through lipid membrane is followed by an active transport of the drug out of the cell by P-gp in an adenosine triphosphate (ATP) dependent manner (taken from Johnstone et al., 2000).*

ATP binding and hydrolysis are thought to be essential for the correct functioning of P-gp. The process requires two molecules of ATP to efflux one xenobiotic molecule (Gottesman and Pastan, 1993). The drug and ATP initially bind to the protein at their specific binding sites, where nucleotide hydrolyses to ADP yields energy for the extrusion of the drug. The release of ADP from the nucleotide binding site ends the first catalytic cycle followed by a conformational

change that reduces affinity for both substrate and nucleotide. The second catalytic cycle is initiated by the hydrolysis of a second ATP molecule and release energy is utilised to reorient the proteins to its original drug binding confirmation. Subsequent release of ADP completes another catalytic cycle, bringing the P-gp molecule back to its original state, where it again binds to both substrate and nucleotide to initiate the next cycle. This catalytic cycle of P-gp lends itself to the development of ATP directed P-gp inhibitors capable of interfering with the two cycles, where drug and nucleotide biding sites co-ordinate to function and efflux the substrates by the ATP driven process, however no such molecules are currently commercially available (Sauna *et al.*, 2001).

Evidence for a direct interaction of many P-gp substrates has been obtained most commonly through direct drug binding studies and photoaffinity labelling experiments (Liu *et al.*, 1996; Cornwell *et al.*, 1986). The reconstitution of purified P-gp into phospholipid vesicles that are capable of drug transport has indicated that transport can occur even in the absence of electrochemical gradients (Shapiro and Ling, 1995). Drug-stimulated ATPase activity has also been shown to be in direct proportion to the ability of P-gp to transport these drugs (Ambudkar, 1995). In addition, discrete amino acid substitutions in P-gp, have previously been used to probe the specificity of the transporter (Gottesman *et al.*, 1995; Taylor *et al.*, 2001).

Recently, Rosenberg and co-workers (2003) reported that the three-dimensional conformation of P-gp changes upon binding of a nucleotide to the intracellular nucleotide-biding domain. In the absence of nucleotide, the two transmembrane domains form a single barrel with a central pore that is open to the extracellular surface and spans much of the membrane depth, while upon binding nucleotides, the transmembrane domains reorganize into three compact domains that open the central pore along its length in a manner that could allow access of hydrophobic drugs directly from the lipid bilayer to the central pore of the transporter.

1.4.3 Expression of P-glycoprotein

In humans, the P-gp is the product of MDR gene, of which two different forms have been identified: MDR1 and MDR2. In rodents, three forms have been identified: mdr1a, mdr1b and mdr2 (Romaldson *et al.*, 2004). The gene responsible for P-gp expression, named MDR1 (Ueda *et al.*, 1986), is located on chromosome 7q21 and is transcribed into a 4.5 kilobase mRNA. P-gp is normally expressed in liver, kidney, intestine, brain and placental tissue, where it protects against the uptake of toxic compounds (Bendayan *et al.*, 2002; Takano *et al.*, 2005; Thiebaut *et*

al., 1987). Previous studies have shown that P-gp is expressed in the upper respiratory tract at the lateral membrane of the nasal mucosa, apical side of ciliated epithelial cells and on the lateral surfaces of serous glands (Lechapt-Zalcman *et al.*, 1997; Wioland *et al.*, 2000). In the lower respiratory tract, there is conflicting evidence. One study stated that P-gp was located at the luminal side of both human and rat type 1 pneumocytes (Campbell *et al.*, 2003), while other work has reported the absence of this protein in both type 1 or type 2 pneumocytes (Scheffer *et al.*, 2002). P-gp has also previously been shown to be present also in alveolar macrophages (Scheffer *et al.*, 2002; van der Valk, 1990).

1.4.4 P-glycoprotein function

The main physiological role for P-gp is the removal of toxic compounds from the body (Johnstone *et al.*, 2000). It has also been postulated that since P-gp is expressed in a wide variety of tissues throughout the body, it must have other physiological functions. P-gp has been linked with lipid transport, e. g. intercellular cholesterol movement (Fielding and Fielding, 1997), immunity and apoptosis (Johnstone *et al.*, 2000). P-gp is also though to play a role in the regulation of Cl^- and K^+ channels (Valverde *et al.*, 1992). However, the conductance of the channels is unaffected by the level of P-gp expression (de Greef *et al.*, 1995).

The precise function of P-gp in the lung is still unknown, but its expression at the apical membrane of epithelial cells may indicate that P-gp has a role in the transportation of compounds from the interstitium to lumen. Lipophilic amines such as fentanyl accumulate in the lungs and it has been proposed that P-gp may be one reason for this build up (Waters *et al.*, 2000).

1.4.5 P-glycoprotein substrates

P-gp affects the transport of wide range of substrates (Gottersman and Pastan, 1993) (Table 1). The majority of those affected are compounds of natural origin (derived from plants, bacteria or fungi) or structurally similar agents. The substrates range in size from 250 Da (cimetidine) to approximately 1900 Da (gramicidin D) (Schinkel, 1997). The single common feature that the substrates share is that they are all ampiphilic. Specific classes of compound transported by P-gp molecule include anti-cancer drugs such as anthracyclines, vinca alkaloids, epipodophyllotoxins and taxanes (Schinkel, 1997; Germann *et al.*, 1996), anti-HIV drugs such as amprenavir and

indinavir, H_2 antagonist such as ranitidine, immunosuppressants such as cyclosporine A (Saeki *et al.*, 1993), cardiac glycosides like digoxin (Tanigawara *et al.*, 1992; Schinkel, 1999; Takano *et al.*, 2005) and antibiotics e. g. rifampicin (Schuetz *et al.*, 1996) (Table 4).

1.4.5.1 Digoxin

Digoxin is a cardioactive glycoside that is often used as a model substrate for the P-gp efflux pump (Ito *et al.*, 1992 and 1993; de Lannoy *et al.*, 1992; Schinkel *et al.*, 1995). Previous *in vitro* permeation studies performed on immortalised gastrointestinal Caco-2 epithelial cells that are known to over-express P-gp, have shown preferential efflux secretion of digoxin (Cavet *et al.*, 1996). Practically this is determined via comparison of the transepithelial basal-to-apical (B-A) digoxin flux to the apical-to-basal (A-B) flux. Cavet and coworkers (1996) also showed the abolition of the active efflux transport in the presence of P-gp inhibitors verapamil, nifedipine and vinblastine. Likewise, LLC-PK1 cells transfected with the human MDR1 gene in order to induce P-gp expression have demonstrated that digoxin is a substrate for P-gp (Tanigawara *et al.*, 1992). It has also been employed to demonstrate the P-gp functionality *in vivo*. Schinkel *et al.* (1995) proved that after administration of digoxin to mdr1a–/– mice e. g. not expressing P-gp, concentrations of digoxin in brain and plasma were 35- and 2-fold higher, respectively, compared with wild-type which contained normal levels of the efflux transporters.

1.4.6 P-glycoprotein inhibitors

In order to reduce the sensitivity of cancer cells to P-gp efflux and thus reduce its effect on chemotherapy, inhibitors of the P-gp transport mechanism have been investigated (Robert and Jarry, 2003). Inhibitors of P-gp can be divided into several categories. The first-generation (e. g. verapamil and cyclosporin A) have been widely used *in vitro* however, due to the potential for serious toxic side effects including nephrotoxicity, congestive heart failure and hypertension, their use in cancer patients has not previously been attempted (Sikic *et al.*, 1997). Second-generation inhibitors are more P-gp specific, resulting in a reduced potential for side-effects. A commonly used P-gp inhibitor, PSC833, is a cyclosporine D analog, which has been shown to effectively reverse multidrug resistance in murine leukaemia and human breast cell lines thus restoring cell sensitivity to chemotherapy (Hamilton *et al.*, 2002). Some of the P-gp inhibitors are in fact substrates for the transporter themselves, but PSC833 interacts specifically with P-gp without being transported (Archinal-Mattheis, 1995). The third generation of inhibitors are mostly synthetic compounds which demonstrate lower toxicity, higher affinity and specificity for P-gp compared to the previous two generations. These agents can significantly alter

pharmacokinetics of anticancer drugs. The most promising third-generation substance for use in in humans are MS-209, which is orally active, LY3359, LY335979, VX-710/Birocadar (also inhibits MRP1) and GF120918 (Hamilton, 2002).

Table 1: *A selected list of compounds that interact with P-glycoprotein (Stouch et al., 2002).*

Drug Class	Examples
Anticancer drugs	Vinca alkaloids (Vincristine, Vinblastine) Anthracyclines (Doxarubicin, Daunorubicin) Epipodophyllotoxins (Etioposide, Teniposide) Taxol (Paclitaxel, Docetaxel) Actinomycin D, Mitomycin C Topotecan, Mithramycin
Other cytotoxic agents	Colchicine, Emitine, Puromycin
Calcium channel blocker	Diltiazem, Felopdipine, Verapamil Nicarpedine, Morphine
HIV protease inhibitors	Ritinovir, Indinavir, Saquinavir
Antifungals	Itraconazole, Ketacopnazole
Hormones	Hydrocortisone, Progesterone, Testosterone Dexamethasone, Estradiol
Immunosuppressants	Cyclosporine, FK506, Rapamycin
Detergents	Triton X-100, Tween 80, Solutol HS-15
Hydrophobic peptides	Gramicidin D, Valinomycin, *N*-acetyl-leucyl-norleucine
Other compounds	Digoxin, Tamoxifen, Terfenadine Rhodamine 123, Calcein-AM

1.4.6.1 Verapamil

Verapamil is a first generation P-gp inhibitor. This calcium channel blocker was the first substance shown to inhibit the P-gp activity (Tsuro *et al.*, 1981). Verapamil has been tested in many different cell lines and was even shown to be effective in MDR-1-transfected Madin Darby canine kidney cells that constitutively express low levels of transport proteins (Braun *et al.*, 2000). The major limitation of this inhibitor is the lack of P-gp specificity. Verapamil has previously also been shown to inhibit other transporters including the organic cation transport system (OCT) (Azsalos *et al.*, 1999). As previously mentioned, the use of this compound in human clinical studies is limited due to severe toxic cardiovascular effects caused by the dex-(D-) isomer (Ferry *et al.*, 1985).

1.4.6.2 GF120918A

GF120918A (HCl salt of GF120918, 9,10-Dihydro-5- methoxy-9-oxo-N-[4-[2-(1,2,3,4-tetrahydro-6,7-dimethoxy-2-isoquinolinyl)ethyl]phenyl]-4-acridine-carboxamide) is a third generation P-gp inhibitor with high potency and specificity for P-gp (Hyafil *et al.*, 1993; Witherspoon *et al.*, 1996; Evers *et al.*, 2000). The substance was originally developed by Glaxo Wellcome, Inc during the screening of acridone carboxamide derivatives as potential P-gp inhibitors. GF120918A has been used both *in vitro* and *in vivo* to investigate the role of transporters in the disposition of various test molecules. Previous studies carried out in both rats and humans have shown that this inhibitor has low toxicity and less side-effects compared to other P-gp inhibitors (Hyafil *et al.*, 1993). For example, full reversion of multidrug resistance by verapamil requires at about 10 μM concentration, when tested in cell culture models, whereas plasma levels above μM result in atrioventricular block in patients (Pennock *et al.*, 1991). In comparison, GF120918 fully reverses multidrug resistance at 0.05 to 0.1 μM (Hyafil *et al.*, 1993). The assays previously performed using different MDR cell lines including murine, Chinese hamster and human have shown that GF120918 is about 100-200 times more potent than verapamil and about 2 orders of magnitude more potent than other MDR inhibitors such as amiodarone. The specificity of GF120918 was shown by Hyafil *et al.* (1993) through the absence of any effects on MDR-negative cell lines. These effects were supported by the inhibition of [^{3}H]-azidopine observed by photoaffinity labelling (Hyafil *et al.*, 1993). Unlike verapamil, GF120918A is not transported by P-gp and is related at the receptor hence it has been shown to be still active several hours after being taken away from the cell culture medium (Hyafil *et al.*, 1993).

1.4.7 Assays for P-glycoprotein interaction

The interaction of substrates with P-gp is still largely an unknown process for many compounds and therefore is still the subject of discussion in the literature. However, several assays have been designed to assess the identification, location and function of P-gp substrates and inhibitors. None of the assays alone provide all the information about P-gp action and each has advantages and disadvantages. The following sections provide a summary of previous work which has been performed to develop methods to assess P-gp action. It is important to gain an appreciation of the assays so that studies into P-gp function can be critically appraised.

1.4.7.1 Transport studies

Transport studies are the most commonly employed method for the evaluation of active transport activity in cells and therefore this type of study is videly used to screen the effects of P-gp substrates and inhibitors. In this method the drug transport across cell layers grown on supports in both the apical to basolateral (A-B) and basolateral to apical (B-A) direction is determinated (Figure 7). The calculated ratio of compound permeation rates in each direction across the cell layer allows the predominant transport direction (if any) to be identified and therefore P-gp localisation within cells to be shown. However, interpretation of data from these type of studies can be complicated due to heterogenity of cells in culture and the compound specific method of transport across cell layers (Stouch *et al.*, 2002). Selecting appropriate substrates and high specificity inhibitors for P-gp is important so that the contribution of non-P-gp transport mechanisms can be minimised. If the studies are performed with these issues in mind, transport studies are a suitable method of P-gp activity evaluation *in vitro*.

1.4.7.2 Immunohistochemistry

The precise localisation of P-gp in cells can be detected by immunohistochemistry. The method is based on the binding of a primary antibody to the P-gp and then the interaction with a fluorescently labeled secondary antibody which is subsequently visualised using confocal laser scanning microscopy (CLMS). There is a wide range of antibodies capable of recognising P-gp. The JSB-1 and C219 antibodies have previously been used to detect the P-gp on the apical side of bronchial epithelium in the airways of the lung (Scheffer *et al.*, 2002). In addition, several studies have reported successfully using a clone MRK16 (Hamada & Tsuruo, 1986) and clone F4 (Chu *et al.*, 1994) antibodies. Due to the reproducible proportionality of the reaction of P-gp with antibodies this method allows the quantification of the P-gp.

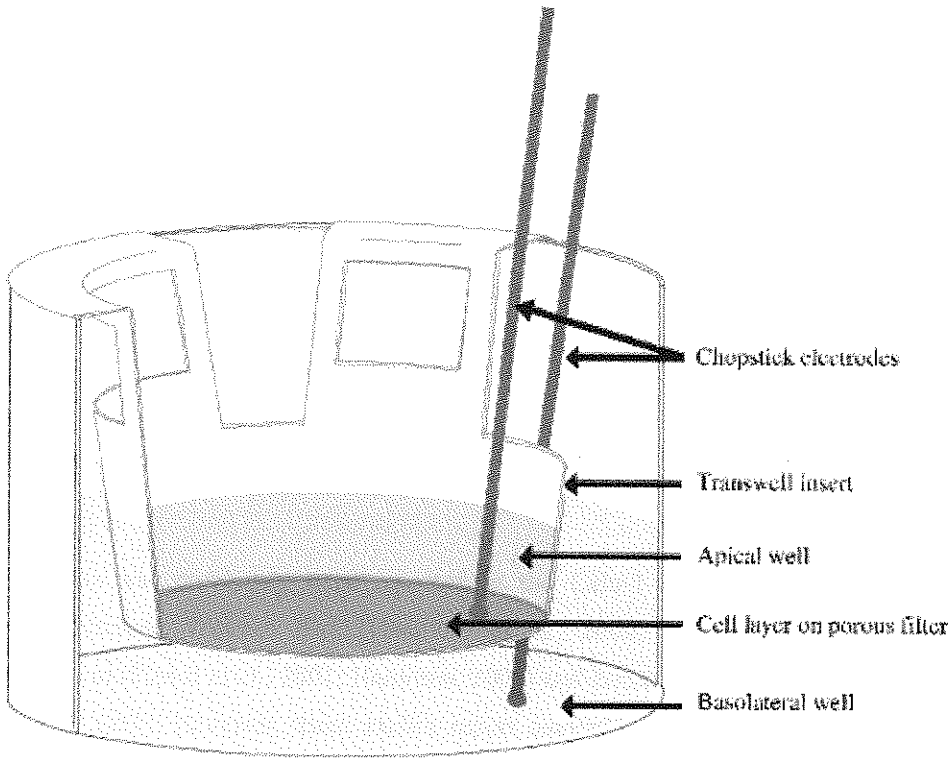

***Figure** 7: A diagram showing Transwell® support. Cells are grown on the porous filter. Cell culture medium is in the basolateral and/or apical well. For evaluation of the cell layer barrier properties, the transepithelial electrical resistance (TER) is measured with chopstick electrodes connected to voltohmmeter (taken from Grainger, 2008).*

CLMS is very useful tool in molecular biology, despite the cost of the equipment and procedures. The principle of CLMS is the emission of light by fluorescent molecules that are energised with a laser or any other light source with high intensity. The continuous light signal that is emitted by the molecules is captured and detected by cameras. Spectral variants of fluorescent markers used for labeling the molecules permit dual-labeling if compounds can be selected with minimal overlap in their emission spectrum and thus allow for co-localisation determinations to be made. Moreover, the resolution of laser microscope is higher than at conventional fluorescence techniques and therefore CLSM allows location visualisation of proteins in biological systems with high resolution. Furthermore, the generation of a three-dimensional image allows the better understanding of the connection between cell compartments, e. g. permits the following of transported substrates in cells with time course. However, CLMS requires a certain level of expertise to prepare the samples and operate the equipment before suitable images are achieved.

1.4.7.3 Accumulation of substrate in cells

The measurement of P-gp substrates accumulation in cells as a result of P-gp efflux transport inhibition by agents that are co-administered with the transported molecule is another method to identify the presence of P-gp. Compounds evaluated by this method are usually fluorescently labeled (Kessel *et al.*, 1991) or photoaffinity analogs of anti-tumor agents (Beck *et al.*, 1992). According to the level of fluorescence emitted by the cell as a result of increased accumulation of drug in the presence of the inhibitor, the activity of the P-gp is measured.

1.4.8 P-glycoprotein in Calu-3 cells

P-gp expression has previously been reported in the Calu-3 cell line using a variety of techniques including: Western Blot (Hamilton *et al.*, 2002; Patel *et al.*, 2002), protein immunodetection (Florea *et al.*, 2001; Hamilton, 2001) and confocal laser scanning microscopy (Florea *et al.*, 2001). However, these studies report contradictory results with respect to the location of this active transporter (Hamilton *et al.*, 2002; Florea *et al.*, 2001; Hamilton, 2001[b]). The presence of P-gp predominantly at the basolateral side of the plasma membrane was demonstrated by Western blott analysis and confocal laser scanning microscopy by Florea *et al.* (2001), but Hamilton *et al.* (2001[b]) showed by immunofluorescent staining that P-gp was predominantly expressed on the apical side of Calu-3 cell membrane. One reason for these differences may be the different cell culture conditions used in the two studies. Whilst Florea *et al.* (2001) cultured the cells using Dulbecco's Modified Eagle Medium (DMEM), Hamilton employed Ham's F12:DMEM. Data generated by Brouillard *et al.* (2001) supports this hypothesis. They showed using Northern blotting that the level of P-gp expression in cells was inducible by culture conditions. Treating the cells with submicromolar concentrations of ouabain stimulated MDR-1 gene expression within 24 h. Immunoblotting and immunohistology demonstrated that ouabain also increased the membrane P-gp content, and as a consequence caused the Calu-3 cells to become resistant to doxorubicin and vinblastine.

Not only has the P-gp transporter been shown to be present in Calu-3 cells, several groups also have investigated its function. However, as with its location, there have been conflicting reports with regards to the manner in which it influences transport in this cell line (Florea *et al.*, 2001; Hamilton *et al.*, 2001a; Hamilton *et al.*, 2001b; Patel *et al.*, 2002) (a summary of these studies is presented in Table 2).

Hamilton *et al.* (2001[b]) investigated the role of P-gp in the Calu-3 cell model using transport and accumulation studies. The metabolic inhibitor sodium azide decreased the efflux of rhodamine 123 (Rh123, P-gp substrate) out of Calu-3 cells to the same degree as cyclosporine A (CsA, P-gp inhibitor), suggesting the presence of efflux in Calu-3 cells. The B-A transport of Rh123 was significantly higher than the movement of the compound in the reverse direction. This secretory efflux was reduced by 25-fold in the presence of CsA. The work described by Hamilton and coworkers (2001[b]) also showed that Rh123 efflux was mainly P-gp mediated through the cell accumulation of Rh 123 and calcein-AM (a known P-gp substrate) in the presence of the P-gp inhibitors CsA, vinblastine and taxol. However, significant inhibition of P-gp activity was not observed until after 2 h post inhibitor application and this was thought to demonstrate that the P-gp efflux pump pathway was energy dependent. In a second study Hamilton *et al.* (2001[a]) examined the influence of glucocorticosteroids on P-gp mediated transport of Rh123 in Calu-3 cells. The potency of the P-gp inhibition was found to be compound and dose dependent. A ca 2.4 fold increase of Rh123 accumulation compared to the untreated control was found with 100 mM budesonid (P-gp inhibitor), whereas the most potent inhibitor was progesterone with a 4.0-fold increase of Rh123 accumulation at 100 mM. This work agreed with the previous study that P-gp was functional in Calu-3 cells and that it was responsible for B-A transport, i.e. efflux.

In contrast to the work by Hamilton *et al.* (2001a, 2001b) and Patel *et al.* (2002), results published by Florea *et al.* (2001) suggested that a P-gp transporter can also be present on the basolateral membrane of Calu-3 cells. Two methods were employed in this work to study the effect of P-gp inhibition upon flunisolide transport. To abolish possible ATP-dependent secretory transport caused by P-gp, a non-specific inhibition of cellular metabolism was evoked by low temperature (4°C), 2-deoxy-D-glucose and sodium azide. Polarized transport of flunisolide was inhibited at all conditions; moreover the transport was abolished using P-gp inhibitors verapamil, SDZ PSC 833 and LY335979. In conclusion, these results showed that the active apical to basolateral transport of flunisolide across Calu-3 cells was facilitated by P-gp located in the basolateral plasma membrane.

The wide range of test compounds employed in cell layer transport studies makes comparison across studies very difficult. In addition, when trying to rationalise the data generated in this field, the specificity of the substrate for the P-gp transport mechanism must be considered. Cavet *et al.* (1997) investigated transepithelial ciprofloxacin fluxes in the A-B and B-A directions in Calu-3 cell layers. This group reported that the transport was similar throughout the 1.0 mM to 3.0 mM ciprofloxacin concentration range. A-B ciprofloxacin flux was inhibited by the addition of a 100-fold excess of norfloxacin, enoxacin, and ofloxacin, while B-A flux was unaffected. However, equivalent studies in Caco-2 epithelia (over-expressing the P-gp), which showed the

absence of a specific secretory pathway and therefore ciprofloxin was shown not to be a P-gp substrate. This demonstrates that the P-gp transport mechanism in Calu-3 cells shows compound selectivity.

Although previous studies report contradictory results about the localisation and the direction of P-gp specific drug transport across the Calu-3 cell layer these studies were typically highly variable and based on the transport of a selected number of compounds. One of the most commonly used agents, Rh123 in not specific substrate for P-gp and could be actively transported by other mechanisms, for example by OCT (van der Sandt *et al.*, 2000). The presence of OCT in Calu-3 has not been demonstrated yet and the impact of OCT on Rh123 transport is not fully examined. For this reason, the transport data of Rh123 in Calu-3 cell line should be interpreted carefully. The studies by Cavet *et al.* (1997), Hamilton (2001a, 2001b) and Patel *et al.* (2002) demonstrate the need for a systematic study of P-gp transport using a highly specific substrate and inhibitor using an optimised cell culture protocol in order to resolve the precise location and function of P-gp in the lung. Only upon completion of such a study can the impact of this active transport mechanism upon drug delivery to the lung be assessed.

1.4.9 P-glycoprotein in normal human bronchial epithelial cells

To date, there has only been limited information published on the expression of P-gp in primary NHBE cells. Recently, Lin *et al.* (2006) showed the expression of P-gp in the NHBE cell layers that development tight junctions *in vitro* which demonstrates that these primary cells can be used to as a model to investigate systemic drug absorption in the airways of the lung. In work of Lin and coworkers (2006) the presence of P-gp in NHBE cells was demonstrated by functional transport studies. The B-A permeability of R123 was significantly higher compared to the transport in the reverse direction. Furthermore, the P-gp expression in the cells was demonstrated by RT-PCR of MDR1. The transport of fenoxfenadine hydrochloride (P-gp substrate) was not affected by P-gp efflux, possibly due to low expression of the P-gp transporter and/or to its saturation with high concentration of fenoxfenadine hydrochloride. However, as mentioned previously, because Rh123 is not a specific substrate for P-gp and could be actively transported by other transporters, for example organic cationic transporter OCT (van der Sandt *et al.*, 2000) this study does not conclusively prove the function of P-gp in NHBE cells. Transport studies using more specific P-gp inhibitors and substrates are required to elucidate the efflux transport mechanisms in NHBE.

***Table 2**: A summary of literature citing Calu-3 and normal human brochial epithelial (NHBE) cells as being P-glycoprotein expressing. A=apical,*

Study	Cells	Substrate(s)	Inhibitor(s)	Direction of polarized transport	Time in culture (days)	Passage	Other method of P-gp detection	Location of P-gp enzyme at cell membrane
Florea *et al.* (2001)	Calu-3	Flunisolide	NaN_3, 2-deoxy-D-glucose SDZ PSC 833, LY335979 Verapamil 4°C	A→B	18	20-62	Western blot Immunohistochemistry	Basolateral
Hamilton *et al.* (2001)[a]	Calu-3	Rhodamine 123	Testosterone Progesterone Propranolol	B→A	4	19-40	-	Apical
Hamilton *et al.* (2001)[b]	Calu-3	Rhodamine 123 Calcein-acetoxy-methylester	Cyclosporine A Vinblastine Taxol Sodium azide	B→A	13-15	19-40	Western blot	Apical
Patel *et al.* (2002)	Calu-3	Cyclosporine A Saquinavir Ritonavir	Quinidine	B→A	10	-	Western blot	Apical
Lin *et al.* (2006)	NHBE	Rhodamine 123 Fexofenadine	Verapamil	B→A	6-8	2-3	RT-PCR	Apical

1.5 Lung drug absorption models

1.5.1 Cell culture models

The major barrier to drug absorption in the airways of the lung is the epithelium (see Section 1.2.7). Therefore, in order to better understand the mechanisms of drug transport in the respiratory tract, models of the pulmonary epithelium are essential. As a consequence, numerous cell layers, cultured *in vitro,* under conditions designed to maintain the characteristics of airway epithelium have been developed (Table 3).

***Table 3**: Summary of the advantages and limitations of immortal cell culture models for in vitro drug transport and metabolism studies (adapted from Forbes, 2000).*

Advantages	Limitations
• Small amounts of compounds are required for experiments • Easier and more economical than *in vivo* experiments which reduces animal usage • Rapid, with a high throughput capacity • Provides mechanistic information about epithelial transport • Environmental conditions, such as temperature and pH, can be controlled • Drug analysis is simplified by the use of aqueous buffer solutions	• Models are usually based on a single cell type and the cells are monoclonal in nature • Tight junctions may not be representative of the target tissue • Non-representative cell cycles affect transport and metabolism mechanisms • Cell lines derived from adenocarcinomas often have untypical phenotypes

In terms of human derived cell culture models, both immortal cell lines and primary cultures can be used to mimic both the upper airway and alveolar epithelia (Mathias *et al.*, 1996). The most commonly used cell lines are 16HBE14o- (immortalized human bronchial cells), Calu-3

(adenocarcinoma human bronchial cells) and A549 (human type II-like alveolar cells). The primary airway epithelial cells that can be culture *in vitro* are known as normal human bronchial epithelial cells (NHBE).

1.5.1.1 Immortalised cell lines

Immortalised cell lines provide a model that is more controllable, reproducible and sustainable compared to primary cell lines. The immortalised nature of cells provides a continuous source of epithelial reproduction, however eventually the cells exhibit dedifferentiated ultrastructural characteristics and they can sometimes lose their ability to form tight junctions (Gruenert *et al.*, 1995).

a.) *Calu-3*

The Calu-3 cell line has been recently shown to be a suitable model of the upper airway epithelium (Grainger *et al.*, 2006). Calu-3 cell lines were originally derived from bronchial carcinoma of a 25 year-old white Caucasian male. The formation of tight junctions, and hence confluent cell layers, when grown on porous support membranes, makes this cell line relatively easy to grow and thus it is widely used for drug transport studies in the airways (Florea *et al.*, 2003; Foster *et al.*, 2000; Wan *et al.*, 2000). When cultured *in vitro* Calu-3 are composed of a mixed phenotype of ciliated and secretory cells that differentiate to exhibit hermetic barrier properties. The cell line when grown as a confluent monolayer commonly displays a high transepithelial electrical resistance (TER > 1000 $\Omega.cm^2$) and low permeability for paracellular transport markers (Cavet *et al.*, 1997; Singh *et al.*, 1997). The cells are of cuboidal and polygonal in shape and approximately 30% of the cells in a typical monolayer form apically located cilia (Pezron *et al.*, 2002). The morphology of Calu-3 cells has been found to be dependent on the culture conditions, e. g. the exposure of cells to a liquid-liquid interface (LLI) or an air-liquid interface (ALI) interface (Mathias *et al.*, 2002). Under LLI conditions the cilia appear to be shorter and thicker than under ALI condition (Florea *et al.*, 2003). In previous work Calu-3 cells have shown the ability to express metabolic enzymes CYP2E1, CYP2B6, CYP1A1 (Foster *et al.*, 2000). The CYP enzymes have not been shown to be inducible under culture conditions. However, Berger *et al.* (1999) detected the secretion of mucin and other high molecular weight glycoproteins by this cell line. Mucus production is governed by the presence and expression of various MUC genes. The MUC1 gene has been detected in all carcinoma cells, but it does not always lead to the production of mucus (Berger *et al.*, 1999). Finkbeiner *et al.* (1993) screened a number of cells derived form lymphsarcinomas and discovered that Calu-3 contained the cystic fibrosis transmembrane conductance regulator (CFTR). Calu-3 also carries

peptide transporters (Mathias *et al.*, 2002; Pezron *et al.*, 2002) and active transporters such as P-gp (Hamilton *et al.*, 2002).

1.5.1.2 Primary pulmonary cell cultures

Primary airway cells cultured *in vitro* are more representative of the native pulmonary epithelium *in vivo* compared to immortalised cell lines because they possess a mixed ciliated epithelium and produce a mucus layer *in vitro*, which appears similar to that produced by the epithelium. The major limitations of attempting to culture primary cell lines, which originate from nondiseased human tissue without immortalisation, are their lack of availability, the limited amount of cells generated by *in vitro* culture and the donor-donor variations (Lin *et al.*, 2006; Forbes, 2000).

Primary airway epithelial cells cultured under ALI conditions on support membranes do form a pseudostratified epithelial layer with overlapping cytoplasmic regions (van Scott *et al.*, 1986). In culture ciliated, non-ciliated, basal and secretory cells forming cilia are all present. In addition, microvilli and a glycocalyx proteins can often be found on the apical cell membrane of primary cell lines (Liedtke *et al.*, 1988). When cultured on a support membrane without a collagen coating and with serum-free medium, scanning electron microscope (SEM) images have previously shown that NHBE cells show less prominent cilia (Lin *et al.*, 2006). On the basolateral membranes of primary cell lines desmosomes have been detected (Jetten *et al.*, 1987) and the formation of tight junctions has been confirmed by the F-actin stain (Lin *et al.*, 2006).

The barrier properties for primary cell monolayers are highly dependant on the culture conditions. For example the differentiation of primary airway epithelial cells *in vitro*, has previously been shown to be influenced by the composition of the extracellular matrix (Jiang *et al.*, 1993; Mette *et al.*, 1993), the presence of growth factors (Keenan *et al.*, 1991), the addition of hormones (Jetten *et al.*, 1991; Lechner *et al.*, 1985), and the presence of an ALI interface (Yamaya *et al.*, 1992; Grainger *et al.*, 2006). However, even when primary cells are grown in optimal conditions, they tend to lose the epithelial barrier properties and differentiation after two or three passages (Forbes, 2000).

The optimisation of cell culture media to maintain the viability of freshly isolated cells has been subject of numerous previous studies (Gruenert *et al.*, 1990; van Scott *et al.*, 1986). It was generally agreed in this previous work that LHC and Dulbecco's modified Eagle's medium/ Ham's F-12 solutions (Widdicombe *et al.*, 1992) provide an environment in which primary cells can grow. However, for long-term studies, the use of serum in cell culture medium has been

shown to be detrimental (Lin *et al.*, 2006; Lechner *et al.*, 1985). Blood-derived serum contains tumour growth factor-l3 (TGF-P) which inhibits airway epithelial cell proliferation and can induce squamous differentiation (Lechner *et al.*, 1983). As a consequence, serum is often replaced in primary cell line growth mediums by growth factors (van Scott *et al.*, 1988). For example, in a study by Yamaya *et al.* (1992) serum in the culture medium was replaced with Ultroser G. Medium additives can also be used to promote specific characteristics of cells, for example retinoic acid promotes cell differentiation, and growth factors (EGF, TGF-P FGF) can modulate the proliferative capacity of the cells (Willey *et al.*, 1984). Another variable that is considered important in the culture of primary cells is the selection of an appropriate surface on which the cells are grown. When tracheal epithelial cells were cultured on Vitrogen gels with an ALI interface, improved cytological and electrical resistance characteristic were observed. As it is believed that the type cell growth surface can have an effect on cell growth a wide range of different supports are available including fibroblast feeder layers, collagen films or gels and collagen-fibronectin bovine serum albumin layers. The surface upon which the cells are grown has been shown to modify the activity of receptors on the cell surface (Yamaya *et al.*, 1991), change the architecture of cells (Yamaya *et al.*, 1992) and regulate cell gene expression (Cromwell *et al.*, 1992).

Most commonly cells are grown *in vitro* on a porous-bottomed insert placed in a tissue culture well to which medium is added. Submerging only one side of the cells in the medium (usually the basolateral side) generates air-liquid interface (ALI) culture conditions which closely simulates the environment in the human airways. Aerobic respiration under ALI promotes glycoprotein secretion and cell differentiation. Grainger *et al.* (2006) showed that when airway cells were grown using an ALI they produced a more columnar shaped epithelium with a more rugged apical topography compared to cells grown under LLI conditions and apical protrusions appearing to be cilia-like structures were observed (Grainger *et al.* 2006). However, typical airway ciliated cell phenotypes are still not produced regardless of the presence of an ALI.

1.5.2 Animal lung models

Methods that employ animals to evaluate drug deposition, metabolism and clearance from the respiratory tract are essential to the pharmaceutical development of inhaled compounds (Table 2). The most commonly employed animal models are the dog, rabbit and rat which each exhibit a monopodial airway branching system similar to humans. However, there are known to be several differences in the morphology and physiology of the human lung compared to other

animal species (summarised in Table 2). For example, the major airway branches in these animal models typically display larger diameters and a smaller angle of branching compared to human (Sweeney *et al.*, 1991). In addition, the pulmonary circulation only supplies the alveolar region in humans, whereas in several animals e.g. rats it also supplies blood to the bronchioles and terminal bronchioles (Chediak *et al.*, 1990; Effros *et al.*, 1994).

Table 4: *Comparison of the key properties of the human and rat lung airways (adapted from Tronde, 2002).*

Property	Human	Rat
General		
Lung lobes	Left lung: 2 Right lung: 3	Left lung: 1 Right lung: 4
Branching	dichotomous	strongly monopodial
Respiratory bronchioles	several generations	absent
Structure of gas exchange barrier		
Average body weight (kg) *(n= 8)*	74	0.140
Thickness of gas diffusion barrier (μm)	0.62	0.38
Gas exchange surface area/unit lung volume (cm^2/cm^3)	371	750
Capillary volume/ unit lung volume (mL/cm^3)	0.057	0.092
Cellular composition in alveoli (%)		
Average body weight (kg) *(n =8)*	74	0.360
Type I alveolar cells	8	9
Type II alveolar cells	16	14
Endothelial cells	30	46
Interstitial cells	36	28
Macrophage	9	3
Alveolar surface covering (%)		
Type I alveolar cells	93	96
Type II alveolar cells	7	4

Although it is accepted that the pathology of disease states such as asthma and COPD should ideally be studied in isolated human airway tissue, ethical constraints limit the availability of human tissue and therefore several types of *in vitro* techniques have been developed to study of disease and drug absorption in the airways of the lung, including:

- airway strip and ring preparations for pharmacological testing of drug action
- lung parenchymal strips
- isolated perfused airways
- isolated perfused lungs - rabbit (Brazzel *et al.*, 1982), rat (Byron *et al.*, 1988; Ryrfeldt *et al.*, 1978) and guinea pig (Ryrfeldt *et al.*, 1978).

1.5.2.1 Isolated perfused rat lung

The most commonly employed animal model to study inhaled drug delivery is the isolated rat lung. The isolated perfused rat lung (IPL) model allows the evaluation of drug disposition in tissues that retain integrity. A detailed investigation of pulmonary dissolution, absorption, tissue binding and pulmonary transport can be performed in the IPL. Moreover, the absorption and metabolism can be studied without the contribution of systemic metabolism and elimination. In comparison with whole animal preparations, transport experiments in the IPL allow greater control over experimental parameters that could change over the time course of an *in vivo* experiment, for example lung perfusion rate and air pressure. In addition, the concentration and recovery of the test compounds can also be finely controlled and multiple samples can be easily extracted from the IPL. Although the lungs of guinea pigs, rabbits and mice have also previously been used to study airway drug disposition, in comparison to rat, the other models are more difficult to manipulate manually. In addition, animals smaller than the rat allow only a limited number of blood samples to be taken during the experiment as a consequence of a low blood volume. The use of artificial perfusion systems or diluted blood can circumvent these sampling problems if smaller animals are preferred due to the cost implications.

A major limitation of the IPL model is the limited viability time of the organ even when maintained using adequate physiological conditions. Many methods have been developed in attempt to prolong the viability of IPL tissue, for example the use of subambient temperature (Niemeier *et al.*, 1972) or storage in preservation solutions prior to perfusion (Reignier *et al.*, 1995; Xiong *et al.*, 1999), however even these techniques have failed to improve viability over the experiment period. The absence of bronchial circulation and lymphatic drainage is also considered as a disadvantage of the model. The non-functioning lymphatic system, fluid

extravasation and use of artificial perfusion medium may lead to weight gain as the system deteorates during perfusion (Fisher *et al.*, 1980; Kroll *et al.*, 1986). However, the IPL preparation has been shown to have a stable metabolic activity for up to 5 h (Tronde *et al.*, 2005).

a) Lung isolation

In order to prepare the rat lung the animal is usually injected with lethal dose of an anaesthetic. When a deep anaesthesia is achieved, an incision is made in the skin at the neck and the trachea is exposed. A cannula is inserted in a trachea through the cut between 4th and 5th cartilage ring, tied in place and connected to ventilator (Byron *et al.*, 1986). Alternatively the lungs can be ventilated manually using a syringe connected to the cannula. The abdomen is cut horizontally, the diaphragm is pierced and the viscera are pulled out to expose and cut the abdominal vessel. The thorax is opened and heparin is injected either into right ventricle or intravenously. The pulmonary artery and vein are cannulated and the blood is flushed out from the pulmonary circulation with a perfusion solution pre-warmed to 37°C. The lungs are either left *in situ* or removed from the thorax and placed in a water vapour-saturated glass or Perspex chamber isothermally regulated to 37°C. A number of different chambers have been designed to hold the lungs, for example Niemeier *et al.* (1972) described the maintenance of IPL in the artificial thorax which consisted of water-jacketed glass chamber sealed by cover. The inner part of the chamber was the organ holder with the connections for cannulating the trachea (ventilation) and the pulmonary artery and left atrium (perfusion). During the experiment the lungs are typically perfused via the pulmonary artery with an oxygenated artificial perfusion solution or whole blood under either constant pressure or constant flow conditions. In most studies the preparation is ventilated with preheated and humidified gas by oscillating negative pressure in the chamber. Alternatively positive pressure is used to induce ventilation.

To date, many different IPL set-ups, ranging in complexity, have been described in literature. However, the high cost of the complex perfusion systems have led to a recent trend to attempt and simplify the IPLL model whilst maintaining the optimal features for investigation of drug absorption. Such an IPL model has been developed by Bosquillon *et al.*, (2008) who showed that even a very simple system is suitable system for evaluation of drug absorption in the lung (Figure 8). In the model developed by Bosquillon and co workers (2008) the lungs are maintained at ambient temperature (21°C) without any specialist chamber and the preparation is perfused under single-pass conditions with modified Krebs-Ringer solution at pH 7.4, 37°C. The lungs are inflated with a constant volume of inhaled air during the experiment. This simple

model has generated data that correlated well with previous permeation studies performed *in vitro* using cell culture models (Bosquillon *et al.*, 2008).

b) Single-pass and re-circulating lung perfusion

There are two types of perfusion systems that have been developed to supply the IPL with essential nutrients after excision from the animal. These two systems are commonly referred to as a single-pass perfusion and a recirculatory perfusion. When a single dose of test compound is administered to the airways of the lung and the perfusion solution is collected at the venous vessels, this is known as single pass perfusion. Re-circulatory perfusion occurs when the perfusate is re-infused into the pulmonary artery after a single pass creating a perfusion loop. The total amount of the delivered drug is the same in both perfusion systems, but the volume of perfusate is much larger using the single-pass system. Van Putte *et al.* (2002) showed no difference regarding drug absorption from IPL between single-pass and re-circulating lung perfusion. However, the single-pass technique is more suitable for kinetic studies as it ensure constant drug concentration in the perfusate.

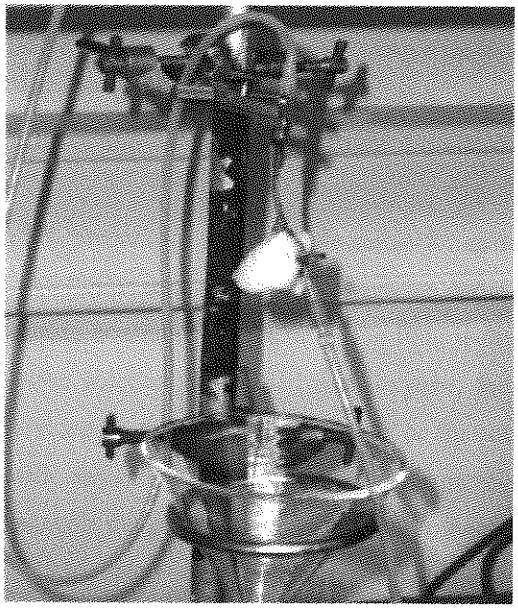

***Figure 8**: Simple isolated perfused rat lung model developed by Bosquillon et al. (2008). The air-filled lungs are vertically suspended above a funnel and maintained uncovered at 21°C. The volume of inhaled air in the lung is kept constant using cannula with syringe connected to the trachea. The lungs are perfused via cannula (green) with oxygenated modified Krebs-Ringer solution.*

c) Drug administration

Administration of a drug to IPL is performed either by intratracheal injection (Schanker *et al.*, 1978 and 1983) or by aerosol inhalation (Byron *et al.*, 1986; Schanker *et al.*, 1986; Tronde *et al.*, 2002[a]). In both methods, the drug is administered through tight fitting cannula that is kept in place during entire experiment to reduce the removal of the drug by lung airway mucociliary clearance. Drug absorption from IPL can be monitored either by measuring the disappearance of substance from the organ or by appearance in the perfusion solution. Using the first method, the apparent rate constant can be obtained, but this approach is limited to substances that are not metabolised by the lung tissue. Moreover, if measuring the disappearance of drug it is necessary to analyse the entire respiratory tract to detect the unabsorbed drug (Burton *et al.*, 1974). As a consequence the detection of the drug in the perfusate is considered more convenient. In addition, assaying the compound in the perfusate allows drug transport to be characterised by kinetic parameters such as absorption half life ($t_{1/2}$) and absorption constant (ka_{lung}) (Tronde *et al.*, 2002[b]).

d) The viability of the isolated perfused lung

During an IPL experiment, the lungs are typically inspected visually for any sight of translucent areas indicating development of oedema, hence damage. Lung viability can be further verified by monitoring the pH of the perfusion solution and the drug metabolising activity in the perfused tissue, e. g. monitoring of microsomal MFO activity.

Although the viability of an IPL preparation can be made stable for up to 5 hours (Tronde *et al.*, 2005), the preparation can deteriorate and generate oedematous areas during the experiment. One of the major concerns during continued perfusion of the lung is that no longer inflates and deflates. Although the perfusion solution is fortified with oxygen, the perfused lung requires more oxygen than can be provided by the use of the red cells or fluorocarbons in the perfusion solution. The difficulties with oxygen supply in the IPL preparation can be reduced by ventilation of the preparation with oxygen delivered at supranormal tension, to minimise the tissue hypoxia (Kroll *et al.*, 1986). However, such ventilation again requires the set up of a complex IPL apparatus and even very simple models such as the one developed by Bosquillon *et al.* (2008) have previously reported 2 hours viability of the IPL preparation using constant volume of inhaled air without ventilation.

e) Applications of the isolated perfused lung

The main disadvantage of the IPL is the limited viability of the preparation (Bassett *et al.*, 1992; Fisher *et al.*, 1980) which prevents the investigation of slow pharmacokinetic processes. However, a wide range of compounds are processed rapidly by the lung and therefore the IPL model has previously been employed to study the absorption, tissue sequestration, and metabolism of large a number of substances (Table 3). Jeppsson *et al.* (1994) looked at the comparative duration of action of three drugs used in the treatment of asthma. Schanker (1981) found that in similar manner to drug absorption in the G. I. tract, the rate of accumulation of an organic compound in the lung tends to depend on the physicochemical properties of the drug. Isolated and perfused lung models have successfully been applied to investigate drug dissolution (Niven *et al.*, 1988; Tronde *et al.*, 2002), drug absorption (Sakagami *et al.*, 2002), and disposition (Audi *et al.*, 1998; Ryrfeldt *et al.*, 1989). Tronde *et al.* (2002) proved the suitability of the rat IPL model for use in metabolic studies and hence the IPL model is widely used for metabolism studies (Dollery *et al.*, 1976; Gillespie *et al.*, 1985; Longmore, 1982). For example, the lung metabolism of tetrapeptides was shown to be higher after delivery to the airways compared to vascular delivery. Although the IPL model is widely used for studying different aspects of pulmonary drug delivery, there is still only limited information on the presence and activity of active transporter systems in this model. It is important to elucidate the activity of transporters such as the P-glycoprotein (P-gp) system as active processes may have a dramatic effect of the rate at which therapeutic agents are absorbed across the airway epithelium.

1.5.3 Correlation among lung absorption models

In vitro models require correlation with *in vivo* conditions if the data is to be used to support the use of therapeutic agent. To date, there is little information on how data obtained from experiments performed on cell lines correlate with data from IPL and *in vivo* models. Mathias *et al.* (2002) compared Calu-3 cell line, a primary culture model and an *in vivo* study (data taken from Schanker, 1986 and co-workers) and found that the permeability characteristics of Calu-3 cells correlated well with primary cultured rabbit tracheal epithelial cells (R^2= 0.91) and the rate of drug absorption from the rat lung *in vivo* (R^2= 0.94). Tronde *et al.* (2003a) determined that the apparent first-order absorption rate in the IPL correlated to the apparent permeability of Caco-2 cell monolayers, despite the later being a colon adenocarcinoma derived cell line. An *in vitro-in-vivo* correlation (R^2= 0.98) was also found in this study for the IPL drug absorption half-life and the pulmonary absorption half-life obtained in rats *in vivo* (Tronde *et al.*, 2003a). Good

correlation between the permeability characteristic of simple IPL model and 16HBE14o- cell line was also recently found by Bosquillon *et al.* (2008). These results illustrate the capability of a wide range of epithelial cell lines to be used for permeability screening, especially when the drugs are absorbed passively. However, no comparison between cell culture models and the IPL has been performed with regards to the presence and activity of transporter systems in these models.

Table 5: *Compounds assessed by using isolated perfused lung model.*

COMPOUND	REFERENCE
Atenolol	Tronde (2002, 2003a)
Beclometazone	Hartiala (1979)
Budesonide	Ryrfeldt (1989), Tronde (2002, 2003a), Cassara (2003)
Bupivicaine	Foth (1995)
Chlorpromazine	Mehendale (1975)
Corticosteroids	Burton (1974)
Cyanocobalamin	Tronde (2002, 2003a)
Diphehydramin	Yoshida (1989)
Dextrans	Mathias (2002), Tronde (2002, 2003a),
Enalapril	Tronde (2002, 2003a)
Fenfluramine	Valodia (2000)
Fluorescein	Byron (1986, 1988), Niven (1990), Ehrhardt (2002, 2003)
Formoterol	Tronde (2002, 2003a), Jeppsson (1994)
Imipramine	Yoshida (1989)
Losartan	Tronde (2002, 2003a)
Mannitol	Schanker (1983)
Metoclopramide	Yoshida (1989)
Metoprolol	Tronde (2002, 2003a)
Phenylbutazone	Yoshida (1989)
Progesterone	Hartiala (1979)
Propranolol	Tronde (2002, 2003a), Mathias (2002)
Quinine	Yoshida (1989)
Salmeterol	Jeppsson (1994)
Sulphanilamide,	Yoshida (1989), Hemberger (1978)
Talinolol	Tronde (2002, 2003a)
Terbutaline	Ryrfeldt (1989), Tronde (2002)
Testosterone	Hartiala (1979)

2 AIMS OF THE THESIS

The overall aim of the thesis was to systematically investigate the presence and activity of P-gp transporter on drug absorption in the airways using three different *in vitro* biological models. Through the careful design of these comparative experiments it was anticipated that the presence and location and activity of P-gp in the airways of the lung would be identified such that the significance of this transporter on inhaled drug delivery could be determined.

To achieve this aim, the specific objectives were:

- Optimise the cell culture conditions for NHBE cells.
- Investigate the influence of the specific P-gp inhibitor GF120918A on the transport of the P-gp substrate digoxin in NHBE cells.
- Compare the impact of P-gp on digoxin absorption in NHBE, Calu-3 and Caco-2 cells.
- Investigate the influence of time in culture and cell passage on the P-gp activity in the NHBE, Calu-3 and Caco-2 cells.
- Investigate the presence of the P-gp efflux transporter in IPL using immunohistochemistry.
- Study the activity of the P-gp in an IPL model performing transport studies using P-gp substrate digoxin and P-gp inhibitors verapamil and GF120918A.

3 MATERIALS AND METHODS

3.1 Materials

Normal human bronchial epithelial (Clonetics™, 1st passage) (NHBE) cells were obtained from Cambrex Bio Science, Inc. (Walkersville, MD, USA). Calu-3 and Caco-2 cells were purchased from the American Type Cell Culture Collection (ATCC, Rockville, USA). [^{14}C]-mannitol (2.26 GBq mmol^{-1},7.4 MBq.mL^{-1}, radiochemical purity 98.6%) was purchased from Amersham (Amersham, UK), [^{3}H]-digoxin (869.5 GBq mmol^{-1}, 37 MBq.mL^{-1}, radiochemical purity 97.0% from Perkin Elmer (Bucks, UK). GF120918A was a gift from GlaxoSmithKline (Stevenage, UK). Bronchial epithelial cell basal medium (BEBM), hydrocortisone (0.25 mg.mL^{-1}), insulin (2.5 mg.mL^{-1}), transferrin (5 mg.mL^{-1}), epinephrine (0.25 mg.mL^{-1}), triiodothyronine (3.25 mg.mL^{-1}), gentamycin (25 mg.mL^{-1}), amphotericin-B (25 mg.mL^{-1}), retinoic acid (0.05 µg.mL^{-1}), epidermal growth factor (0.25 µg.mL^{-1}; human recombinant), bovine pituitary extract (BPE; > 14 mg.mL^{-1}), 0.1% (w/v) trypsin-0.1% (w/v) EDTA solution were obtained from Cambrex Bio Science, Inc. Dulbecco´s modified Eagle´s medium/nutrient mixture F12 HAM (DME/F12), Dulbecco´s modified Eagle´s medium (DMEM), fetal bovine serum (FBS), glutamine (200 mM), penicillin 100 UI/ml-streptomycin 100 µg/ml solution, MEM non-essential amino acid solution (100 x), 0.02% (w/v) EDTA / 0.25% (w/v) trypsin solution, Hanks balanced buffer solution (HBSS), verapamil, NaCl, KCl, $CaCl_2$, $MgSO_4$, $NaHCO_3$, KH_2PO_4, 4-(2-hydroxyethyl)piperazine-1-ethanesulfonic acid (HEPES), D-glucose, bovine serum albumin (BSA), ≥ 140 USP units.mg^{-1} heparin, phosphate buffer saline (PBS, 0.01 M, pH 7.4), paraformaldehyde, glycerol, isopentane, dimethylsulfoxide (DMSO), ammonium acetate, Triton X-100, trypan blue, isopropanol, glutaraldehyde, sodium cacodylate, osmium tetraoxide, ethanol, Spur resin, uranyl acetate, lead citrate, phenobarbital, polysine microscope slides and acetone were obtained from Sigma - Aldrich (Poole, UK). Tissue culture flasks and twelve-well polyester Transwell® cell culture supports (0.4 µm pore size, 1.13 cm^2) were purchased from Corning Costar (Corning, UK). Ready Protein^{+}® scintillation cocktail was obtained from Beckman Coulter (High Wycombe, UK). F-4 antibody was purchased from Kamiya (Seattle, US); AlexaFluor 568, 4´-6-diamidino-2-phenylindole (DAPI), FM® 1-43 FX was from Invitrogen (Paysley, UK). Antibody C219 was from Calbiochem (UK). Embedding medium (OCT) was from Raymond A Lamb Laboratories (Eastbourne, UK) and anti-goat serum block from Santa Cruz Bio-Tech (Santa-Cruz, US). SDS RM1 (E) maintenance diet was obtained from Special Diets Services Ltd (Essex, UK). Polyethylene tubing PolyE 240, silk black braid suture thread USP, size 4.0 and Micro

Aneurysm clip was from Harvard Apparatus Ltd (Edenbridge, UK), Dieffenbach's bulldog artery clip, Halstead's artery clamp was from Scientific Laboratory Supplies Ltd (Nottingham, UK). Polypropylene fitting was purchased from Cole-Parmer Instrument Co Ltd (London, UK). Microsyringe was obtained from Hamilton (Bonaduz, Switzerland) and semi micro rexaloy clamp from Fisher Scientific (Loughborough, UK). Statistical testing was performed by using SPSS version 11.0 obtained from SPSS Ltd (London, UK).

3.2 Calu-3 cell culture

3.2.1 Cell culture maintenance

Cell stocks were cultured in 162 cm^2 tissue culture flasks using DME/F12 supplemented with 10% (v/v) FBS, 1% glutamine, 1% penicillin, 1% streptomycin and 1% MEM non-essential amino acid solution as the cell culture medium. The cells were maintained in BB16 ell culture incubator (Heraeus Instruments, Hanau, Germany) at 37°C in a humidified atmosphere of 95% air / 5% CO_2. The cell culture medium was changed every 2-3 days. The cells were subcultured once a week (method described below). All processes were carried out using sterile techniques appropriate to cell culture using a class II flow cabinet (Class 2 safety, Howorth Airtech, Hants, UK)..

3.2.2 Subculturing of cells

When cells reached approximately 90% confluency (determined visually), they were washed twice with 10 mL PBS and detached from the culture flask by addition of 5 mL 0.02% (w/v) EDTA / 0.25% (w/v) trypsin solution at 37°C under stirring conditions. The detachment process took up to 20 min during which the cells were visually inspected using an optical microscope (type s, Wilovert, Wetzlar, Germany) to determine the point at which approximately 95% of the cells were released from the walls of the flask. The trypsin was inactivated by addition of 10 mL pre-warmed cell culture media. The cells were harvested from the inactivated trypsin suspension by centrifugation, the supernatant was removed and the cells were resuspended in 6 mL of fresh prewarmed cell culture media. A 2 mL aliquot of the cell suspension was placed into a 162 cm^2 tissue culture flask containing 25 mL of prewarmed cell culture media to maintain the cell stock. A 100 µL sample was withdrawn from the remaining portion of cell suspension and mixed with 100 µL of trypan blue which

stains dead cells blue where live cells remain white. The sample was mixed using a pipette for 2 min and allowed to stand for 10 min before the cell density was counted with a Neubauer hemocytometer. The hemacytometer chambers were evenly filled with the cell suspension using a pipette and left undisturbed for 1 min on the bench allowing the deposition of the cells on the counting plane. The cells were counted in two 1 x 1 x 0.1 mm areas. The cell concentration (c) was calculated according to the Equation 4:

$$c = 2n10^4 \qquad \text{Equation 4}$$

where n represented the average the cell count from both 1 x 1 x 0.1 mm areas. Using calculated cell density, the cell suspension was diluted with fresh cell culture medium to provide the cell concentration desired for further experiments i. e. for seeding Transwell® inserts (method described in subsequent Sections)

3.2.3 Cell freezing

To keep a permanent stock of the cells, the cell lines were kept frozen. When the cells reached full confluency in the 162 cm^2 flasks, they were prepared for cryopreservation. The cell culture media was changed the day before the freezing process. The next day, the cells were detached from tissue culture flask as described in Section 3.2.2. Cells were harvested at a concentration of 3 x 10^6 cells.mL^{-1}. A cryoprotectant 10% (w/v) DMSO was added and the suspension was divided into 1 mL ampoules. The cell suspensions were slowly frozen in a -80°C freezer using a cell freezer container that contained isopropanol. After 24 hours, the ampoules were transferred to storage barrel with liquid nitrogen and stored until required.

3.2.4 Cell revival

The ampoule containing the frozen cell suspension was transferred from the liquid nitrogen and quickly thawed in water bath at 37°C (NE5-28D, Bennett Scientific Ltd. Newton Abbot, UK). The thawing was complete within 1 min. The cells were transferred into 10 mL cell culture media prewarmed to 37°C and washed for 1 min by gentle shaking by hand. The cells were isolated by centrifugation (1500 rpm for 5 min using a Allegra X 22R Centrifuge was from Beckman Coulter Wallac, Finland).and the supernatant containing DMSO was removed. The cells were resuspended in 1 mL of fresh cell culture media and transferred into a 162 cm^2 tissue culture flask containing 25 mL of cell culture media which was prewarmed to 37°C. The

cells were allowed to attach to the walls of the flask overnight and next day the medium was changed to remove non-viable cells floating in the cell culture medium from the flask. The cells were maintained using standard cell culture conditions as described in Section 3.2.1. Prior to their use for transport experiments, the cells were subcultured at least twice in order to restore the cells' metabolism that was affected by freezing.

3.2.5 Transwell culture conditions

For transport experiments, a 500 µL aliquot of a cell suspension (passage 39 and 54, concentration 1.0 x 10^5 cells cm^{-2}) obtained from subculturing the cells (method described in Section 3.2.2) was applied to the apical side of the 12-well polyester Transwell® cell culture supports (0.4 µm pore size, 1.13 cm^2). A 1500 µL aliquot of cell culture medium was applied to the basolateral side of the Transwell® support. The cells were allowed to attach to the Transwells® overnight, the media was removed from the apical compartment and the cell layer which remained attached to the support was cultured under air-liquid interface (ALI) conditions. The cell culture medium on the basolateral side (500 µL) was changed every 2-3 days. Under ALI culture conditions the cell layers became confluent (i.e. formed tight junctions within a few days and this was assessed visually as the time after which the culture medium ceased to permeate up into the apical chamber of the Transwell® under hydrostatic pressure from fluid in the basolateral chamber. The cells were maintained at 37°C in an incubator under 5% CO_2 conditions and used for transport studies at day 14 or 21 post seeding.

3.3 Normal human bronchial epithelial cells

3.3.1 Cell culture maintenance

Frozen passage-1 stocks were defrosted according the suppliers instructions (Clonetics) which involved slowly thawing the cells in a 37°C waterbath. The whole volume of the vial was transferred into a 162 cm^2 tissue culture flask containing NHBE cell culture medium, i.e. BEBM supplemented with hydrocortisone (0.5 $\mu g.mL^{-1}$), insulin (5 $\mu g.mL^{-1}$), transferrin (10 $\mu g.mL^{-1}$), epinephrine (0.5 $\mu g.mL^{-1}$), triiodothyronine (6.5 $\mu g.mL^{-1}$), gentamycin (50 $\mu g.mL^{-1}$), amphotericin-B (50 $\mu g.mL^{-1}$), retinoic acid (0.1 $ng.mL^{-1}$), epidermal growth factor (0.5 $ng.mL^{-1}$) and BPE (35 $mg.mL^{-1}$). The cells were kept at 37°C in a humidified atmosphere of 95% air /

5% CO_2 in an incubator. The cell culture medium was changed every 2 days. The cells were split after 7 days in culture using method described in Section 3.2.2.

3.3.2 Transwell cell culture conditions

When the NHBE cells in culture reached approximately 70% – 80% confluency (day 7), the cells were washed twice with 10 mL PBS and detached from the flask using 5 mL 0.1% (w/v) trypsin-0.1% (w/v) EDTA solution. A 6 mL aliquot of NHBE media was added to inactivate the trypsin and a haemocyanometer was used to check the cell viability and concentration as described in Section 3.2.2. Cells were seeded for permeability experiments on Transwell® inserts at a density of 2.5×10^5 cells.cm^{-2} (Lin *et al.*, 2006) (method described in Section 3.2.5) and were cultured using 2 different growth media: (a) NHBE cell culture medium (described previously) or (b) BEBM:DME/F12 (50:50) with all supplements included in the NHBE medium except for BPE (Lin *et al.*, 2006). After 24 h, the medium on the basolateral side of the cell layer was changed and the medium on the apical side of the cell layer was removed to directly expose the cells to ALI culture conditions. Medium in the basolateral compartment (1500 µL) was changed every other day for 7 days and then every day. The cells were kept at 37°C in a humidified atmosphere of 95% air / 5% CO_2 in an incubator. Cell layers were used for drug transport studies, at day 14 and 21 in culture.

3.4 Caco-2

3.4.1 Flask culture maintenance

Cell stocks were cultured in 162 cm^2 tissue culture flasks in DMEM supplemented with 10% (w/v) FBS, 1% (w/v) glutamine, 1% (w/v) penicillin-streptomycin and 1% (w/v) MEM non-essential amino acid solution (for the purpose of this study defined as Caco-2 cell culture medium). The cells were maintained in an incubator at 37°C in a humidified atmosphere of 95% air / 5% CO_2. Cells were subcultured twice a week following the same protocol described above on Section 2.2.2 for Calu-3 cell line.

3.4.2 Transwell culture

For the Caco-2 transport experiments, the cells (passage 45-56) were seeded at 2.5 x 10^5 cells.cm^{-2} on 12-well polyester Transwell® supports (0.4 μm pore size, 1.13 cm^2). To seed the Transwell®, 500 μL of the cell suspension was added to the apical side of the support and 1500 μL of the Caco-2 cell culture medium added to the basolateral side of the support. After the cells had attached to the Transwells® (usually overnight), the media was changed on both sides of the cell layer and the cells were grown at a liquid-liquid interface (LLI). The Caco-2 cell culture medium on both the apical and basolateral side of the cells was changed every 2-3 days during which they were maintained at 37°C in a humidified atmosphere of 95% air / 5% CO_2 in an incubator. On the day 21 of culture on the Transwell® supports the Caco-2 cells were used for permeation studies.

3.5 Transepithelial electrical resistance measurement

The transepithelial electrical resistance (TER) value of cell layers cultured on Transwell® supports was measured daily (day 1-21) for NHBE during growth on the supports and at the beginning and end of each transport experiment using an EVOM voltohmmeter with silver chopstick electrodes (World Precision Instruments, Stevenage, UK). To enable measurement of TER, warmed medium was added to the apical (0.4 ml) and basolateral (0.9 ml) side of the cell layers, and the cells were left to equilibrate for 10 min in an incubator (37°C, atmosphere of 95% air / 5% CO_2). One electrode was placed in the liquid on the basolateral side of the cells and one in the apical fluid and readings were taken in triplicate (one measurement from three different positions in both chambers). TER was calculated by subtracting the background resistance due to the blank Transwell® insert and medium using Equation 5:

$$R_{cells} = (R_{cells} + R_{filter}) - R_{filter} \qquad \text{Equation 5}$$

where R_{cells} represents the resistance of the cells and R_{filter} was the resistance of the filter. Due to the dependency of the resistance upon the area, TER values were corrected for the support surface area to obtain a value that was independent of the support employed. Cells layers of Calu-3, Caco-2 and NHBE with appropriate TER i.e. higher than 300 Ω.cm^2 were used for permeability studies.

3.6 Scanning electron microscopy

The NHBE cells (passage 2) were cultured for 7 days on Transwell® filter inserts and then fixed by immersion in a 50:50 cell culture medium: 2.5% (w/v) glutaraldehyde, 0.1 M sodium cacodylate buffer at pH 7.2. After 10 min the immersion solution was aspired to waste and the cells were re-suspended in a 2.5% (w/v) glutaraldehyde mixed with 0.1 M sodium cacodylate buffer pH 7.2 for two hours. The glutaraldehyde solution was removed and the cells were washed with PBS and stored at room temperature prior to imaging.

Immediately prior to taking the scanning electron microscopy (SEM) images of the cell layer they were washed three times in 2.5% glutaraldehyde, 0.1 M sodium cacodylate buffer, pH 7.2. The cells were incubated in the washing solution for 10 min intervals during each wash. After washing the cells were incubated in an aqueous solution of 1% (w/v) osmium tetroxide for 90 minutes and then the cells were washed twice with Milli-Q water, again immersing the cells for a period of 10 min during both washes. The cells were subjected to a series of ethanol/water washes, which contained increasing levels of ethanol from 30%, 50%, 70%, 90%, to 100% (v/v). The cells were submerged in the ethanol co-solvent solutions for 15 minutes each. The cell layers were incubated in a pure ethanol solution overnight. After the last ethanol wash, the Transwell® inserts were removed and transferred to ethanol solution in critical point drying holders. The Transwell® inserts containing the cell layers were dried out using carbon dioxide in a E3000 critical point dryer (Polaron, Ringmer, UK).and the inserts were removed from the holders and mounted on stubs with adhesive carbon pads. The inserts were sputter coated with gold in E5100 sputter coater (Polaron, Ringmer, UK). The samples were examined using a Philips SEM501B SEM operated at 15 kV and images recorded with Deben Pixie 3000 digital scan generator and imaging system.

3.7 Transmission electron microscopy

The cells were fixed onto Transwell® filter inserts using glutaraldehyde as described in Section 3.6. The inserts were separated from their polystyrene holders and 2 mm^2 stripes were removed from the inserts. The cells were subjected to a series of acetone/water washes increasing in acetone content from 30%, 50%, 70%, 95%, to 100% (v/v). During each wash the cells were held in the solution for 15 min. The cell layers were then submersed in a pure ethanol solution overnight. Following day the cells samples were subjected to a second series

of washes using an acetone:Spurr resin solution again the cells were submerged for 15 min in washes with an increasing rates of Spurr resin ranging from 3:1, 1:1, 1:3 (v/v). The cells were then treated with Spurr resin for two 24 hr periods and embedded in the resin by heating at 60°C for 24 h. Ultrathin transverse sections of the embedded cells were cut using a OMU4 ultracut ultramicrotome (Reichart Ltd which is now part of Leica Microsystems, Milton Keynes, UK). These sections were stained in uranyl acetate and lead citrate. The samples were imaged using a 100CX transmission electron microscope (JEOL, Herts, UK)..

3.8 P-glycoprotein cell culture transport studies

Drug transport studies were performed using a methodology similar to that reported by Manford *et al.*, 2005. The passage of a drug was measured in both the A-B and the B-A directions. Studies were performed under stirring conditions at 37°C in a humidified atmosphere of 95% air / 5% CO_2 in an incubator. Prior to initiation of the transport experiment, the cell layers were washed with HBSS by adding 500 µL / 1500 µL of HBSS to the apical / basolateral side of the cells respectively. During the washing process, the TER of each cell layer was measured after 30 min equilibration in HBSS at 37°C in an incubator (method described in Section 3.5). The HBSS was aspirated to waste from both chambers after the measurement of TER was complete and 510 µL or 1510 µL of the test solution was added to the apical (for A-B transport) or basolateral (for B-A transport) sides of the cells, respectively. This was defined as the donor solution. In a similar manner 1500 µL or 500 µL of fresh pre-warmed HBSS containing 0.1% (w/v) BSA was added either to the basolateral or apical side of the cells as appropriate. This was defined as the receiver solution. Immediately after the initiation of the measurement, 10 µL of test solution was removed from the donor solution of each well to assay the initial donor concentration (C_0). After 30, 60, 90 and 120 min, 500 µL (A-B transport) or 100 µL (B-A transport) samples were removed from each receiver solution and this volume was replaced immediately with pre-warmed HBSS containing 0.1% (w/v) BSA to maintain the constant volume. At the final experimental time point (120 min) a 10 µL sample was removed from each donor solution to assess the final donor concentration. In order to confirm the integrity of the cell layers during the experiment, the TER of each cell layer was measured after study completion again using the method described in Section 3.5. Each transport experiment was repeated using 6-12 cell layers.

[^{3}H]-digoxin was used as a model drug and the test solutions were prepared by diluting the concentrated solution as received from manufacturer with HBSS supplemented with 0.1% (w/v) BSA to provide a final concentration of 5.0 nM (unless otherwise stated). The non-

specific P-gp inhibitor verapamil was used at a concentration of 100 μM in HBSS (unless otherwise stated) and the specific inhibitor GF120918A was used at a 2.0 μM in HBSS (unless otherwise stated). To aid the solubility of the GF120918A, the test solution contained 1% (v/v) DMSO. [^{14}C]-mannitol was used as a marker of paracellular transport at a concentration of 8.9 μM in HBSS. Transport experiments were performed in the A-B and B-A directions in presence or absence of P-gp inhibitors using Calu-3, Caco-2 and NHBE cells. For inhibition studies, verapamil and GF120918A were added to both donor and acceptor solutions to ensure a continuous inhibition of the P-gp efflux pump irrespective of its localisation on the cell surface.

To quantify the digoxin samples from both donor and receiver solutions containing digoxin were placed in 5 ml polypropylene vials and 5 ml of Ready Protein$^{+®}$ scintillant was added to each sample. The digoxin content was assayed by liquid scintillation counting using a 1209 Rackbeta dual scintillation counter (Beckman Coulter, UK) as counts per minute (CPM). The apparent permeability coefficient (P_{app}) was calculated according the Equation 6:

$$P_{app} = \frac{dQ/dt}{AC_0} \qquad \text{Equation 6}$$

where dQ/dt (mol s^{-1}) represents the increase of drug in the receiver solution per time interval (s), A (cm^2) was the surface area of the filter supporting the cell layer and C_0 (mol cm^{-3}) was the initial drug concentration in the donor solution. Normal confluent cell should display a paracellular mannitol permeability of < 1.0 x 10^{-6} $cm.s^{-1}$ (Forbes and Ehrhardt, 2005). Cell layers with $P_{app\ mannitol}$ > 1.0 x 10^{-6} $cm.s^{-1}$ were excluded from calculations due to insufficient barrier properties. Efflux was defined as a ratio of the permeability coefficient in the B-A direction divided by the permeability coefficient from the A-B direction and calculated according the Equation 7.

$$Efflux = \frac{P_{app}(B-A)}{P_{app}(A-B)} \qquad \text{Equation 7}$$

Recovery of the drug from the transport experiments was calculated by summation of the total amounts of drug in the apical and basolateral chambers and dividing by the amount of drug added in the original donor solution, according Equation 8:

$$MassBalance = \frac{C_c}{C_0} x100\% \qquad \text{Equation 8}$$

where C_0 is the quantity of drug applied into apical chamber and C_c is calculated cumulative concentration of the drug in basolateral chamber at the final time point of the permeation experiment. All the data are expressed as mean ± standard deviation (SD). Statistical testing was performed by using SPSS version 11.0 software and data were analysed by Student's t test, with the significance set at $p < 0.05$.

3.9 Isolated perfused rat lung

3.9.1 Animals

Male Wistar rats, weighing approximately 300 g, were obtained from Harlan UK Ltd (Oxon, Oxfordshire). They were fed with a SDS RM1(E) maintenance diet and housed at 21°C, 45%-60% humidity with a 12 hour light/dark cycle. The surgical protocol was established under the UK Schedule 1 Programme (Animal Licence exempt).

3.9.2 Surgical protocol

The rats were injected with a lethal dose of pentobarbital (130 $mg.kg^{-1}$ body weight) and as soon as they were unconscious, they were placed and secured in a supine position on a board inclined at approximately 45°. A midline incision was made from the neck of the animal to its abdomen using a scalpel blade. The viscera were pulled out from the abdominal cavity and rats were exsanguinated by severing the main abdominal vessels. The trachea was exposed and carefully pierced through one wall with a 21G needle. A 3 cm long cannula made of a polyethylene tubing mounted on a blunt 21G needle was introduced into the trachea. This was securely tied with two suture threads and a 25 mm Dieffenbach's bulldog artery clip. The diaphragm was cut open and the rib cage laterally incised with scissors taking care not to damage the lung tissue. After the thymus was removed, the heart was slightly twisted in order to expose the pulmonary artery and then stretched down using a Halstead's artery clamp. A vertical incision was made though both atria and the pulmonary artery was cannulated using an identical method to the intratracheal cannula. Just 2 or 3 mm of the cannula was introduced into the vessel. This was secured with a Micro Aneurysm clip and the perfusion was initiated. The perfusion system consisted in reservoir of the solution and peristaltic pump connected to the intravascular cannulae by silicone tubing and a polypropylene fitting. The perfusion

solution was a modified Krebs-Ringer buffer (NaCl 118 mM, KCl 4.7 mM, $CaCl_2$ 2.5 mM, $MgSO_4$ 1.2 mM, $NaHCO_3$ 24.9 mM, KH_2PO_4 1.2 mM, HEPES 10 mM, D-glucose 11 mM, 4.5% (w/v) BSA and heparin 35 $kU.mL^{-1}$) at pH 7.4 (Tronde *et al.*, 2002). The solution was oxygenated by constant bubbling of a 5 % CO_2 95% O_2 gas mixture and kept at 37°C by partial immersion of the perfusate reservoir in a water bath. The rate of perfusion was 8 $mL.min^{-1}$. The lungs were manually ventilated with 2 ml air using a 10 ml syringe connected to the intratracheal cannulae by silicone tubing. Once the tissue had blanched, the pericardium was dissected free and the inflated lungs were carefully removed from the chest cavity whilst maintaining the perfusion. The air-filled lungs were vertically suspended above a funnel using a semi micro rexaloy clamp and kept on the bench at 21°C.

3.9.3 Immunohistochemical localization of P-glycoprotein in rat lung tissue

Rats were injected with a lethal dose of pentobarbital (130 $mg.kg^{-1}$ body weight). Surgery was performed in Section 3.9.2. After tracheotomy, the pulmonary artery was cannulated, and prewarmed PBS was infused into the left ventricle to flush the blood out of the lungs. When the tissue was blanched, the lungs were carefully cut away from the chest cavity, the connective tissue removed and the lungs were rinsed with PBS to wash out the surface blood. To expand the lungs and maintain cell integrity during freezing, approximately 10 mL of 25% embedding medium was injected into the tracheal cannula. Lungs were immersed in ice-cold isopentane for 3 min. Tissue was stored at -80°C until use.

The frozen lung was removed from the storage, cut in small blocks and placed in embedding medium. The frozen blocks were cut into 10 µm slices using cryostat at -20°C. The lung sections were placed on polysine microscope slides and stored at -80°C. Slides were fixed with acetone for 10 min on the bench, washed with PBS and placed in a moist container to prevent the samples drying out. The excess moisture was removed from the slide, taking care not to dry out the sample. The tissue was exposed to 0.1% (v/v) Triton X 100 with 0.5% (v/v) FBS in PBS for 60 min at 37°C in order to increase the permeability of the cell membrane. After subsequent washing with 10 mL PBS, 50 mM ammonium acetate in PBS was added to the tissue for 10 min. To inhibit any non-specific binding of the antibody, the sections were exposed to anti-goat serum block for 30 min at room temperature. After washing with PBS the samples were incubated with mouse monoclonal P-gp antibody C219 (10 $\mu g.mL^{-1}$; 60 min) that recognizes an internal, highly conserved amino acid sequence: VQEALD and VQAALD, corresponding to the C-terminal and N-terminal regions, respectively, found in both MDR1 and MDR3 isoforms of P-gp. Slides were washed with PBS and exposed to a red-fluorescent

goat anti–mouse IgG antibody AlexaFluor 568 (10 $\mu g.mL^{-1}$; 60 min) that react with the Fc portion of the heavy chain of mouse IgG2a. The tissue cell nuclei were stained with 1 $mg.mL^{-1}$ 4′-6-diamidino-2-phenylindole (DAPI) in PBS for 10 min, and washed with 10 mL PBS. Finally, samples were coated with glycerol 10% (w/v), sealed with a cover slip and viewed using Leica DMIR E2 confocal microscope (Leica Microsystems, Milton Keynes, UK).

3.9.4 Transport experiments

[^{3}H]-digoxin and [^{14}C]-mannitol were diluted to a concentration of 45.8 nM and 65.6 μM in HBSS respectively. The non-specific P-gp inhibitor verapamil was used at 100 μM either in the perfusion solution or co-admistered with [^{3}H]-digoxin. The specific P-gp inhibitor GF120918A was used at a concentration of 2.0 μM in HBSS containing 1% (v/v) DMSO and it was co-administered with [^{3}H]-digoxin. Due to limited availability of GF120918A, the inhibitor was not used in the perfusion solution.

After isolation, the lung preparation was allowed to stabilise for 2-3 min. The lungs were deflated and the test compound was instilled into the IPL airways through the tracheal cannula using a calibrated 100 μL microsyringe. The solution was applied 3 mm above the trachea bifurcation over a period of 1-2 s. The lungs were re-inflated with approximately 0.5 ml of air using 10 mL syringe connected to the tracheal cannula. Air volume in lung and the perfusion flow was kept constant during the experiment was not influenced by the drug administration. The perfusion buffer collected from the left atrium was sampled (0.5 mL) at predetermined time intervals for 90 min. The tissue viability was verified by visual inspection for signs of oedema, the ratio of dry vs wet weight after 90 min and the transfer profile of mannitol from airways to perfusate.

The concentration of transported agents in perfusate was assayed by liquid scintillation counting using a 1209 dual scintillation counter after dilution in 5 mL of Ready Protein$^{+®}$ scintillant as CPM. Each transport experiment was carried out on at least 4 IPL preparations. The cumulative amount of the test compounds transported from the airways to the perfusate in 90 min was calculated as a mass-fraction of the given dose recovered in the perfusate (Tronde *et al.*, 2002). The absorption half-life ($t_{1/2}$, min) was calculated as the time needed for transfer of 50% of the amount of digoxin and mannitol recovered in the perfusate after 90 min (Tronde *et al.*, 2002). The apparent absorption rate constant (ka) was calculated according to the Equation 9.

$$ka = \frac{\ln 2}{t_{1/2}}$$ Equation 9

All the data are expressed as mean ± SD. Statistical testing was performed by using SPSS version 11.0 software and data were analysed by Student's *t* test, with the significance set at $p < 0.05$. The IPL preparations showing any signs of oedema during the experiment (determined visually) were excluded from calculation due to impaired viability.

4 RESULTS

4.1 Normal human bronchial epithelial cell growth condition optimisation

4.1.1 Morphology of normal human bronchial epithelial cells cultured on Transwells

NHBE cells (passage 1) cultured in a cell culture flask with NHBE cell culture medium showed epithelium like morphology (Figure 9). These cells were subcultured (passage 2) and seeded on Transwell® supports in BEBM:DME/F12 (50:50) and the cell layer appeared to be confluent (determined visually) 14 days after seeding (Figure 10A). In contrast, using the NHBE medium to culture the cells on the Transwell® supports impaired growth of the cells and a confluent layer was not formed even after 14 days in culture (Figure 10B). These data are consistent with SEM, TEM and TER measurements.

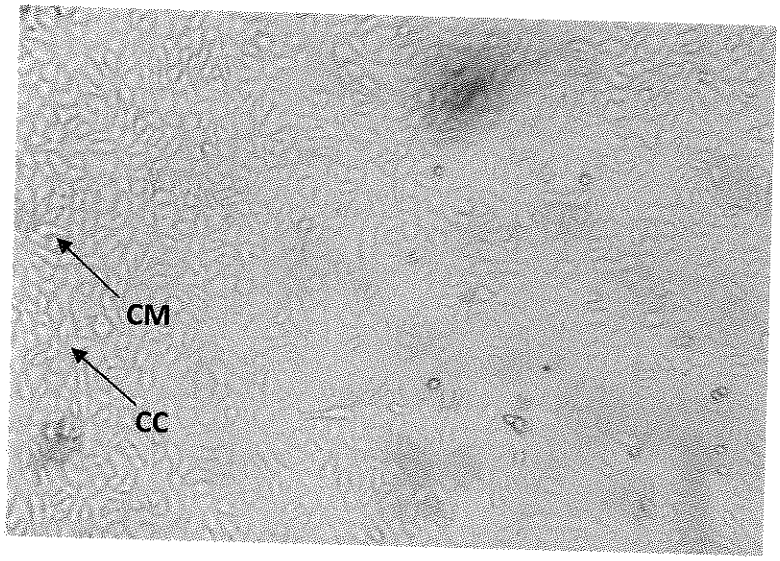

***Figure 9**: Morphology of normal human bronchial epithelial (NHBE) cells observed using a light microscopy (100 x). Cells of passage 1 in a cell culture flask. CM = cell membrane, CC = cell cytoplasm.*

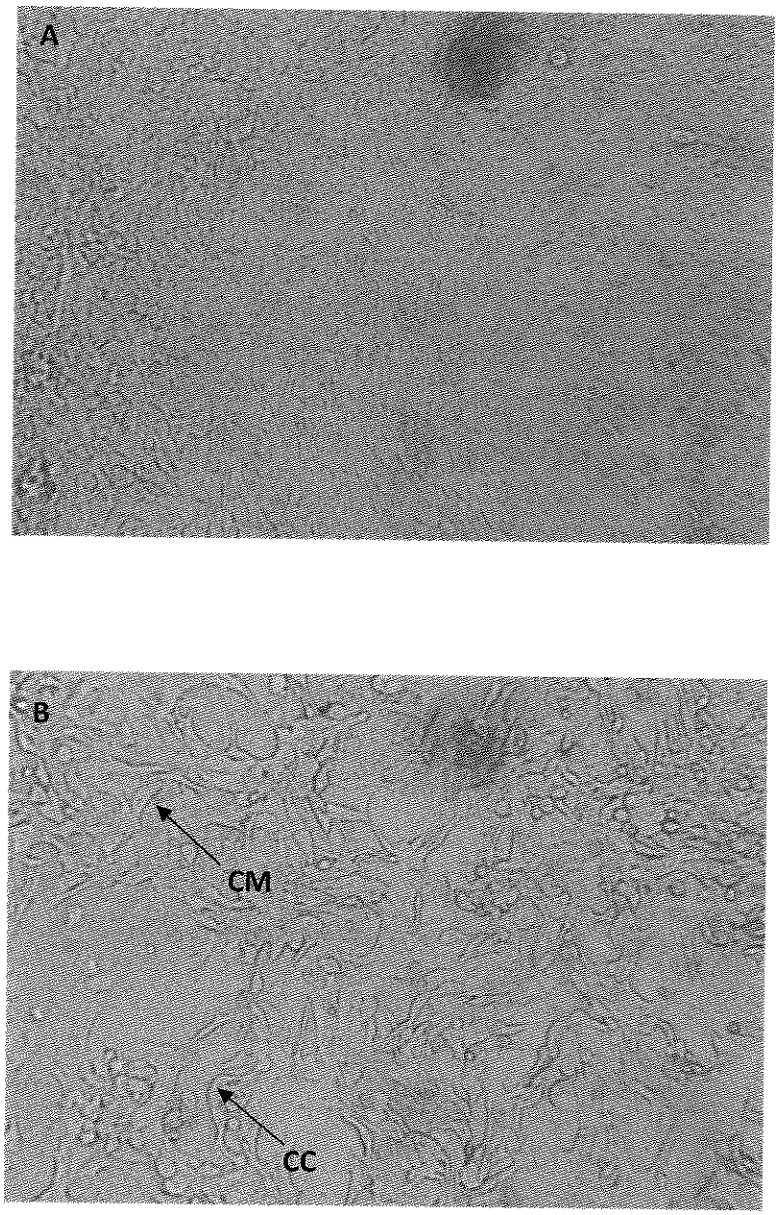

***Figure 10**: Morphology of normal human bronchial epithelial (NHBE) cells observed using a light microscope (100 x). Cell layer of passage 2 cells after 14 days post seeding on Transwell® support grown using either (A) bronchial epithelial cell basal medium (BEBM): Dulbecco's modified Eagle's medium/nutrient mixture F12 HAM (DME/F12) (50:50) medium(B), or (B) NHBE cell culture medium. CM = cell membrane, CC = cell cytoplasm.*

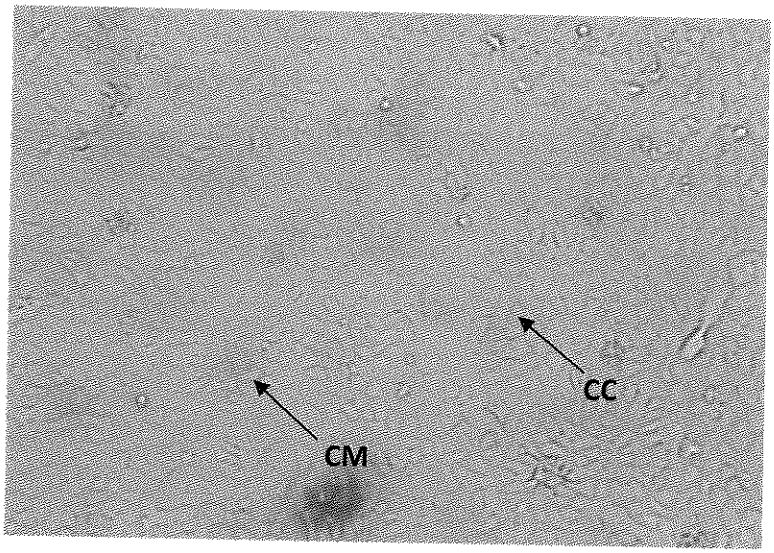

***Figure 11**: Morphology of normal human bronchial epithelial (NHBE) cells observed using a light microscope (100 x). Cells of passage 3 in a cell culture flask. CM = cell membrane, CC = cell cytoplasm*

NHBE cells of passage 2 cultured in a cell culture flask using NHBE cell culture media reached confluency (determined visually) on day 7 in culture (Figure 11). However, were subcultured (passage 3) and seeded on Transwell® supports in a similar manner to cells of passage 2, they did not exhibit a confluency irrespective of the growth media employed (Figure 12A, 12B).

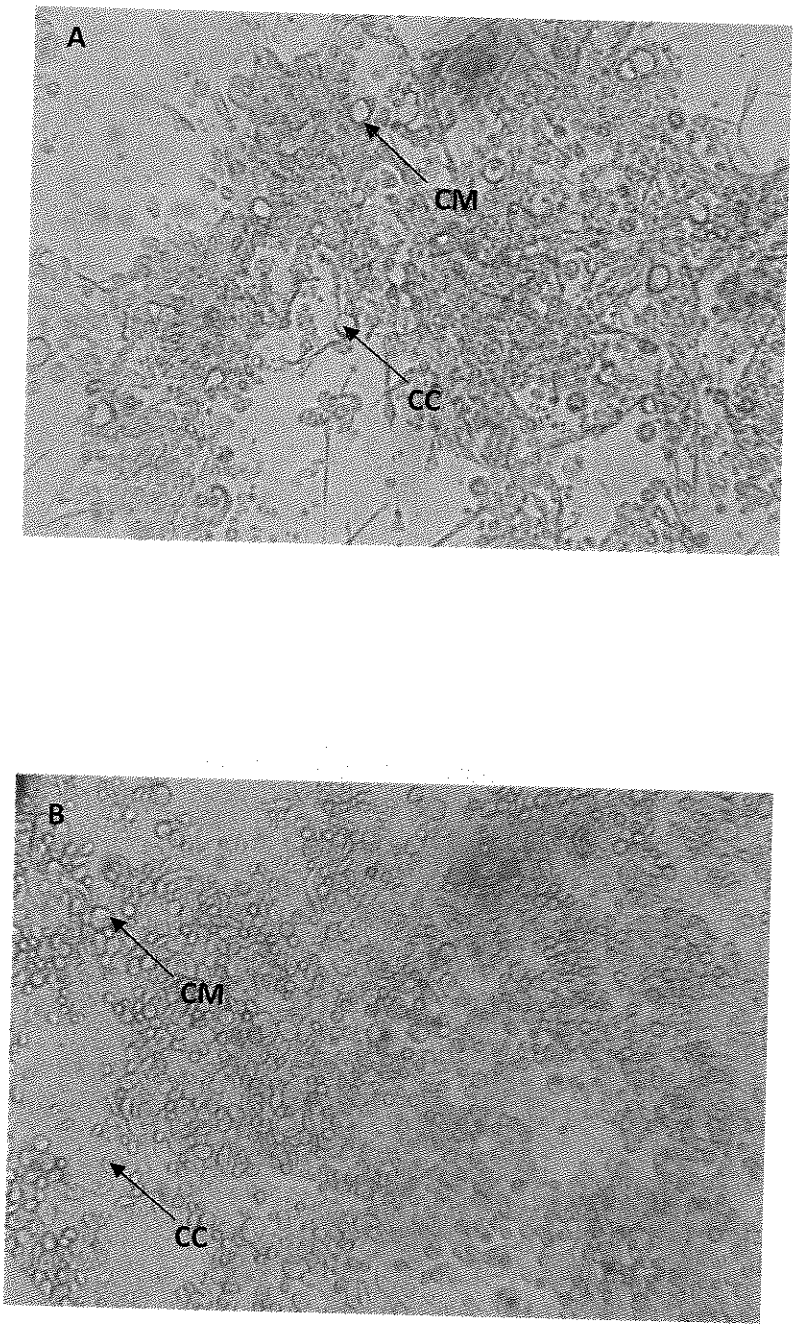

***Figure 12**: Morphology of normal human bronchial epithelial (NHBE) cells observed using a light microscope (100 x). Cell layer of passage 3 cells after 14 days post seeding on Transwell® support grown using either (A) bronchial epithelial cell basal medium (BEBM): Dulbecco's modified Eagle's medium/nutrient mixture F12 HAM (DME/F12) (50:50) medium(B), or (B) NHBE cell culture medium. CM = cell membrane, CC = cell cytoplasm.*

4.1.2 Scanning and transmission electron microscopy

SEM revealed that NHBE (passage 2) formed a confluent cell layer when cultured using serum free BEBM:DME/F12 (50:50) medium on day 7 in culture (Figure 13). Conversly, the confluency of the cells grown using NHBE cell culture medium was impaired (Figure 13). Cells grown using either condition viewed by TEM were shown to exist as a multilayer of 4-6 cell layers with clear evidence of desmosomes (Figures 15 and 16). Rare apical projections (microvilli) were also observed when the cells were imaged using TEM. The microvilli were more pronounced in preparations grown using BEBM:DME/F12 (50:50) (Figure 16) than those grown using NHBE cell culture medium (Figure 15). Individual cells and cell-to-cell boundaries were seen clearly under both conditions. Desmosomes were observed using both NHBE cell culture medium and BEBM:DME/F12 (50:50), but the formation of tight junctions was observed only using BEBM:DME/F12 (50:50).

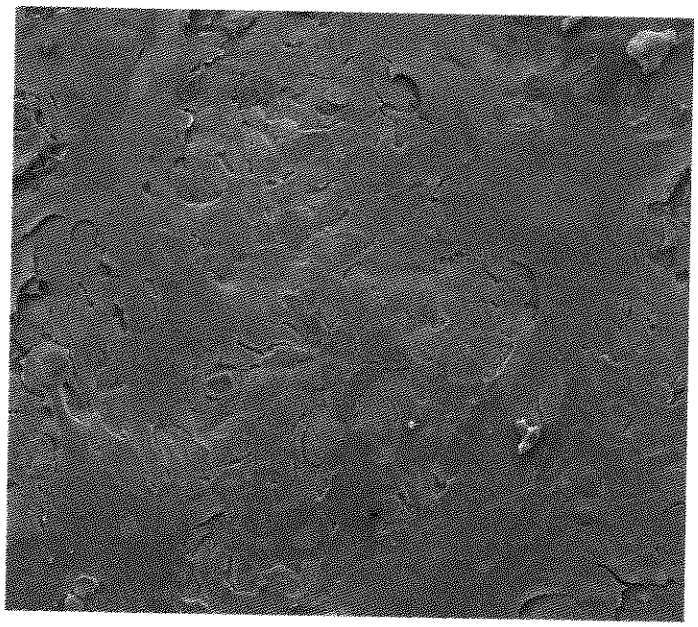

***Figure 13**: Scanning electron microscopy (SEM) of normal human bronchial epithelial (NHBE) cells (passage 2) cultured using bronchial epithelial cell basal medium (BEBM): Dulbecco's modified Eagle's medium/nutrient mixture F12 HAM (DME/F12) after 7 days in culture.*

***Figure 14**: Scanning electron microscopy (SEM) image of normal human bronchial epithelial (NHBE, passage 2) cells cultured using NHBE cell culture medium after 7 days in culture.*

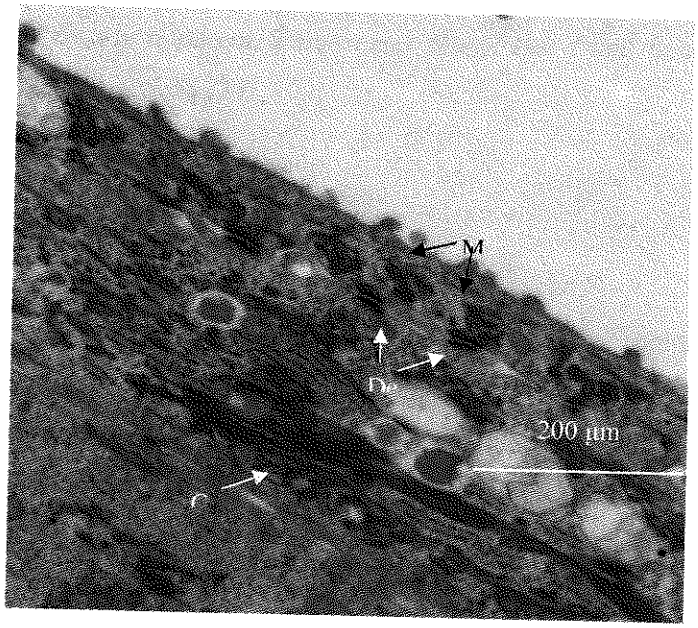

***Figure 15**: Transmission electron microscopy (TEM) image of normal human bronchial epithelial (NHBE) cells cultured using NHBE cell culture medium after days 7 in culture with clearly apparent desmosomes (Des), cell - cell boundaries (CB) and thick microvilli (MV).*

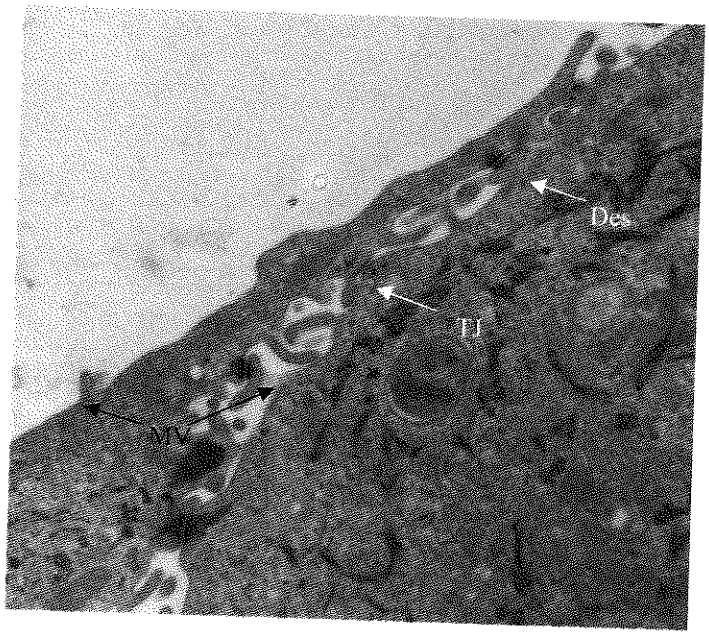

***Figure 16**: Transmission electron microscopy (TEM) image of normal human bronchial epithelial (NHBE) cells cultured (passage 2) using bronchial epithelial cell basal medium (BEBM): Dulbecco's modified Eagle's medium/nutrient mixture F12 HAM (DME/F12) after 7 days in culture with clearly apparent desmosomes (Des), cell - cell boundaries (CB), thick microvilli (MV) and tight junctions (TJ).*

4.1.3 Transepithelial electrical resistance

NHBE cells of passage 2 cultured in a 162 cm^2 flask using NHBE cell culture medium reached confluency on day 7 in culture (determined visually). When these cells were seeded on to Transwell® supports and grown using either NHBE cell culture medium or BEBM:DME/F12 (50:50) they exhibited a measurable TER from day 3 in culture (Figure 17). On day 3 the TER of cells cultured under both conditions from passage 2 were not significantly different ($p > 0.05$, NHBE cell culture medium and BEBM:DME/F12 (50:50) 74 ± 14 $\Omega.cm^2$ and 73 ± 13 $\Omega.cm^2$, respectively). The TER of passage 2 cells grown using BEBM/DME F12 (50:50) reached a maximum (1117 ± 293 $\Omega.cm^2$) on day 21 after seeding whereas those cells grown using NHBE cell culture did not change significantly ($p > 0.05$) during the course of the experiment. These data are consistent with results from SEM, TEM and optical microscopy.

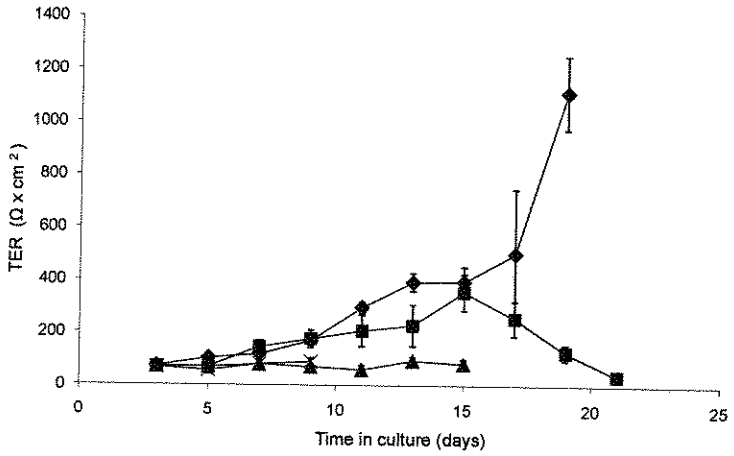

***Figure 17**: Transepithelial electrical resistance (TER) of normal human bronchial epithelial (NHBE) cell layers grown on Transwell® supports as a function of days in culture. Cells (passage 2 and 3) were cultured in either NHBE cell culture medium or a mixture of bronchial epithelial cell basal medium (BEBM): Dulbecco's modified Eagle's medium/nutrient mixture F12 HAM (DME/F12) (50:50). ♦ BEBM:DME/F12 (50:50), passage 2; ■ BEBM:DME/F12 (50:50), passage 3; ▲ NHBE cell culture medium, passage 2; x NHBE cell culture medium, passage 3. Data represent mean ± SD (n=12).*

NHBE cells of passage 3 cultured in a 162 cm^2 flask in NHBE cell culture medium also reached confluency on day 7 in culture (determined visually). In a similar manner to cells from passage 2, when seeded on to Transwell® supports they exhibited a measurable TER from day 3 in culture, irrespective of the growth media employed (Figure 17). Again on day 3 the TER of the passage 3 cells cultured under either condition were not significantly different ($p > 0.05$, NHBE cell culture medium and BEBM:DME/F12 (50:50) 74 ± 14 $\Omega.cm^2$ and 71 ± 12 $\Omega.cm^2$, respectively) and these values were not significantly different to passage 2 cells ($p > 0.05$). The TER of passage 3 cells grown using BEBM/DME F12 (50:50) reached a maximum (355 ± 68 $\Omega.cm^2$) on day 15 after seeding whereas those cells grown using NHBE cell culture did not change significantly ($p > 0.05$) during the course of the experiment (for these cells the culture was terminated after day 9). This data is also consistent with results from SEM, TEM and optical microscopy.

4.2 Cell culture transport studies method development

4.2.1 Digoxin dose ranging studies

In order to determine the influence of the digoxin concentration on the transport of this drug across the cell barrier, a set of transport experiments with Calu-3 cells (passage 40, day 21 in culture) was performed using 4 different digoxin concentrations (5.0 – 5.0 x 10^3 nM). The transport of the lowest digoxin concentration (0.005 μM) was linear both in A-B and B-A directions (R^2_{A-B} = 0.9998; R^2_{B-A} = 0.9996) (Figure 18). Cumulative digoxin concentration at 120 min of the experiment was significantly higher ($p < 0.05$) in A-B direction (1.80 ± 0.30 x 10^{-14} M) than in B-A direction (7.20 ± 0.14 x 10^{-14} M).

The transport when 50 nM digoxin was applied was also linear both in A-B and B-A directions (R^2_{A-B} = 0.9974; R^2_{B-A} = 0.9998) over the 120 min experiment (Figure 19). The cumulative digoxin concentration at 120 min was 1.70 ± 0.12 x 10^{-14} M in A-B direction e. g. significantly higher ($p < 0.05$) than in B-A direction (7.51 ± 0.76 x 10^{-14} M).

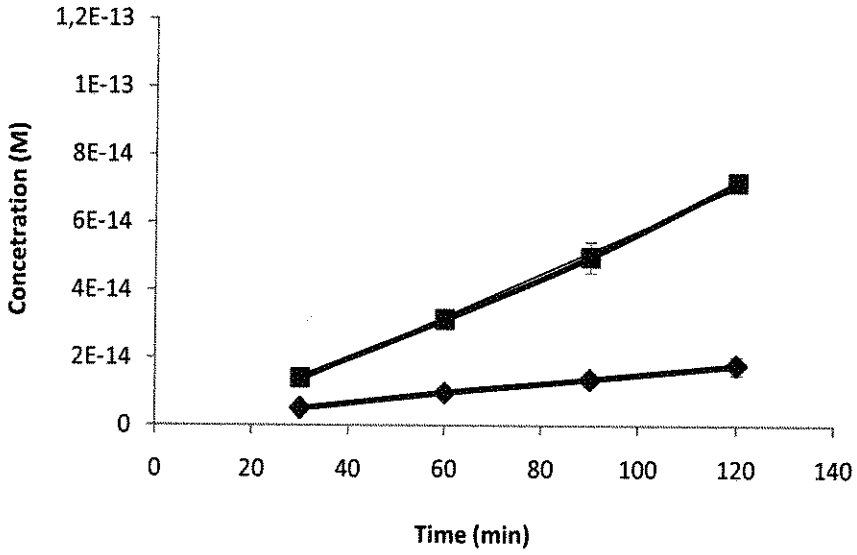

***Figure 18**: Cumulative concentration of digoxin (5 nM) in the apical to basolateral (♦) and basolateral to apical (■) direction across Calu-3 cells (passage 40, day 21 in culture). Data represent mean ± SD (n ≥ 3).*

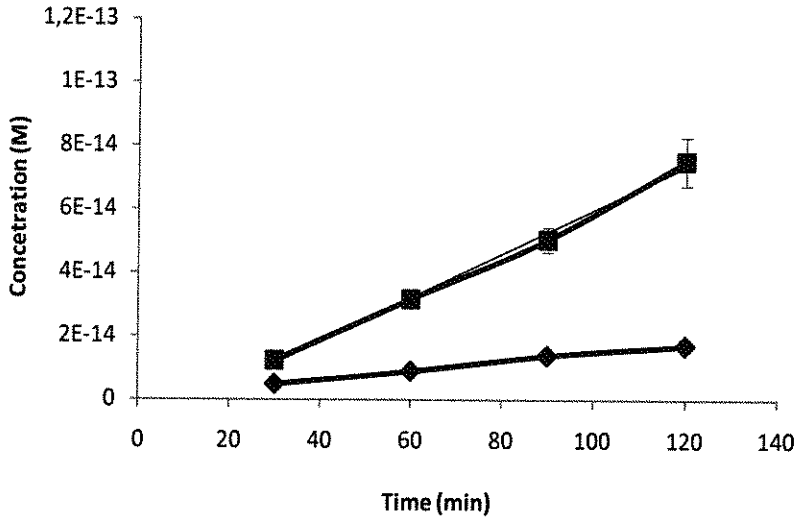

***Figure 19**: Cumulative concentration of digoxin (50 nM) in the apical to basolateral (♦) and basolateral to apical (■) direction across Calu-3 cells (passage 40, day 21 in culture). Data represent mean ± SD (n ≥ 3)*

The transport of 500 nM digoxin was linear both in A-B and B-A directions ($R^2_{A-B} = 0.9564$; $R^2_{B-A} = 0.9997$) (Figure 20). Cumulative digoxin concentration at 120 min was 5.6 times less in the in A-B direction ($1.42 \pm 0.05 \times 10^{-14}$ M) compared to the in B-A direction ($7.94 \pm 0.15 \times 10^{-14}$ M).

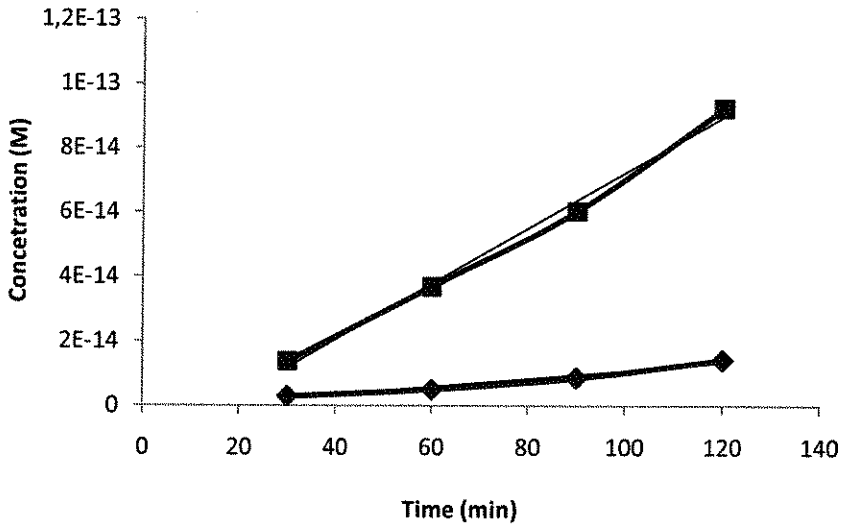

***Figure 20**: Cumulative concentration of digoxin (500 nM) in the apical to basolateral (♦) and basolateral to apical (■) direction across Calu-3 cells (passage 40, day 21 in culture). Data represent mean ± SD (n ≥ 3).*

In similar manner to the three lower concentration, the transport of 5000 nM digoxin both in A-B and B-A directions was again linear ($R^2_{A-B} = 0.9183$; $R^2_{B-A} = 0.9997$) (Figure 21). Cumulative digoxin concentration at 120 min of the experiment was statistically different ($p < 0.05$) to the 50 nM digoxin transport rates ($2.12 \pm 0.01 \times 10^{-14}$ M in A-B direction and $9.23 \pm 1.34 \times 10^{-14}$ M in B-A direction).

Recovery of digoxin ranged from 91 ± 5 % to 108 ± 6 % across all the experiments. The cell layers was shown to remain intact as no decrease in TER was detected during any of the transport experiments (TER of the start of experiment 397 ± 14 $\Omega.cm^2$, end 487 ± 13 $\Omega.cm^2$). The mannitol transport (P_{app}) ranged from $0.59 \pm 0.05 \times 10^{-6}$ $cm.s^{-1}$ to $0.72 \pm 0.07 \times 10^{-6}$ $cm.s^{-1}$ and hence the cell lines did provide a significant barrier. The cumulative transport of digoxin was significantly higher in the B-A than A-B direction ($p < 0.05$) at all used drug concentrations and as efflux was observed at all concentrations used, the lowest digoxin concentration (5 nM) was used in all subsequent transport experiments (Table 4).

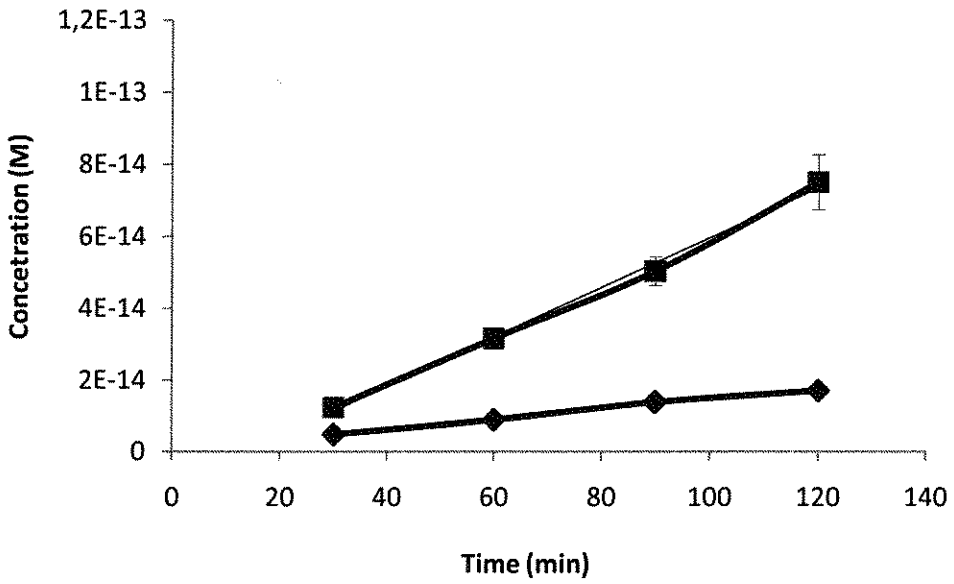

***Figure 21**: Cumulative concentration of digoxin (5000 nM) in the apical to basolateral (♦) and basolateral to apical (■) direction across Calu-3 cells (passage 40, day 21 in culture). Data represent mean ± SD ($n \geq 3$).*

***Table 6**: Summary of digoxin transport across the Calu-3 cells (passage 40, day 21 in culture). Set of transport experiments with Calu-3 cells was performed using 4 different digoxin concentrations (5.0 – 5.0 x 10^3 nM). R^2 is linearity of the transport, c_{120} (M) is cumulative digoxin concentration at 120 min and P_{app} ($cm.s^{-1}$) is digoxin apparent permeability. Data represent mean ± SD ($n \geq 3$).*

Digoxin (nM)	A - B			B - A			Efflux ratio
	R^2	C_{120} (x 10^{-14} M)	P_{app} (x 10^{-6} cm.s^{-1})	R^2	c_{120} (x 10^{-14} M)	P_{app} (x 10^{-6} cm.s^{-1})	
5	0.9998	1.80 ± 0.30	0.49 ± 0.05	0.9996	7.20 ± 0.14	1.90 ± 0.01	3.86
50	0.9974	1.70 ± 0.12	0.49 ± 0.02	0.9998	7.51 ± 0.76	2.16 ± 0.28	5.33
500	0.9564	1.42 ± 0.05	0.37 ± 0.10	0.9997	7.94 ± 0.15	2.20 ± 0.17	5.98
5000	0.9183	2.12 ± 0.01	0.44 ± 0.02	0.9997	9.23 ± 1.34	2.12 ± 0.18	4.81

4.2.2 Inhibitor dose ranging studies

In order to optimise the concentration of the P-gp inhibitors, the effect of verapamil and GF120918A on digoxin transport across Caco-2 cell layers (passage 45-56, 21 days post-seeding), which are known to over-express P-gp was assessed. In the absence of verapamil, the P_{app} of digoxin was 0.17 ± 0.02 $cm.s^{-1}$ in A-B direction (Figure 22) and this was significantly lower ($p < 0.05$) than the B-A direction (P_{app} B-A 5.52 ± 0.24 $cm.s^{-1}$). In the presence of verapamil, the A-B transport of digoxin was significantly higher ($p < 0.05$, P_{app} = 2.17 ± 0.12 $cm.s^{-1}$) compared to when the inhibitor was absent. The addition, the P-gp inhibitor verapamil significantly ($p < 0.05$) decreased B-A transport rate to a make it similar to the rate of the A-B route i.e. a P_{app} of 2.68 ± 0.55 $cm.s^{-1}$. The integrity of the cell layers was not disrupted by the addition of verapamil as no decrease in TER was detected during the experiment (start 1022 ± 48 $\Omega.cm^2$, end 1014 ± 46 $\Omega.cm^2$). Likewise, the mannitol transport ranged from 0.16 ± 0.09 x 10^{-6} $cm.s^{-1}$ to 0.88 ± 0.67 x 10^{-6} $cm.s^{-1}$ which showed a significant barrier was maintained during the experiment.

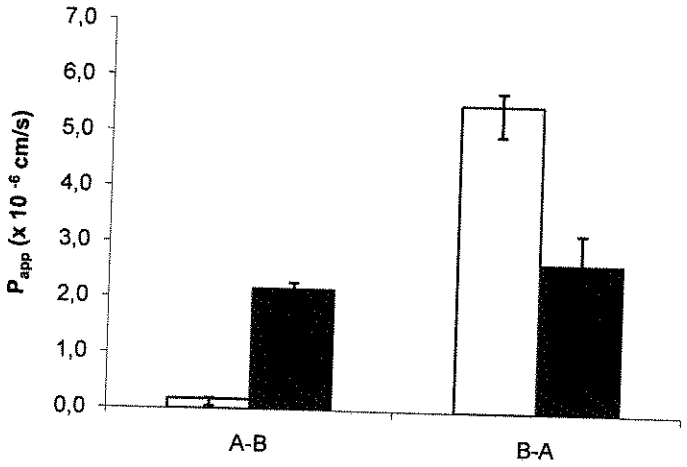

Figure 22: *Apparent permeability coefficient (P_{app}) of [^{3}H]-digoxin in the apical to basolateral (A-B) and basolateral to apical (B-A) direction across Caco-2 (passage 45-56, day 21 in culture) in presence (■)/absence (□) of verapamil. Data are expressed as mean ± SD, n = 6.*

The presence of 0.5 µM GF120918A did not have any significant impact ($p > 0.05$, Figure 23) on the A-B transport of digoxin. P_{app} of digoxin; in the absence of GF120918A the A-B transport rate was $0.70 \pm 0.22 \times 10^{-6}$ cm.s^{-1} and in its presence it was $0.99 \pm 0.65 \times 10^{-6}$ cm.s^{-1}. However, the digoxin absorption rate in B-A direction in the presence of GF120918A was significantly reduced ($p < 0.05$) from $6.02 \pm 0.41 \times 10^{-6}$ cm.s^{-1} to $4.17 \pm 0.20 \times 10^{-6}$ cm.s^{-1}. The addition of GF120918A did not affect cell layer integrity. The TER ranged from 1071 ± 153 Ω.cm^2 at the beginning of the experiment to 972 ± 135 Ω.cm^2 at the end. The mannitol transport varied from $0.26 \pm 0.03 \times 10^{-6}$ cm.s^{-1} to $0.54 \pm 0.24 \times 10^{-6}$ cm.s^{-1}.

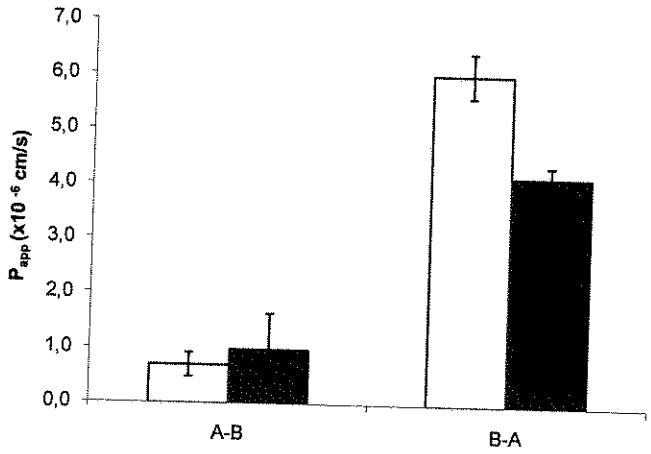

***Figure 23**: Apparent permeability coefficient (P_{app}) of [^{3}H]-digoxin in the apical to basolateral (A-B) and basolateral to apical (B-A) direction across Caco-2 (passage 45-56, day 21 in culture) in presence (■)/absence (□) of 0.5 μM GF120918A. Data are expressed as mean ± SD, n = 6.*

Increasing the concentration of GF120918A to 2.0 μM did not have any impact on the A-B transport of digoxin in similar manner to 0.5 μM GF120918A (Figure 24). The P_{app} of 0.54 ± 0.21 x 10^{-6} cm.s^{-1} in A-B direction in the absence of this inhibitor was not significantly different ($p > 0.05$) from the A-B value of 1.34 ± 0.66 x 10^{-6} cm.s^{-1}. In the presence of inhibitor, the P_{app} was of 2.44 ± 0.13 x 10^{-6} cm.s^{-1} in B-A direction, but without it the digoxin transport rate in B-A direction was 5.84 ± 0.68 x 10^{-6} cm.s^{-1}. Hence, although the inhibitor significantly reduced the B-A transport of digoxin it did not completely abolish it. The integrity of the cell layers was maintained during the experiment as verified by monitoring the TER (start 1014 ± 64 Ω.cm^2, end 965 ± 73 Ω.cm^2). The mannitol transport ranged from 0.26 ± 0.05 x 10^{-6} cm.s^{-1} to 0.98 ± 0.6 x 10^{-6} cm.s^{-1}.

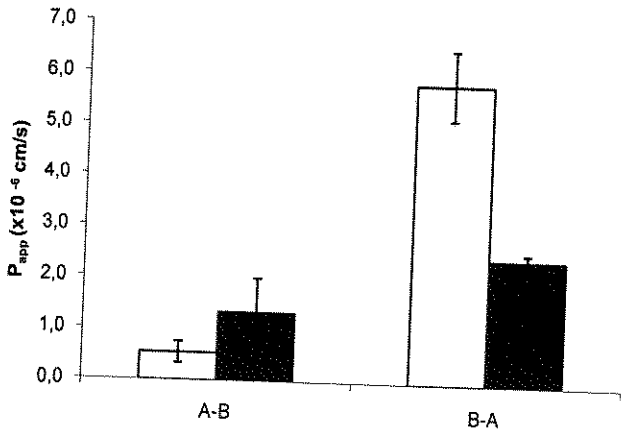

Figure 24: *Apparent permeability coefficient (P_{app}) of [^{3}H]-digoxin in the apical to basolateral (A-B) and basolateral to apical (B-A) direction across Caco-2 (passage 45-56, day 21 in culture) in presence (■)/absence (□) of 2.0 μM GF120918A. Data are expressed as mean ± SD, n = 6.*

The digoxin efflux ratio i. e. the A-B transport rate as a function of the B-A rate, in Caco-2 cells was influenced by the type and concentration of used inhibitor. In the presence of verapamil, the B-A digoxin transport was reduced to such an extent that the transport was symmetrical i. e. no significant difference between A-B and B-A. In the presence of 0.5 μM and 2.0 μM GF120918A, the digoxin efflux ratio was decreased by 51 % and 83 %, respectively. As 2.0 μM GF120918A also made digoxin transport symmetrical, this concentration was used for all transport experiments described in subsequent Sections.

4.3 The effect of P-glycoprotein on digoxin transport

4.3.1 Normal human bronchial epithelial cells

The transport of digoxin across NHBE layers was dependant upon the post seeding culture time (Figure 25, 26). NHBE cells (passage 2), cultured using BEBM:DME/F12 (50:50) showed no

significant difference ($p < 0.05$) in digoxin transport rate in A-B and B-A direction in the absence of GF120918A when assessed 14 days post seeding. The P_{app} of digoxin in A-B and B-A direction was $0.72 \pm 0.12 \times 10^{-6}$ cm.s^{-1} and $0.75 \pm 0.17 \times 10^{-6}$ cm.s^{-1}, respectively in the absence of the inhibitor. On day 21 in culture, the was P_{app} of $0.68 \pm 0.01 \times 10^{-6}$ cm.s^{-1} in A-B direction and unlike the cells when cultured in the Transwell supports for 14 days this was significantly higher ($p < 0.05$) than the P_{app} of $0.26 \pm 0.06 \times 10^{-6}$ cm.s^{-1} in B-A direction in the absence of GF120918A.

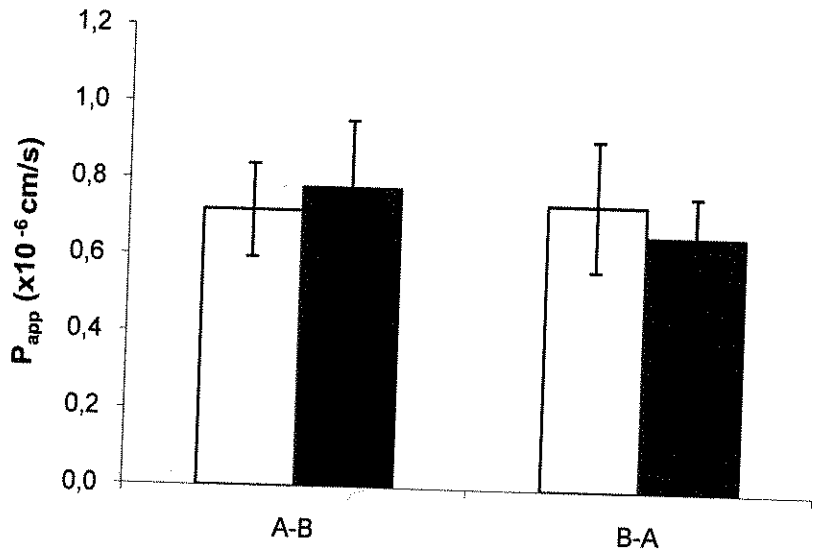

***Figure 25**: The transport of [^{3}H]-digoxin across normal human bronchial epithelial (NHBE) cells, passage 2. Figure shows results from the transport experiment after 14 days in culture in the presence of GF120918A (2 μM) (■) and the absence of this inhibitor (□). Data are expressed as mean ± SD, n > 3.*

GF120918A did not have any significant impact on digoxin transport using the cells that has been cultured for 14 days post-seeding (Figure 25). Digoxin transport across NHBE cells in the presence of GF120918A gave a P_{app} of $0.78 \pm 0.18 \times 10^{-6}$ cm.s^{-1} in A-B direction and $0.67 \pm 0.11 \times 10^{-6}$ cm.s^{-1} in B-A direction, both of which were statistically ($p > 0.05$) similar compared to transport in the absence of the P-gp inhibitor. However, on the day 21, the P_{app} of digoxin was significantly different ($p > 0.05$) in both directions (A-B, $0.41 \pm 0.07 \times 10^{-6}$ cm.s^{-1} and $0.70 \pm$ B-A 0.07×10^{-6} cm.s^{-1}) as a result of the inhibitor's addition. Therefore, the presence of efflux in NHBE cells was culture time-dependant. On day 14, digoxin efflux was not detected, but on the day 21 post seeding, the digoxin transport was clearly polarised in A-B direction and influenced by the specific P-gp inhibitor (Figure 26). TER (start 523 ± 58 Ω.cm^2, end 511 ± 74 Ω.cm^2) and

mannitol permeability (ranged from 0.35 ± 0.09 x 10^{-6} cm.s^{-1} to 1.16 ± 0.38 x 10^{-6} cm.s^{-1}) were monitored and found to be acceptable during the experiment thus verifying the barrier properties of the cells.

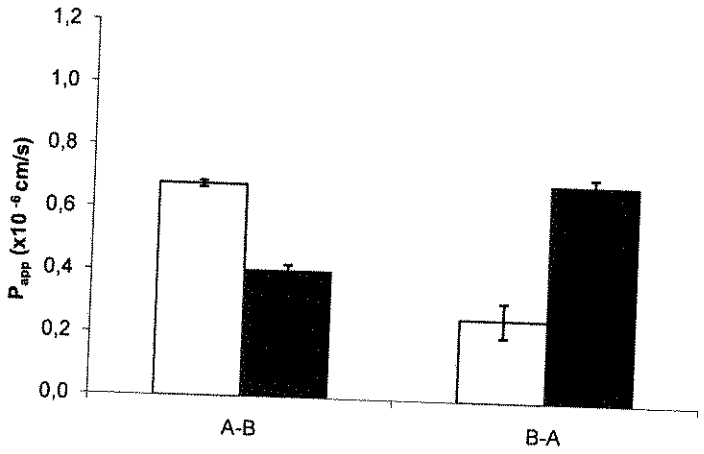

***Figure 26**: The transport of [^{3}H]-digoxin across normal human bronchial epithelial (NHBE) cells, passage 2. Figure shows results from the transport experiment after 21 days in culture in the presence of GF120918A (2 μM) (■) and the absence of this inhibitor (□). Data are expressed as mean ± SD, n > 3.*

NHBE cells (passage 3) cultured in BEBM:DME/F12 (50:50) displayed a TER of 341 ± 16 Ω.cm^2 after 14 days in culture hence were considered to have formed a suitable barrier for transport experiments. However, the mannitol permeability data ($P_{app\ mannitol}$ > 1.0 x 10^{-6} cm.s^{-1}, data not shown) implied that the cell layer had impaired barrier properties and, therefore the cells were not used for further studies. NHBE (passage 2 and 3) cultured using NHBE cell culture medium did not posses barrier properties suitable for transport experiments (determined by TER < 150 Ω.cm^2) during the 9 days in culture, therefore it was not possible to perform permeation experiments using these cells.

4.3.2 Calu-3

In a similar manner to NHBE cells the transport rate of digoxin across Calu-3 layers was dependant upon the post seeding culture time (Figure 27). Digoxin P_{app} in Calu-3 cells of

passage 33 after 14 days culture in the A-B direction was $1.50 \pm 0.40 \times 10^{-6}$ cm.s^{-1} and in the B-A direction it was $1.89 \pm 0.55 \times 10^{-6}$ cm.s^{-1}. As the A-B and B-A transport rates were not significantly different ($p > 0.05$), there was not considered to be any selective efflux of the substrate after growing the cells on Transwell® supports for 14 days. After 21 days in culture the A-B digoxin, the P_{app} was $1.53 \pm 0.05 \times 10^{-6}$ cm.s^{-1} and significantly higher ($p < 0.05$) than in the reverse direction at $1.29 \pm 0.07 \times 10^{-6}$ cm.s^{-1}. Therefore, after 21 days growth the transport in the A-B was dominant.

In the presence of the GF120918A, the transport of digoxin across Calu-3 (passage 33) cells was also dependent upon the post seeding culture time (Figure 27, 28). Digoxin P_{app} in the A-B direction was $1.39 \pm 0.07 \times 10^{-6}$ cm.s^{-1} and in the B-A $2.13 \pm 0.59 \times 10^{-6}$ cm.s^{-1} and therefore no significant efflux ($p > 0.05$) was present after 14 days in culture. Allowing the cells to grow for 21 days on the Transwell® supports gave a dominant A-B digoxin transport of $1.48 \pm 0.11 \times 10^{-6}$ cm.s^{-1}, which was significantly higher ($p < 0.05$) than the P_{app} of $1.21 \pm 0.03 \times 10^{-6}$ cm.s^{-1} in the B-A direction. The barrier properties of the cells were maintained during the experiment as verified by the TER (begin 560 ± 75 Ω.cm^2, end 504 ± 76 Ω.cm^2) and mannitol permeability (P_{app} ranged from $0.30 \pm 0.01 \times 10^{-6}$ cm.s^{-1} to $0.34 \pm 0.30 \times 10^{-6}$ cm.s^{-1}). In addition, the transport rate of mannitol was not influenced by the presence of GF120918A ($p < 0.05$, data not shown).

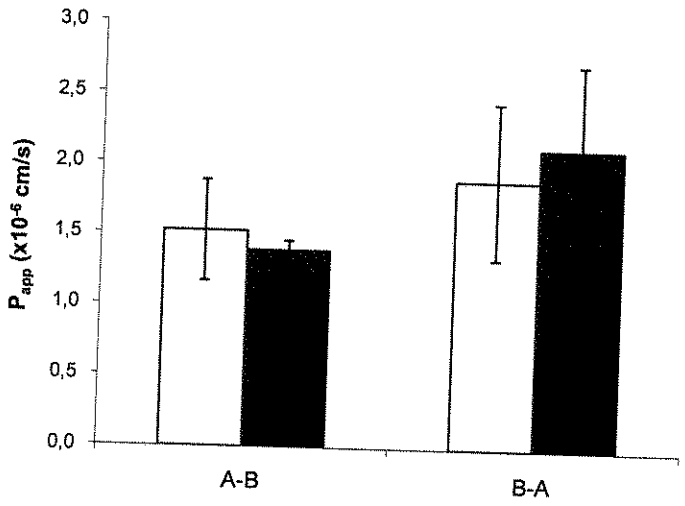

***Figure 27**: Apparent permeability coefficient (P_{app}) of [^{3}H]-digoxin in the apical to basolateral (A-B) and basolateral to apical (B-A) direction across Calu-3 (passage 33) after 14 days culture on Transwell® supports in the presence (■) and the absence (□) of GF120918A (2 μM). Data represent mean ± SD ($n \geq 3$).*

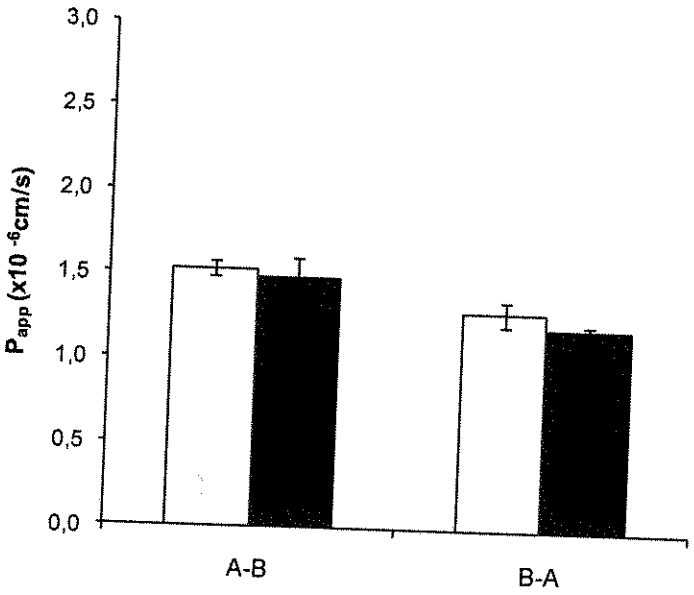

***Figure 28**: Apparent permeability coefficient (P_{app}) of [^{3}H]-digoxin in the apical to basolateral (A-B) and basolateral to apical (B-A) direction across Calu-3 (passage 33) in the presence (■) and the absence (□) of GF120918A (2 μM). Data represent mean ± SD ($n \geq 3$).*

The dominant mode of transport of digoxin across Calu-3 cells, passage 53, was not dependant upon the post-seeding culture time (Figure 29, 30). Transport of digoxin was polarised in the B-A direction on day 14 in culture ($P_{app\ A-B} = 0.59 \pm 0.00 \times 10^{-6}$ cm.s^{-1} was significantly lower ($p < 0.05$) than in the reverse direction, $P_{app\ B-A} = 1.23 \pm 0.14 \times 10^{-6}$ cm.s^{-1}) and on day 21 in culture ($P_{app\ A-B}$ of $0.76 \pm 0.03 \times 10^{-6}$ cm.s^{-1} was significantly lower ($p < 0.05$) than in the reverse direction $P_{app\ B-A} = 1.58 \pm 0.10 \times 10^{-6}$ cm.s^{-1}).

After culturing the cells for 14 days on Transwell® supports the P_{app} of digoxin was $0.56 \pm 0.03 \times 10^{-6}$ cm.s^{-1} in A-B direction and significantly higher ($p < 0.05$) in the B-A at $1.12 \pm 0.01 \times 10^{-6}$ cm.s^{-1} in the presence of the inhibitor. On day 21 the B-A digoxin transport was significantly also higher ($p < 0.05$) than in the reverse direction ($P_{app\ B-A} = 1.01 \pm 0.03 \times 10^{-6}$ cm.s^{-1}, $P_{app\ A-B} = 0.81 \pm 0.04 \times 10^{-6}$ cm.s^{-1}) in the presence of the inhibitor. The barrier properties of the cells were maintained during the experiment and were verified by TER (begin 396 ± 18 Ω.cm^2, end 537 ± 34 Ω.cm^2) and mannitol permeability (P_{app} ranged from $0.13 \pm 0.01 \times 10^{-6}$ cm.s^{-1} to $0.28 \pm 0.04 \times 10^{-6}$ cm.s^{-1}).

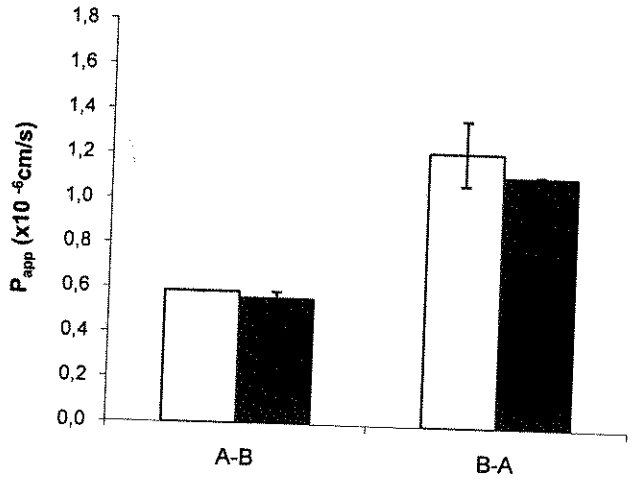

***Figure 29**: Apparent permeability coefficient (P_{app}) of [^{3}H]-digoxin in the apical to basolateral (A-B) and basolateral to apical (B-A) direction across Calu-3 (passage 53) cells in the presence of GF120918A (2 μM) (■) and the absence of this inhibitor (□) on day 14 in culture. Data represent mean ± SD (n ≥ 3).*

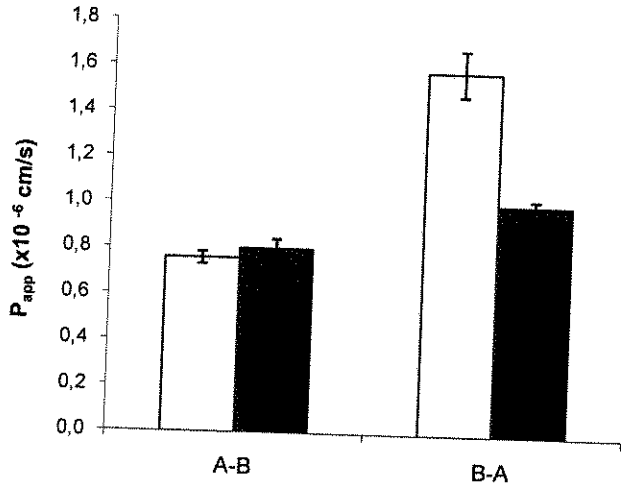

***Figure 30**: Apparent permeability coefficient (P_{app}) of [^{3}H]-digoxin in the apical to basolateral (A-B) and basolateral to apical (B-A) direction across Calu-3 (passage 53) in the presence of GF120918A (2 μM) (■) and the absence of this inhibitor (□) on day 21 in culture. Data represent mean ± SD (n ≥ 3).*

4.3.3 Comparison of digoxin efflux in the three cell models

A significantly higher ($p < 0.05$) digoxin efflux ratio was observed in Caco-2 compared to Calu-3 cells (Figure 31). The P_{app} of digoxin in Calu-3 (21 days in culture, passage 53) in absorptive and secretory directions were $0.76 \pm 0.02 \times 10^{-6}$ cm.s^{-1} and $.58 \pm 0.01 \times 10^{-6}$ cm.s^{-1} respectivly which gave an efflux ratio of 2.08. The Calu-3 efflux was reduced by 40.0 % using GF120918A. The Caco-2 cells gave a A-B P_{app} of $0.54 \pm 0.21 \times 10^{-6}$ and a B-A P_{app} of $5.84 \pm 0.68 \times 10^{-6}$, hence an efflux ratio of 10.73. The Caco-2 efflux was reduced by 81.1 % when the cells were exposed to GF120918A. In contrast to Calu-3 and Caco-2, the P_{app} value of NHBE cells in the secretory direction was significantly lower ($p < 0.05$) than in the absorptive direction ($P_{app\ A\text{-}B} = 0.68 \pm 0.01 \times 10^{-6}$, $P_{app\ B\text{-}A} = 0.26 \pm 0.06 \times 10^{-6}$). In the presence of GF120918A the A-B transport was reduced by 40% and B-A increased by 164 %.

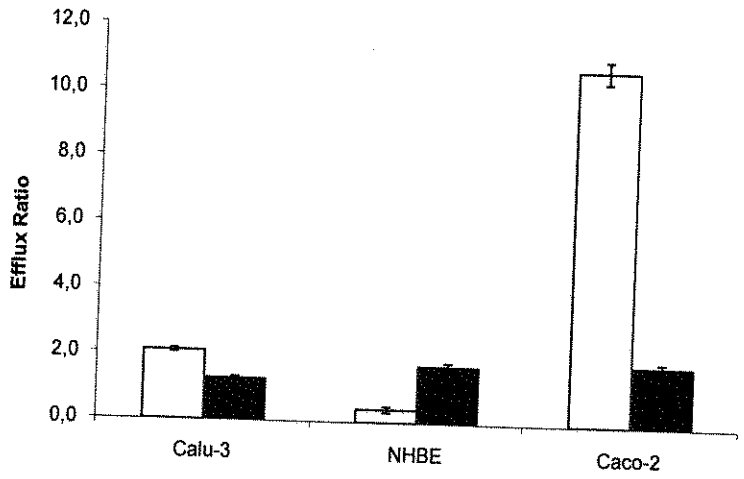

***Figure 31**: The transport of [^{3}H]-digoxin across Calu-3 (passage 53), normal human bronchial epithelial cells (NHBE, passage 2), and Caco-2 (passage 56) cells. Figure shows results from the transport experiment in the presence (■) and absence (□) of GF120918A (2 μm) after 21 days culture on a Transwell® support. The efflux ratio is the apparent permeability coefficient P_{app} (basolateral to apical) divided by the P_{app} (apical to basolateral). Data are expressed as mean ± SD, $n \geq 3$.*

4.4 Isolated perfused rat lung

4.4.1 Immunohistochemical localization of P-glycoprotein in rat lung tissue

The immunohistochemistry showed that the P-gp was present both in the alveolar and bronchial tissue of the IPL preparation (Figure 32). Red compact dots in the plasma membrane and in the cytoplasm (nuclei are stained in blue) show the localisation of P-gp. After incubation with Alexa Fluor® 568 goat anti-mouse IgG secondary antibody, heterogenous epithelial labelling for P-gp was observed in the alveolar tissue (Figure 32A). The staining of the P-gp protein was always much stronger on the membrane of the cells than that in the interstitium between the cells. No staining was observed within the cell cytoplasm. Staining of the bronchial rat lung tissue also confirmed the presence of the P-gp molecule (Figure 32B) within the epithelium. It was not possible to localize the P-gp specifically to any cell compartment. The staining was very heterogenous both inside and outside the cells. Isolated weak intracytoplasmatic P-gp labeling was detected. The staining in the bronchial tissue did not reveal the predominant localisation of the P-gp protein either on the basolateral or apical cell membrane.

4.4.2 Transport experiments

Digoxin transport across the airway epithelium using the IPL was dependant on the method of inhibitor application (Figure 33 and Table 7). The % of digoxin transported in 90 min was 41 ± 17 % ($t_{1/2}$ = 14 ± 2 min, ka = 0.049 ± 0.006 min^{-1}) in the absence of an inhibitor and the co-administration of verapamil did not have any significant impact ($p > 0.05$) on the digoxin transport; % of digoxin transported in 90 min was 54 ± 3 % ($t_{1/2}$ = 12 ± 3 min, ka = 0.059 ± 0.017 min^{-1}). In similar manner to verapamil, the co-administration of GF120918A with the digoxin did not have any significant impact ($p > 0.05$) on the digoxin transport; the % of digoxin transported in 90 min was 46 ± 7 % ($t_{1/2}$ = 14 ± 3 min, ka = 0.052 ± 0.013 min^{-1}) in the presence of GF120918A. Using verapamil in the perfusion solution increased the amount of digoxin transported in 90 min to 62 ± 5 % ($t_{1/2}$ = 13 ± 3 min, ka = 0.056 ± 0.014 min^{-1}). It was not possible to perform the experiment with GF120918A in the perfusion solution due to limited availability of this inhibitor.

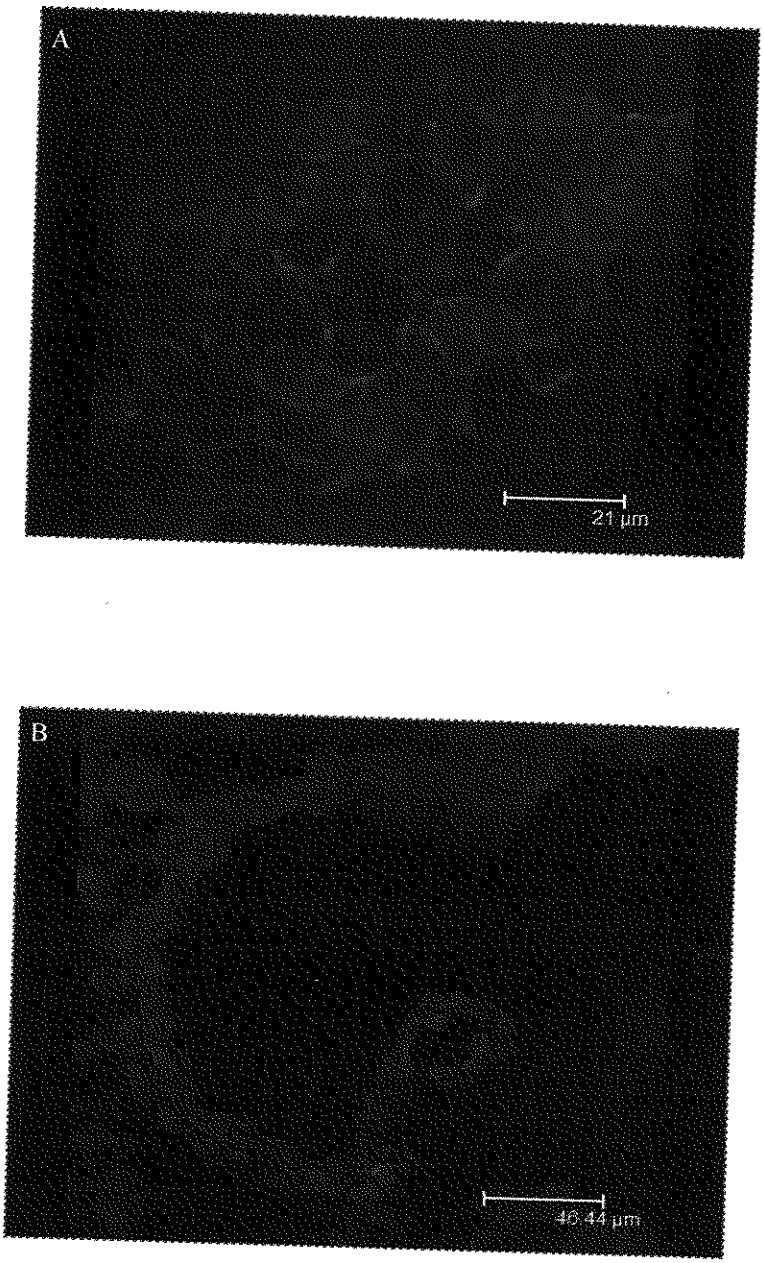

***Figure 32**: Confocal microscopy of P-glycoprotein expression in rat lung. Acetone-fixed cryostat sections of (A) alveolar and (B) brochial tissue. Alexa Fluor® 568 goat anti-mouse IgG secondary antibody (red) was used to visualise anti-P-glycoprotein mouse mAb (C219). Nuclei stained with DAPI (blue).*

The digoxin absorption profile was not significantly different ($p > 0.05$) when GF120918A and verapamil were co-administered with digoxin, however the presence of verapamil in perfusion solution significantly ($p < 0.05$) increased digoxin absorption in IPL preparation between 2 and 25 min of the experiment compared to the untreated control. After 2 min of the experiment the amount of digoxin transported was 3.3 ± 0.9 % and 6.4 ± 2.3 % in the absence and presence of the inhibitor, respectively. At 25 min, the amount of transported digoxin was 28.7 ± 9.9 % and 43.5 ± 6.7 %, in the absence and presence of the inhibitor, respectively.

The cumulative amount of mannitol transport during all experiments was 48.5 ± 5.0 % and this was not affected by the presence of the inhibitors (Table 7). No lung oedema was present during any of the experimental reported herein (determined visually).

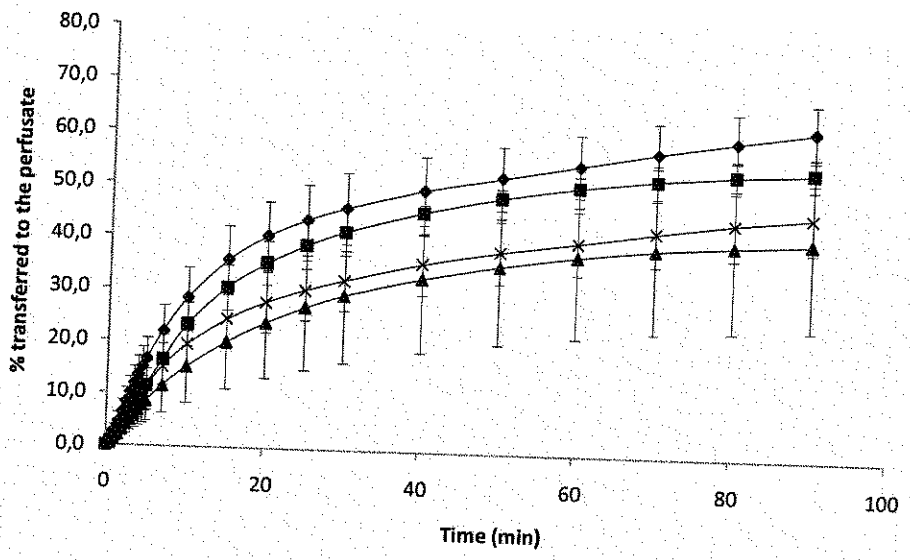

***Figure 33**: Cumulative percentage of administered [^{3}H] digoxin dose (45.8 nM co-administered with [^{14}C] mannitol, 65.6 μM) transferred to the perfusate vs time in presence/absence of P-glycoprotein inhibitors (♦) verapamil in perfusion solution, (■) verapamil co-administered with [^{3}H]-digoxin, (x) GF120918A co-administered with [^{3}H]-digoxin, (▲) no inhibitor. Data are expressed as mean ± SD, n=4.*

***Table 7**: Rate of [^{3}H]-digoxin (45.8 nM) and [^{14}C]-mannitol (65.6 μM) absorption across the epithelium of the isolated and perfused rat lung in presence/absence of two P-glycoprotein inhibitors GF120918A (2.0 μM, co-administered with [^{3}H]-digoxin) and verapamil (100μM, *verapamil co-administered with [^{3}H]-digoxin and [^{14}C]-mannitol, $^{\Delta}$verapamil in perfusion solution). The absorption half-life ($t_{1/2}$, min) and apparent absorption rate constant (ka) are also presented. Data is expressed as the mean ± SD, n=4.*

[^{3}H]-digoxin			
	abs $t_{1/2}$ (min)	ka (min^{-1})	% transported in 90 min
- inhibitor	14 ± 2	0.049 ± 0.006	41 ± 17
+ GF120918A	14 ± 3	0.052 ± 0.013	46 ± 7
+ verapamil*	12 ± 3	0.059 ± 0.017	54 ± 3
+ verapamil$^{\Delta}$	13 ± 3	0.056 ± 0.014	62 ± 5
[^{14}C]-mannitol			
	abs $t_{1/2}$ (min)	ka (min^{-1})	% transported in 90 min
- inhibitor	27 ± 2	0.026 ± 0.002	51 ± 10
+ GF120918A	27 ± 4	0.027 ± 0.005	50 ± 2
+ verapamil*	29 ± 6	0.025 ± 0.005	45 ± 6
+ verapamil$^{\Delta}$	28 ± 4	0.026 ± 0.004	48 ± 2

5 DISCUSSION

Numerous studies have generated data in an attempt to shown the impact of P-gp on the oral absorption of drugs, but due to the anatomical and physiological complexity of the lung, the exact function and localisation of P-gp in this organ is not yet fully understood. Studying transport across the lung epithelium can be simplified using cell lines. *In vitro* transport models allow accurate drug dosing, precise localisation, bypass of mucociliary and/or macrophage clearance and the control of barrier integrity. In addition, the cell barrier can be manipulated through the variation of cell type. However, the functional expression of numerous important surface membrane proteins in the cell cultured *in vitro* is constantly questioned due to the lack of an easy method to test their presence and/or functionality. Hence, the relevance of cell culture models and justification used to select the most appropriate to model transport in the lung is a source of continuing debate in literature.

In this study, the activity of the P-gp was assessed in Calu-3 (passage 33 and 53), Caco-2 (passage 45-56) and NHBE (passage 2) cells grown on Transwell® supports by performing drug transport experiments. This data was compared to a rat IPL model to investigate the P-gp activity in native lung epithelia and immortalised cells *in vitro*. The transport rate of the known P-gp substrate digoxin was determined in the absence and presence of the P-gp inhibitors verapamil and GF120918A. It was anticipated that the transport rates of digoxin would be able to provide an indication of the P-gp activity present in the two airway cell models and rat lung tissue.

5.1 Normal human bronchial epithelial cells growth conditions optimisation

NHBE cells have recently been described in the literature as a suitable *in vitro* model for human airway epithelium (Lin *et al.*, 2006). However, there currently no standard, universally accepted protocol that details the manner in which these cells should be grown *in vitro*. Previous work has evaluated the influence of cell culture conditions on both the barrier properties of these cells and the expression of P-gp (Lin *et al.*, 2006) and this has produced several different methodologies of culturing bronchial epithelial cells (Lin *et al.*, 2006; Yamaya *et al.*, 1992; Gruenert *et al.*, 1990; van Scott *et al.*, 1986). Lin *et al.* (2006) used FBS free BEBM:DME/F12 (50:50) and ALI conditions for culturing NHBE cells, but the supplier of the cells (Cambrex Bio Science, Inc)

suggests an alternative set of conditions. As a consequence the first objective in this work was to optimise the cell culture media in which the NHBE cells should be grown.

When NHBE cells of passage 1 were suspended in a tissue culture flask using NHBE cell culture medium, the cells underwent extensive morphological change, losing their cuboidal appearance and becoming flattened over their first days in culture. The cells reached confluency on day 7 post seeding showing epithelium-like morphology, which was similar to the observation described by Lin *et al.* (2006). After subculturing (i. e. passage 2) and seeding of the cells on Transwell®, the growth of passage 2 cells in NHBE cell culture medium appeared impaired. The cells that did not form a confluent cell layer showed markedly attenuated cytoplasmic extensions even though the same cells of passage 2 appeared confluent in the cell culture flask. These visual observations suggested that not only the medium composition, but also the manner in which the cells are cultured i. e. either in flask (liquid interface) or at an air liquid interface can significantly influence the cell morphology (Wiesel *et al.*, 1983; Yamaya *et al.*, 1992). In addition to the changes in cell morphology, it was apparent that the cell proliferation was impaired by presence of the serum in the cell culture medium, when the cells were grown on the Transwell® supports. Lechner *et al.* (1983) previously reported that the addition of serum to cell culture medium can inhibit airway epithelial cell proliferation and induce squamous differentiation. Therefore the data generated in the present study strengthens the recommendation that the use of blood-derived serum is not recommended for long-term studies with primary cultures.

NHBE cells of passage 2 grown in BEBM:DME/F12 (50:50), i. e. identical medium to Lin *et al.* (2006) formed a tight cell layer which was suitable for drug transport studies based on the mannitol permeabilities and TER values obtained for each Transwell® insert ($P_{app\ mannitol} < 1.0 \times 10^{-6}$ cm.s^{-1}, Forbes and Ehrhardt, 2005; TER > 300 Ω.cm^2, commonly accepted laboratory standard values). The mannitol permeability suggested that BEBM:DME/F12 (50:50) medium produced cell layers with tight junctions that were maintained for 21 days post-seeding. This finding confirms work of Lin *et al.* (2006) who successfully cultured the NHBE cells (passage 2 and 3) on cell culture flasks without a collagen coating using serum free BEBM:DME/F12 (50:50) for 15 days (the previous work of Lin et al. (2006) used the increase of TER value with time in culture to investigate the confluency of the cells in similar manner as in present study). This finding indicates that the cells loose epithelial barrier properties after three passages, which has been described previously with primary cell *in vitro* (Forbes, 2000).

Cells of passage 3 cultured either in NHBE cell culture medium or BEBM:DME/F12 (50:50) did not form a confluent cell layer when seeded on Transwell® supports and grown under ALI

conditions. As a result only passage 2 cells were suitable for transport studies using these culture conditions. The TER of NHBE passage 3 cultured on Transwell® supports in the BEBM:DME/F12 (50:50) medium reducing with the time in culture has previously been described by Davidson *et al.* (2000). In addition, the loss of differentiation after only two or three passages has been previously described in literature (Forbes, 2000) and this phenomena is commonly described as one of the main disadvantages of culturing primary cells.

5.2 Cell culture transport method development

5.2.1 Digoxin dose ranging studies

In order to determine the influence of concentration on the transport of digoxin across a cell barrier *in vitro*, a series of transport experiments were performed with Calu-3 cells. This cell line was chosen for the pilot experiment as it was thought to be the most relevant in which to model transport across the airways of the lung. All the digoxin concentrations utilised in the experiments showed polarised transport in the B-A direction suggesting the localisation of the P-gp molecule on the apical membrane of Calu-3 cells. Although significant differences in cumulative transport were observed for different digoxin concentrations, an increase in concentration did not depress the relative efflux ratio. A lack of efflux depression indicated that the P-gp transporter was not saturated even at the highest digoxin concentration used. A lack of transporter saturation is essential if a correlation between substrate transport and protein activity, a assumption commonly made in cell culture activity studies, is required. To ensure that P-gp transport was not saturated, the lowest concentration of those tested was used in all transport experiments. A similar digoxin concentration for transport experiments has previously been used by Cavet *et al.* (1997) in a study investigating the impact of P-gp on ciprofloxacin transport across Calu-3 cells.

5.2.2 Inhibitor dose ranging studies

Previous work have described the P-gp activity in the intestinal Caco-2 cell line (Artursson *et al.*, 2001). Therefore, this cell line was used to characterise the influence of P-gp inhibitor concentration and type on digoxin transport across a typical cell layer. Although a number of inhibitors are known to interact with P-gp including MS-209 (Hamilton, 2002), cyclosporin A (Sikic *et al.*, 1997), PSC833 (Mattheis, 1995), in this work verapamil (non-selective) and GF120918A (selective) were used to represent two very different types of P-gp inhibitor.

Verapamil is known to be non-specific inhibitor that can interact with several efflux transporters in Caco-2 cells, e. g. multidrug resistance associated protein (MRP, Azsalos *et al.*, 1999) and organic cation transporter (OCT, Horio *et al.*, 1989). Data presented in the current study agreed with previous literature and showed that verapamil completely depressed the digoxin efflux in the Caco-2 cell line. Such a dramatic effect suggested that all the transporters contributing to this efflux were inhibited. Conversely, using GF120918A, a far less pronounced efflux depression was observed which indicated a much more specific effect. However, a confounding issue was that the GF120918A efflux inhibition was found to be concentration dependent; a lower rate of efflux inhibition was attained using 0.5 μM GF120918A (Letrent *et al.*, 1999) compared to 2.0 μM (recommended by GlaxoSmithKline Ltd). The lower concentration may have only resulted in a partial block of the P-gp transporters, but with the current data this cannot be discerned. Due to the limited availability it was not possible to investigate a full range of GF120918A concentrations on the P-gp activity.

5.3 The effects of P-glycoprotein on digoxin transport

5.3.1 Normal human bronchial epithelial cells

Primary cells provide the closest *in vitro* representation of the airway epithelium. In this study, the NHBE cells, which were sourced from nondiseased human tissue without immortalization, were selected to establish the influence of the cell type upon P-gp expression in cell layers. However, in order to investigate transport across primary cell lines it is important to establish optimum cell culture conditions that will generate suitable barrier properties. Although culture medium and the passage number had been optimised the time of growth on the Transwell supports had not previously been assessed and therefore this variable was incorporated into the transport experiments.

NHBE cells of passage 2 cultured in BEBM:DME/F12 (50:50) were successfully grown on the Transwell® inserts and possessed barrier suitable for the permeation experiments for 21 days in culture. The occurrence of polarised digoxin across the cells was found to be dependent on time in culture. No polarised transport of digoxin was detected after 14 days in culture, but the polarized transport of digoxin in A-B direction was shown on day 21. The possible explanation for the occurrence the high A-B transport after the NHBE cells had been cultured on Transwells for 21 days could be the gradual development of the P-gp transport system with time in culture. A similar effect has been already reported by Lin *et al.* (2006). The ratio of digoxin A-B to B-A

transport was 2.08, suggesting the presence of P-gp transporter on the basolateral cell membrane. The lack of equivalence in transport rates for digoxin in the NHBE cells was reduced by 40 % when GF120918A was applied to the cells. In previous work, Lin *et al.* (2006) found the Rh123 efflux to be polarised in B-A direction using NHBE cells, therefore was assumed that the P-gp was predominantly located on the apical membrane of NHBE cells. In the study by Lin *et al.* (2006) verapamil was used to inhibit this efflux. However, it could be argued that neither of these substances is ideal for evaluation of P-gp activity in cell culture models. As discussed previously, verapamil is a non-specific inhibitor that influences other transporters and it has been reported that Rh123 is a not specific P-gp substrate (Troutman and Thakker, 2003b). Rh123 has also been reported, in the isolated perfused rat kidney, to be preferentially secreted by a transporter of the organic cation carrier systems and not by the P-gp (Masereeuw *et al.*, 1997). The finding that Rh123 is not a specific substrate has been confirmed by van der Sandt *et al.* (2000) in a study where Rh123 was shown to be actively transported by the organic cation carrier system in the LLCK-PK1 and the LLC-PK1:MDR1 cell lines. In light of this information, claims on the presence and activity of P-gp based on Rh123 efflux studies should be made with caution as these compounds are affected by a variety of factors, which may present a misleading picture. The discrepancy between findings on polarisation of digoxin NHBE transport reported by Lin *et al.* (2006) and in current study is similar to that previously described for Calu-3 cell line. Those studies that used non-specific substrates and inhibitors (Hamilton *et al.*, 2002; Patel *et al.*, 2002; Florea *et al.*, 2001; Hamilton, 2001) produced different results than with compounds specific for P-gp probably due to the high number of variables changing in a single experiment when non-specific compounds are used (Cavet *et al.*, 1997).

Digoxin has been used widely in P-gp functionality studies as it appears to be a far more reliable substrate without the metabolic complications known to affect Rh123 (de Lannoy and Silverman, 1992). The key feature that makes digoxin a desirable P-gp probe is that unlike other P-gp substrates (e. g. cyclosporine A) it does not self-regulate its own transport i. e. act as both an inhibitor and a substrate. Not only has digoxin been previously shown to be a highly specific P-gp substrate (Verschraagen *et al.*, 1999; Tang *et al.*, 2002), it has only moderate passive permeability (Hunter and Hirst, 1997) and it is not metabolised (Verschraagen *et al.*, 1999); all of which are desirable properties for active transport probe. Although several other drug transporters have reported to transport digoxin, most notably MDR3 (Lecureur *et al.*, 2000; Smith *et al.*, 2000), the apically located MRP2 (Lowes *et al.*, 2003), the multispecific organic anion transporting polypeptide OATP1 transporter (van Montfoort *et al.*, 2002) and OATP2 (Noe *et al.*, 1997), a comprehensive study by Montfoort *et al.* (2002) showed that digoxin did not appear to possess a high affinity for any of these transporters (van Montfoort *et al.*, 2002). A further advantage of using digoxin as the P-gp probe is that the cell layer integrity doesn't alter

following treatment with the drug. Aside from the inconvenience of working with a tritiated compound, the main disadvantage of [^{3}H]-digoxin, as with most lipophilic compounds, is the potential of binding to the Transwell® inserts. This was prevented in this work by using a surface active protein, 0.1% (w/v) BSA, to enable a full digoxin recovery from the transport experiments.

Although the presence of P-gp in NHBE cells was confirmed in present study and also in literature, further investigation of the localisation of P-gp in the cells is important if NHBE are to be used as a drug absorption model for the airways. Suitable methods that could be used to elucidate the P-gp localisation in the cells are immunohistochemistry and confocal microscopy.

5.3.2 Calu-3

The Calu-3 cell line, derived from human bronchial adenocarcinoma, is widely used for drug transport studies in the airways. When cultured *in vitro*, Calu-3 cells are composed of a mixed phenotype of ciliated and secretory cells that differentiate to exhibit good barrier properties. Moreover, this cell line is relatively easy to grow. Although Calu-3 cells are well described in the literature as a model for drug absorption in airways (Grainger *et al.*, 2006), in a similar manner to NHBE cells, previous studies report contradictory results about the expression of P-gp in this cell line (Hamilton *et al.*, 2001[b]; Cavet *et al.*, 1997).

The Calu-3 cell layers were cultured under ALI growth conditions to mimic *in vivo* conditions using a method previously described by Grainger *et al.* (2006). Using this method, cell layers suitable for digoxin transport studies, based on the TER and mannitol permeability, were obtained for each Transwell® insert. Mannitol permeability suggested the maintenance of their barrier properties between 14-21 days post-seeding for all the employed cell passages. As documented in the literature, the population and the transport properties of cells change after repeated passaging (Artursson, 1991). Therefore, two different passages of Calu-3 were compared in this work to investigate the potential for variability in the cells during passage.

Digoxin efflux in the Calu-3 cells was found to be dependent on the passage number and time in culture. Cells of passage 33 did not reveal any efflux after 14 days in culture. The absence of efflux in Calu-3 cells of passage between 21 and 37, 14 – 21 days post seeding was previously described by Cavet *et al.* (1997). The conclusion of Cavet's work was that P-gp transport was absent from Calu-3 cells (Cavet *et al.*, 1997). However, Florea *et al.* (2001) demonstrated that Calu-3 cells had polarized digoxin transport in A-B direction suggesting the presence of P-gp on

the basolateral membrane. The presence of P-gp at the basolateral surface of Calu-3 cell line has been supported by confocal laser scanning microscopy (Florea *et al.*, 2001). Conflicting data on active transport in cell lines is not uncommon due to the inter-laboratory variation that can occur when working with cell lines. Defining the exact location of transport proteins is difficult as this can be dependent on growth conditions and this has been previously seen in a number of cell types, e. g. in A549 cells (Hamilton *et al.*, 2001a; Trussardi *et al.*, 1998). The abnormal location of active transport systems can account for a variety of pathologies (Loo and Clarke, 1997; Skach, 2000).

Cells of passage 53 used in the current work did demonstrate polarised transport of digoxin in B-A direction irrespective of the time in culture (i. e. 14 - 21 days). Similar results have been previously described in the literature but again there are several conflicting studies (Hamilton *et al.*, 2002; Patel *et al.*, 2002; Hamilton, 2001[b]). Artursson (1991) demonstrated that the transport properties of cells may change during the passaging process. Therefore, one possible explanation for the reported lack of P-gp activity could be that the P-gp transport in Calu-3 is only present in passages around 40 or higher. As a consequence, the often neglected impact of the passage number onto P-gp expression in the cells should be always considered when performing permeation experiments.

In the presence of GF120918A the B-A digoxin transport in passage 53 Calu-3 cells was not influenced on day 14, however, this was reversed after 21 days in culture, which suggested different transport mechanisms dominated at different time points. While Wils and co-workers (1994b) could not find a change in transporter expression when culture time was varied, others have found the expression of P-gp to be culture time dependant (Anderle *et al.*, 1998; Hoskins *et al.*, 1993; Hosoya *et al.*, 1996). For example, using Western blots, Hosoya and co-workers (1996) demonstrated that the order of P-gp expression over a period of 4 weeks was 4w>1w>2w>3w, while in permeation studies the function of P-gp as a transporter protein increased significantly from day 17 to 27 when the cells were seeded on polycarbonate filters. Wils and co-workers (1994a; 1994b) used immunoblotting to show that no increase in P-gp expression from day 4 to 22 occurred when Caco-2 cells were cultured in plastic flasks. Anderle and co-workers (1998) cultured Caco-2 cells in plastic flasks and measured a significant decrease of the P-gp expression over time, whereas cultivation of the cells on polycarbonate filters lead to an increase of the P-gp expression level. Wils and co-workers (1994b) observed that the capacity to express P-gp may be lost during long-term cell cultivation. One explanation for the lack of GF120918A influence on efflux of digoxin on day 14 could be that the efflux present on day 14 in culture is not caused by P-gp transporters but other transport systems such as OCT that cannot be inhibited by GF120918A. It is possible the P-gp activity develops with

time in culture in similar manner to NHBE cells described in Section 5.3.1. On the day 21, the P-gp contributes to the efflux, therefore GF120918A can inhibit the P-gp activity, and the digoxin transport in B-A direction in the presence of the inhibitor was reduced. In light of these results, care has to be taken when comparing results from studies using different post-seeding cell culture conditions.

The contradictory findings regarding the P-gp expression in Calu-3 line reported in literature, aside from highlighting the innate inter-laboratory variation for this cell line, casts doubt over the ability of this cell line to consistently express P-gp. Thus, the Calu-3 drug absorption model may be a more representative model for drug targeted tissue that has been reported to exhibit low level efflux transporter expression. Characterisation of Calu-3 cells with regard to P-gp expression and determining how are these findings related to culture conditions is important if this cell line is to be used as a drug absorption model for the airways. Moreover, there is a concern that the use of carcinoma cell lines derived from the target tissue may not be truly representative of the epithelium *in vivo* (Gres *et al.*, 1998). The potential inability of the Calu-3 cell line to exhibit carrier protein expression levels found *in vivo* has been acknowledged (Mathias *et al.*, 2002; Foster *et al.*, 1998; Hamilton *et al.*, 2002). Calu-3 cells also generate unusually high TER values for a bronchial epithelial derived cell line.

5.3.3 Comparison of the digoxin efflux in three cell models

The Caco-2 cell line was used in this study as positive control cell culture system i.e. a cell line that was known to express P-gp (Cavet *et al.*, 1996).. The results from the study were in agreement with the theory that the Caco-2 cells expressed P-gp and this cell line produced the greatest digoxin efflux ratio of all the cell models employed. However, the reported efflux values for the Caco-2 cells (10.73) are almost double those previously reported by Cavet *et al.* (1996), who described the digoxin efflux ratio in Caco-2 cells as ranging from to 4.7 to 6.4 for 1-200 μM digoxin. This efflux magnitude disparity could be explained by the different culture conditions employed across these two studies. While Cavet *et al*, (1996) cultured the cells on polycarbonate filters, the present study used polyester filters. The effects that a change in support material can have on cells culture in vitro has already been discussed in Section 5.3.2.

NHBE and Calu-3 cells are not thought to express P-gp to the same extent that the carcinoma cell line Caco-2 does. This may be due to the different origins of the cell lines. Caco-2 is intestinal cell line whereas the Calu-3 and NHBE are of lung origin. In Calu-3 cells, the digoxin transport was polarized in the B-A direction suggesting the presence of the P-gp in the apical

cell membrane after 21 days in culture, a result that backs up the data generated by Hamilton *et al.* (2001[b]). In contrast, the efflux observed in NHBE was probably as a result of and active transporter to the basolateral plasma membrane. This result doesn't correspond with work done by Lin *et al.* (2006) who predicted that the transport was on the opposite side of the cell layer.

Variability between laboratories with respect to the permeability of compounds across Caco-2 cell layers has limited the usability of permeability data. For future work, the standardisation of all cell culture parameters such as time in culture, type of membrane support and seeding density (Braun *et al.*, 2000) is essential for comparable data exchange to become reality. Moreover, employment another method in addition to transport experiments for precise investigation of P-gp location in the cells, e. g. immunohistochemistry could help to elucidate the exact localisation, therefore function of P-gp in the cells.

5.4 Isolated perfused rat lung

5.4.1 Immunohistochemical localisation of P-glycoprotein in rat lung tissue

The relatively low levels of P-gp expression in the lung compared with that in other tissues has been well documented (Lechapt-Zalcman *et al.*, 1997; Thiebaut *et al.*, 1987; Pavelic *et al.*, 1993). Positive staining of the rat lung tissue for P-gp in this study proved that P-gp was present in both alveolar and bronchial epithelia confirming literature reports (Lechapt–Zalcman *et al.*, 1997; Wioland *et al.*, 2000; Sakagami *et al.*, 2004). Lechapt–Zalcman *et al.* (1997) reported the localisation of P-gp in bronchial respiratory epithelium and showed a restriction of the protein distribution to the apical surface. With a more sensitive immunodetection method (Sabattini *et al.*, 1998) P-gp was also detected on lateral membranes of ciliated cells and at the circumference of basal cells. Unfortunately in this study was not possible to localize the expression of P-gp either on apical or basolateral side of the epithelial cells due to a lack of image resolution.

5.4.2 Transport experiments

Any *in vitro* drug absorption model should represent the tissue it is modelling in as many aspects as possible, however it is crucial that the active and passive drug absorption characteristics are all present and active in order to provide a usable model.. To provide a contrast to the very simplistic cell line models, a rat IPL was used investigate the P-gp activity in a more complex environment i.e. viable lung airway epithelium. The presence of the P-gp and other transporters,

e. g. MRP1 and MVP in normal human lung tissues has previously been reported in the literature (van der Walk *et al.*, 1990; Flens *et al.*, 1997; Izquiredo *et al.*, 1996a; Wright *et al.*, 1998). Despite the high number of *in vitro* studies, the functional effect of efflux transporter activity on the transport of drugs across the lung barrier in animal models has not been thoroughly investigated. In one of the only studies reporting P-gp activity in the rat lung Tronde *et al.* (2003b) showed functional evidence for P-gp limiting the absorption of talinolol and losartan from the rat lung. However, the role of P-gp in the absorption of these drugs was found to be quantitatively less important in comparison to the passive diffusion across the lung epithelium.

The functionality of the P-gp was tested in the rat IPL model using P-gp substrate digoxin and inhibitors GF120918A and verapamil in the current work. The inhibitors were present either in the digoxin donor solution or in the perfusion solution. Digoxin was rapidly and well absorbed from the air- to the circulation of the IPL, but the similarity of the digoxin absorption profiles in the absence and presence of the GF120918A inhibitor co-administered with digoxin suggested that P-gp did not significantly contribute to the transport of digoxin across the lung epithelium. The absorption rate of digoxin was however significantly increased when verapamil was present in the perfusion solution. A possible explanation for the lack of GF120918A activity could be the presence of an insufficient amount of the inhibitor in the lung tissue. When the inhibitor is co-administered with the substrate and not infused within the perfusate solution the resonance of the inhibitor may be short. Therefore, no influence of the inhibitor on digoxin absorption from IPL could be recorded. In contrast, inclusion of the inhibitor in the perfusate resulted in much higher concentration of inhibitor in the lung and this may be the reason why verapamil could have been present in a sufficient concentration to reduce digoxin efflux in the IPL. Due to the limited availability of the GF120918A it was not possible to perform the transport experiment with this inhibitor present in the perfusion buffer. In addition, as the verapamil is not specific inhibitor of P-gp and therefore no conclusion on the extent of P-gp involvement in the increased absorption of digoxin in IPL can be unambiguously identified. For future studies should be performed to allow a direct comparison using GF120918A administered in the perfusion solution to evaluate the activity of P-gp in rat IPL model.

6 CONCLUSION

The relatively low levels of P-gp expression in the lug compared with that in other tissues has been well documented (Lechapt - Zalcman *et al.*, 1997; Thiebaut *et al.*, 1987; Pavelic *et al.*, 1993). However, the bronchial epithelium has not been characterised to the same extent with respect to the other transported and efflux mechanisms compared to the intestine even though primary cultures of NHBE cells have been recently recognised as suitable model for studies of drug absorption in the airways (Lin *et al.*, 2006). In present study, the influence of different cell culture medium on cell growth and differentiation was investigated. Morphology and barrier properties of the cells were found to be different for different cell culture medium employed. The integrity of the cell layers seemed satisfactory (determined by TER and mannitol transport) when BEBM:DME/F12 (50:50) was used for a 21 day period. Using transport studies, the presence of P-gp in NHBE was detected on day 21 in culture on the basolateral plasma membrane of the cells.

In present study, the functional efflux in the Calu-3 cell line was found to be dependent on passage number and time in culture. The digoxin efflux that was possible to inhibit by specific P-gp inhibitor GF120918A was detected only at passage higher that 53 on day 21 in culture. The transport of digoxin was polarised in B-A direction, therefore the P-gp transporter was assumed to be present on the apical cell membrane.

Digoxin remains one of the most suitable substrates available for P-gp investigation, despite minor interactions with other transporters; therefore it was used in this study for investigation of P-gp impact on drug absorption in IPL model. The presence of P-gp was confirmed by the immunohistochemistry both in alveolar and bronchial tissue and the transport studies confirmed the presence of an active transport mechanism in the IPL. However, due to the limited availability of specific P-gp inhibitor GF120918A it was not possible to include the inhibitor in the perfusate solution and thus completely investigate the involvement of the P-gp transporter in this active transport. Further transport studies in IPL should be performed to clarify the expression relates to transport activity of P-gp in this model.

7 REFERENCES

Adson A., Raub T. J., Burton P. S., Barsuhn C. L., Hilgers A. R., Audus K. L., and Ho H. F. (1994). Quantitative approaches to delineate paracellular diffusion in cultured epithelial cell monolayers. *J Pharm Sci* **83**, 1529-1536.

Ambudkar S. V. (1995). Purification and reconstitution of functional human P-glycoprotein. *J Bioenerg Biomembr* **27**, 23-29.

Ambudkar S. V., Kimchi-Sarfaty C., Sauna Z. E., and Gottesman M. M. (2003). P-glycoprotein: from genomics to mechanism. *Oncogene* **22**, 7468-7485.

Anderle P., Niederer E., Rubas W., Hilgendorf C., Spahn-Langguth H., Wunderli-Allenspach H., Merkle H., and Langguth P. (1998). P-glycoprotein (P-gp) meditated efflux in Caco-2 cell monolayers: The influence of culturing conditions and drug exposure on P-gp expression levels. *J Pharm Sci* **87**, 757-762.

Anderson R. G., Kamen B. A., Rothberg K. G., and Lacey S. W. (1992). Potocytosis: sequestration and transport of small molecules by caveolae. *Science* **255**, 410-411.

Archinal-Mattheis A., Rzepka R. W., Watanabe T., Kokubu N., Itoh Y., Combates N. J., Bair K.W., and Cohen D. (1995). Analysis of the interactions of SDZ PSC 833 ([3'-keto-Bmt1]-Val2]-cyclosporine), a multidrug resistance modulator, with P-glycoprotein. *Oncol Res* **7**, 603-610.

Artursson P. (1991). Cell cultures as models for drug absorption across the intestinal mucosa. *Crit Rev Ther Drug Carrier Syst* **8**, 305-330.

Artursson P., Palm K., and Luthman K. (1996). Caco-2 monolayers in experimental and theoretical predictions of drug transport. *Adv Drug Deliv Rev* **22**, 67-84.

Artursson P., Palm K., and Luthman K. (2001). Caco-2 monolayers in experimental and theoretical predictions of drug transport. *Adv Drug Deliv Rev* **46**, 27-43.

Audi S. H., Roerig D. L., Ahlf S. B., Lin W., and Dawson C. A. (1999). Pulmonary inflammation alters the lung disposition of lipophilic amine indicators. *J Appl Physiol* **87**, 1831-1842.

Azsalos A., Thompson K., Yin J. J., and Ross D. D. (1999). Combinations of P-glycoprotein blockers, verapamil, PSC833, and cremophor act differently on the multidrug resistance associated protein (MRP) and on P-glycoprotein (Pgp). *Anticancer Res* **19**, 1053-1064.

Bassett D. J. P., and Roth R. A. (1992). The isolated perfused lung preparation, in: *In vitro methods of toxicology* (Watson R. R., ed), 143-155, Boca Raton, CRC Press, Florida.

Beck W. T., and Qian X. D. (1992). Photoaffinity substrates for P-glycoprotein. *Biochem Pharmacol* **43**, 89–93.

Berger J. T., Woynow J. A., Peters K. W., and Rose M. C. (1999). Respiratory carcinoma cell lines-MUC genes and glycoconjugates. *Am J Respir Cell Mol Biol* **20**, 500-510.

Bloodgood R. (2005). http://www.med-d.virginia.edu/public/CourseSitesDocs/CellandTissue Structure/handouts/unrestricted/original/MMHndt_Respiratory.html.

Borst P., Evers R., Kool M., and Wijnholds J. (1999). The multidrug resistance protein family. *Biochim Biophys Acta - Biomembranes* **1461**, 347-357.

Bosquillon C., Clear N., Bennett J., and Forbes B. (2008). A simple isolated perfused lung technique for measurement of pulmonary absorption. *J Pharm Pharmacol*. In preparation.

Braun A., Hammerle S., Suda K., Rothen-Rutishauser B., Gunthert M., Kramer S. D., and Wunderli-Allenspach H. (2000). Cell cultures as tools in biopharmacy. *Eur J Pharm Sci* **11**, S51-S60.

Brazzel R. K., and Kostenbauder H. B. (1982). Isolated perfused rabbit lung as a model for intravascular and intrabronchial administration of bronchodilator drugs II: Isoproterenol prodrugs. *J Pharm Sci* **71**, 1274-1281.

Brewis R. A. L., Corrin B., Geddes D. M., and Gibson G. J., eds. (1995). Respiratory Medicine, second edition, W. B. Saunders Company Ltd, London.

Brown R. A., Jr., and Schanker L. S. (1983). Absorption of aerosolized drugs from the rat lung. *Drug Metab Dispos* **11**, 355-360.

Brouillard F., Tondelier D., Edelman A., and Baudouin-Legros M. (2001). Drug resistance induced by ouabain via the stimulation of mdr1 gene expression in human carcinomatous pulmonary cells. *Cancer Res* **61**, 1693–1698.

Bundgaard M., Frokjaer-Jensen J., and Crone C. (1979). Endothelial plasmalemmal vesicles as elements in a system of branching invaginations form the cell surface. *Proc Natl Acad Sci USA* **76**, 6439-6442.

Burger H., Foekens J. A., Look M. P., Meijer-van Gelder M. E., Klijn J. G., Wiemer E. A., Stoter G., and Nooter K. (2003). RNA expression of breast cancer resistance protein, lung resistance related protein, multidrug resistance-associated proteins 1 and 2, and multidrug resistance gene 1 in breast cancer: correlation with chemotherapeutic response. *Clin Cancer Res* **9**, 827-36.

Burton J. A., and Schanker L. S. (1974). Absorption of corticosteroids from the rat lung. *Steroids* **23**, 617-624.

Byron P. R. (1986). Prediction of drug residence times in regions of the human respiratory-tract following aerosol inhalation. *J Pharm Sci* **75**, 433-438.

Byron P. R., and Niven R. W. (1988). A novel dosing method for drug administration to the airways of the isolated perused rat lung. *J Pharm Sci* 77, 693-695.

Byron P. R., Roberts N. S. R., and Clark R. (1986). In isolated perfused rat lung preparation for the study of aerosolized drug deposition and absorption. *J Pharm Sci* **75**, 168-171.

Campbell L., Abulrob A.-N. G., Kandalaft L. E., Plummer S., Hollins A. J., Gibbs A., and Gumbleton M. (2003). Constitutive expression of P-glycoprotein in normal lung alveolar epithelium and functionality in primary alveolar epithelial cultures. *J Pharmacol Exp Ther* **304**, 441–452.

Campbell L., Hollins A. J., Al Eid A., Newman G. R., von Ruhland C., and Gumbleton M. (1999). Caveolin-1 expression and caveolae biogenesis during cell transdifferentiation in lung alveolar epithelial primary cultures. *Biochem Biophys Res Commun* **262**, 744-751.

Camps P. W. L. (1929). A note on the inhalation treatment of asthma. *Guy's Hosp Rep* **79**, 496- 498.

Cassara M. L., Figueroa J. M., Roemele P. E., Florea B. I., and Junginger H. E. (2003). Uptake, accumulation and release of budesonide in an vitro model of human bronchial cells (Calu-3) cultured in monolayers. *Pediatr Res* **53**, 3.

Cavet M. E., West M., and Simmons N. L. (1996). Transport and epithelial secretion of the cardiac glycoside, digoxin, by human intestinal epithelial (Caco-2) cells. *Br J Pharmacol* **118**, 1389-1396.

Cavet M. E., West M., and Simmons N. L. (1997). Transepithelial transort of the fluoroquinoline ciprofloxacin by human airway epithelial Calu-3 cells. *Antimicrob Agents Chemother* **41**, 2693-2698.

Chediak A. D., and Warren A. (1990). The circulation of the airways: anatomy, physiology and potential role in drug delivery to the resporatory tract. *Adv Drug Deliv Rev* **5**, 11-18.

Choi C. (2005). ABC transporters as multidrug resistance mechanisms and the development of chemosensitizers for their reversal. *Cancer Cell Int* **5**, 30.

Chu T., Iin T., and Kawinski E. (1994). Detection of soluble P-glycoprotein in culture media and extracellular fluids. *Biochem Biophys Res Commun* **203**, 506-512.

Conhaim R. L., Eaton A., Staub N. C., and Heath T. D. (1988). Equivalent pore estimate for the alveolar-airway barrier in isolated dog lung. *J Appl Physiol* **64**, 1134-1142.

Cornwell M., Gottesman M., and Pastan I. (1986). Increased vinblastine binding to membrane vesicles from multidrug resistant KB cells. *J Biochem* **262**, 7921-7928.

Crandall E. D., and Kim K. J. (1991). Alveolar epithelial barrier properties, in: *The Lung* (Crystal R. G., West J. B. *et al.,* eds), 273-287, Raven Press Ltd., New York.

Cromwell O., Hamid Q., Corrigan C. J., Barkans J., Meng Q., Collins P. D., and Kay A. B. (1992). Expression and generation of interleukin-8, IL-6 and granulocyte-macrophage colonystimulating factor by bronchial epithelial cells and enhancement by IL-l beta and tumour necrosis factor-alpha. *Immunology* **77**, 330-337.

Dalby R. N., Hickney A. J., and Tianom S. L. (1996). Medical devices for the delivery of therapeutic aerosols to the lung, in *Inhalation Aerosols-Physical and Biological Basis for Therapy* (Hickney A. J., ed), 441-473, Marcel Dekker, New York.

Davidson D. J., Kilanowski F. M., Randell S. H., Sheppard D. N., and Dorin J. R. (2000). A primary culture model of differentiated murine tracheal epithelium. *Am J Physiol Lung Cell Mol Physiol* **279**, L766-L778.

de Greef C., Sehrer J., Viana F., von Acker K., Eggermont J., Mertens L., Raeymaekers L., Droogmans G., and Nilius B. (1995). Volume-activated chloride currents are not correlated with P-glycoprotein expression. *Biochem J* **307**, 713-718.

de Lannoy I. A. M., and Silverman M. (1992). The MDR1 gene product, P-glycoprotein, mediates the transport of the cardiac glycoside, digoxin. *Biochem Biophys Res Commun* **189**, 551–557.

Dean M., Hamon Y., and Chimini G. (2001). The human ATP-binding cassette (ABC) transporter superfamily. *J Lipid Res* **42**, 1007-1017.

Dollery C. T., and Junod A. F. (1976). Concentration of (+/-) propranolol in isolated, perfused lungs of rat. *Br J Pharmacol* **57**, 67-71.

Doring F., Will J., Amashes S., Clauss W., Ahlbrecht H., and Daniel H. (1998). Minimal molecular determinants of substrates for recognition by the intestinal peptide transporter. *J Biol Chem* **273**, 23211-23218.

Effros R. M., and Mason G. R. (1983). Measurements of pulmonary epithelial permeability *in vivo*. *Am Rev Respir Dis* **127**, S59-S65.

Effros R. M., Murphy C., Hacker A., Schapira R. M., and Bongard R. (1994). Reduction and uptake of methylene-blue form rat air spaces. *J Appl Physiol* 77, 1460-1465.

Ehrhardt C., Kneuer C., Fiegel J., Hanes J., Schaefer U. F., Kim K. J., and Lehr C. M. (2002). Influence of apical fluid volume on the development of functional intercellular junctions in the human epithelial cell line 16HBE14o-: implications for use of this cell line as an *in vitro* model for bronchial drug absorption studies. *Cell Tissue Res* **308**, 391-400.

Ehrhardt C., Kneuer C., Laue M., Schaefer U. F., Kim K. J., and Lehr C. M. (2003). 16HBE14o- human bronchial epithelial cell layers express P-glycoprotein, lung resistance-related protein, and caveolin-1. *Pharm Res* **20**, 545-551.

Enna S. J., and Schanker L. S. (1973). Phenol red absorption from the rat lung: Evidence of carrier transport. *Life Sciences* **12**, 231-239.

Endicott J., and Ling V. (1997). The biochemistry of P-glycoprotein-mediated multidrug resistance. *Annu Rev Biochem* **58**, 137-171.

Evans M. J., Van Winkle L. S., Fanuchi M. V., and Plopper C. G. (2001). Cellular and molecular characteristics of basal cells in airway epithelium. *Exp Lung Res* **27**, 401-415.

Evers R., Kool M., Smith A. J., van Deemter L., de Haas M., and Borst P. (2000). Inhibitory effect of the reversal agents V-104, GF120918 and Pluronic L61 on MDR1 Pgp-, MRP1- and MRP2-mediated transport. *Br J Cancer* **83**, 366–374.

Ferry D. R., Glossman H., and Kaumann A. J. (1985). Relationship between the stereoselective negative inotropic effects of verapamil enantiomers and their binding to putative calcium channels in the human heart. *Br J Pharmacol* **84**, 811-824.

Fielding C. J., and Fielding P. E. (1997). Intracellular cholesterol transport. *J Lipid Res* **38**, 1503-1521.

Finkbeiner W. E., Carrier S. D., and Teresi C. E. (1993). Reverse transcription-polymerase chain reaction (RT-PCR) phenotypic analysis for the cell-cultures of human tracheal epithelium, tracheobronchial glands, and lung carcinomas. *J Am Respir Cell Mol Biol* **9**, 547-556.

Fisher A. B., Dodia C., and Linask J. (1980). Perfusate composition and edema formation in isolated rat lungs. *Exp Lung Res* **1**, 13-21.

Flens M. J., Scheffer G. L., van der Valk P., Broxterman H. J., Eijdems E. W., Huysmans A. C., Izquierdo M. A., and Scheper R. J. (1997). Identification of novel drug resistance-associated proteins by a panel of rat monoclonal antibodies. *Int J Cancer* **73**, 249-257.

Florea B. I., Cassara M. L., Junginger H. E., and Borchard G. (2003). Drug transport and metabolism characteristics of the human airway epithelial cell line Calu-3. *J Control Rel* **87**, 131-138.

Florea B. I., van der Sandt I. C. J., Schrier M. S., Kooiman K., Deryckere K., de Boer A. G., Junginger H. E., and Borchard G. (2001). Evidence of P-glycoprotein mediated apical to basolateral transport of flunisolide in human broncho-tracheal epithelial cells (Calu-3). *Br J Pharmacol* **134**, 1555-1563.

Flynn G. L., Yalkowski S. H., and Roseman T. J. (1974). Mass-transport phenomena and models – theoretical concepts. *J Pharm Sci* **63**, 479-510.

Forbes B. (2000). Human airway epithelial cell lines for *in vitro* drug transport and metabolism studies. *Pharm Sci Tech Today* **3**, 18-27.

Forbes B., and Ehrhardt C. (2005). Human respiratory epithelial cell culture for drug delivery applications. *Eur J Pharm Biopharm* **60**, 193-205.

Foster K. A., Avery M. L., Yazdanian M., and Audus K. L. (2000). Characterization of the A549 cell lines and type II pulmonary epithelial cell model for drug metabolism. *Exp Cell Res* **243**, 359-366.

Foth H., Geng W. P., Krug N., and Vetterlein F. (1995). Pulmonary uptake of bupivacaine in isolated perfused rat lung. *Naunyn Schmiedebergs Arch Pharmacol* **351**, 99-106.

Frokjaer-Jensen J. (1991). The endothelial vesicle system in cryofixed frog mesenteric capillaries analyse by othrathin serial sectioning. *J Electron Microsc Tech* **19**, 291-304.

Gan L. S., Yanni S., and Thakker D. R. (1998). Modulation of the tight junctions of the Caco-2 cell monolayers by H2-antagonists. *Pharm Res* **15**, 53-57.

Ganapathy M. E., Huang W., Wang H., Ganapathy V., and Leibach F. H. (1998). Valacyclovir: a substrate for the intestinal and renal peptide transporters PEPT1 and PEPT2. *Biochem Biophys Res Commun* **246**, 470-475.

Gardiner T. H., and Schanker L. S. (1974). Absorption of disodium cromoglycate from the rat lung: evidendce of carrier transport. *Xenobiotica* **4**, 725-731.

Germann U. (1996). P-glycoprotein - a mediator of multidrug resistance in tumour cells. *Eur J Cancer* **32A**, 927-944.

Gillespie M. N., Krechniak J. W., Crooks P. A., Altiere R. J., and Olson J. W. (1985). Pulmonary metabolism of exogenous enkephalins in isolated perfused rat lungs. *J Pharmacol Exp Ther* **232**, 675-681.

Gorin A. B., and Stewart P. A. (1979). Differential permeability of endothelial and epithelial barriers to albumin flux. *J Appl Physiol* **47**, 1315-1324.

Gottesman M., and Pastan I. (1993). Biochemistry of multidrug resistance mediated by the multidrug transporter. *Annu Rev Biochem* **62**, 385-427.

Gottesman M. M., Hrycyna C. A., Schoenlein P. V., Germann U. A., and Pastan I. (1995). Genetic analysis of the multidrug transporter. *Annu Rev Genet* **29**, 607-649.

Grainger C. I. (2008). PhD thesis. King's College London, University of London.

Grainger C. I., Greenwell L. L., Lockley D. J., Martin G. P., and Forbes B. (2006). Culture of Calu-3 cells at the air interface provides a representative model of the airway epithelial barrier. *Pharm Res* **23**, 1482-1490.

Gres M. C., Julian B., Bourrie M., Meunier V., Roques C., Berger M., Boulenc X., Berger Y., and Fabre G. (1998). Correlation between oral drug absorption in humans, and apparent drug permeability in TC-7 cells, a human epithelial intestinal cell line: comparison with the parental Caco-2 cell line. *Pharm Res* **15**, 726-733.

Groneberg D. A., Eynott P. R., Doring F., Dinh T. Q., Oates T., Barnes P. J., Chung K. F., Daniel H., and Fischer A. (2002). Distribution and function of the peptide transporter PEPT2 in normal and cystic fibrosis human lung. *Thorax* **57**, 55-60.

Groneberg D. A., Witt C., Wagner U., Chung K. F., Fischer A. (2003). Fundamentals of pulmonary drug delivery. *Respir Med* **97**, 382–387.

Gruenert D. C. (1987). Differentiated properties of human epithelial cells transformed *in vitro*. *Biotechniques* **5**, 740-749.

Gruenert D. C., Basbaum C. B., and Widdicombe J. H. (1990). Long-term culture of normal and cystic fibrosis epithelial cells grown under serum-free conditions. *In vitro Cell Dev Biol* **26**, 411-418.

Gruenert D. C., Dieter C., Finkbeiner W. E., and Widdicombe J. H. (1995). Culture and transformation of human airway epithelial cells. *Am J Physiol Lung Cell Mol Physiol* **268**, L347-L360.

Grundemann D., Gorboulev V., Gambaryan S., Veyhl M., and Koepsell H. (1994). Drug excretion mediated by a new prototype of polyspecific transporter. *Nature* **372**, 549-552.

Gumbleton M. (2001). Caveolae as potential macromolecule trafficking compartments within alveolar epithelium. *Adv Drug Deliv Rev* **49**, 281-300.

Hamilton[a] K. O., Backstrom G., Yazdanian M. A., and Audus K. L. (2001). P-glycoprotein efflux pump expression and activity in Calu-3 cells. *J Pharm Sci* **90**, 647 – 658.

Hamilton[b] K. O., Yazdanian M. A., and Audus K. L. (2001). Modulation of P-glycoprotein activity in Calu-3 cells using steroids and ß-ligands. *Int J Pharm* **228**, 171–179.

Hamilton K. O., Yazdanian M. A., and Audus K. L. (2002). Contribution of efflux pump activity to the delivery of pulmonary therapeutics. *Current Drug Metabolism* **3**, 1-12.

Han H. K., Oh D. M., and Amidon G. L. (1998). Cellular uptake mechanism of amino acid ester prodrugs in Caco-2/hPEPT1 cells overexpressing a human peptide transporter. *Pharm Res* **15**, 1382-1386.

Harkema J. R., Mariassy A., George J. S., Hyde D. M., and Plopper C. G., (1991). Epithelial cells of the conducting airway; a species comparison, in *The Airway Epithelium – Physiology, Pathophysiology and Pharmacology* (Farmer S. G., and Hay D. W. P., eds), 3–39, Marcel Dekker Inc., New York.

Hartiala J., Uotila P., and Nienstedt W. (1979). Metabolism of progesterone in the isolated perfused rat lungs. *J Steroid Biochem Mol Biol* **11**, 1539-1541.

Hemberger J. A., and Schanker L. S. (1978). Pulmonary absorption of drugs in the neonatal rat. *Am J Physiol-Cell Physiol* **234**, C191-C197.

Hickney A. J., and Thompson D. C. (1992). Physiology of the airways, in *Pharmaceutical Inhalation Aerosol Technology* (Hickney A. J. ed), 1-27, Marcel Dekker, New York.

Higgins C. (1993). The ABC transport channel superfamily: an overview. *Sems Cell Biol* **4**, 1-5.

Higgins C. F., and Gottesman M. M. (1992). Is the multidrug tranporter a flippase? *Trend Biochem Sci*, **17**, 18-21.

Hoskins J., De Herdt S. V., Moore R. E., and Bumol T. F. (1993). The development and characterization of Vinca alkaloid-resistant Caco-2 human colorectal cell lines expressing mdr-1. *Int J Cancer* **53**, 680-688.

Horio M., Chin K.-V., Currier S., Goldenberg S., Williams C., Pastan I., Gottesman M. M., and Handlers J. (1989). Transepithelial transport of drugs by the multidrug transporter in cultured Madin-Darby canine kidney cell epithelia. *J Biol Chem* **264**, 14880-14891.

Hosoya K. I., Kim K. J., and Lee V. H. (1996). Age-dependent expression of P-glycoprotein in Caco-2 monolayers. *Pharm Res* **13**, 885-890.

Hukkanen J. (2000). Xenobiotic-metabolizing cytochrome P450 enzymes in human lung. *Acta Universitas Ouluensis*.

Hunter J., and Hirst B. H. (1997). Intestinal secretion of drugs. The role of P-glycoprotein and related drug efflux system in limiting oral drug absorption. *Adv Drug Deliv Rev* **25**, 129-157.

Hyafil F., Vergely C., Du Vignaud P., and Grand-Perret T. (1993). *In vitro* and *in vivo* reversal of multidrug resistance by GF120918, an acridonecarboxamide derivative. *Cancer Res* **53**, 4595–4602.

Ito S., Koren G., and Harper P. A. (1992). Energy-dependent transport of digoxin across renal tubular cell monolayers (LLC-PK1). *Can J Physiol Pharmacol* **71**, 40–47.

Ito S., Woodland C., Harper P. A., and Koren G. (1993). The mechanism of the verapamil-digoxin interaction in renal tubular cells (LLC-PK1). *Life Sci* **53**, L399-L403.

Iwamoto K., Watanabe J., and Yonekawa H. (1989). Effects of bovine serum albumin and recirculation rate on the uptake of propranolol by rat perfused lung. *J Pharm Pharmacol* **41**, 266-268.

Izquierdo M. A., Scheffer G. L., Flens M. J., Giaccone G., Broxterman H. J., Meijer C. J., van der Valk P., and Scheper R. J. (1996a). Broad distribution of the multidrug resistance-related vault lung resistance protein in normal human tissues and tumors. *Am J Pathol* **148**, 877-887.

Jeppsson A. B., Nilsson E., and Waldeck B. (1994). Formoterol and salmeterol are both long acting compared to terbutaline in the isolated perfused and ventilated guinea-pig lung. *Eur J Pharmacol* **257**, 137-143.

Jetten A. M. (1991). Growth and differentiation factors in tracheobronchial epithelium. *Am J Physiol Lung Cell Mol Physiol* **260**, L361-L373.

Jetten A. M., Brody A. R., Deas M. A., Hook G. E. R., Rearick J. I., and Tacher S. M. (1987). Retinoic acid and substratum regulate the differentiation of rabbit tracheal epithelial cells into squamous and secretory phenotype. *Lab Invest* **56**, 654-664.

Jiang C., Finkbeiner W. E., Widdicombe J. H., McCray P. B., and Miller S. S. (1993). Altered fluid transport across airway epithelium in cystic fibrosis. *Nature Lond* **262**, 424-427.

Johnstone R., Ruefli A., and Smyth M. (2000). Multiple physiological functions for multidrug transporter P-glycoprotein. *Trends Biochem Sci* **25**, 1-6.

Juliano R. L., and Ling V. (1976). A surface glycoprotein modulating drug permeability in Chinese hamster ovary cell mutants. *Biochim Biophys Acta* **455**, 152-62.

Junginger H. E., and Verhoef J. C. (1998). Macromolecules as safe penetration enhancers for hydrophilic drugs - a fiction? *Pharm Sci Tech Today* **1**, 370-376.

Karlsson J., Ungell A., Grasjo J., and Artursson P. (1999). Paracellular drug transport across intestinal epithelia: influence of charge and induced water flux. *Eur J Pharm Sci* **9**, 47-56.

Keenan K. P., and Resau J. H. (1991). Cell-to-cell communication: a differential response to TGF-beta in normal and transformed (BEAS-2B) human bronchial epithelial cells. *Carcinogenesis* **12**, 1993-1999.

Kekuda R., Prasad P. D., Wu X., Wang H., Fei Y. J., Leibach F. H., and Ganapathy V. (1998). Cloning and functional characterization of a potential-sensitive, polyspecific organic cation transporter (OCT3) most abundantly expressed in placenta. *J Biol Chem* **273**, 15971-15979.

Kessel D., Beck W. T., Kukuruga D., and Schulz V. (1991). Characterization of multidrug resistance by fluorescent dyes. *Cancer Res* **51**, 4665–4670.

Kim K.-J., and Malik A. B. (2003). Protein transport across the lung epithelial barrier. *J Physiol Lung Cell Mol Physiol* **284**, L247-L259.

Ko A. C., Hirsh E., Wong A. C., Moore T. M., Taylor A. E., Hirschl R. B., and Younger J. G. (2003). Segmental hemodynamics during partial liquid ventialtion in isolated rat lungs. *Resuscitation* **57**, 85-91.

Kroll F., Karlsson J. A., Nilsson E., Persson C. G. A., and Ryrfeldt A. (1986). Lung-mechanics of the guinea pig isolated perfused lung. *Acta Physiol Scand* **128**, 1-8.

Lansley A. B. (1993). Mucociliary clearance and drug delivery via the respiratory tract. *Adv Drug Deliv Rev* **11**, 299-327.

Lechapt-Zalcman E., Hurbain I., Lacave R., Commo F., Urban T., Antoine M., Milleron B., and Bernaudin J. F. (1997). MDR1-P-gp 170 expression in human bronchus. *Eur Respir J* **10**, 1837-1843.

Lechner J. F., and LaVeck M. A. (1985). A serum-free method for culturing normal human bronchial epithelial cells at clonal density. *J Tissue Culture Meth* **9**, 43-48.

Lechner J. F., McClendon I. A., LaVeck M. A., Shamsuddin A. M., and Harris C. C. (1983). Differential control by platelet factors of squamous differentiation in normal and malignant human bronchial epithelial cells. *Cancer Res* **43**, 5915-5921.

Lecureur V., Sun D., Hargrove P., Schuetz E. G., Kim R. B., Lan L. B., and Schuetz J. D. (2000). Cloning and expression of murine sister of P-glycoprotein reveals a more discriminating transporter than MDR1/P-glycoprotein. *Mol Pharmacol* **57**, 24-35.

Lee V. H. (2000). Membrane transporters. *Eur J Pharm Sci* **11**, S41-S50.

Lee J. Y., Urbatsch I. L., Senior A. E., and Wilkens S. (2002). Projection structure of P-glycoprotein by electron microscopy – evidence for a closed conformation of the nucleotide binding domains. *J Biol Chem* **277**, 40125-40131.

Lee K., and Thakker D. R. (1999). Saturable transport of H2-antagonists ranitidine and famotidine across Caco-2 cell monolayers. *J Pharm Sci* **88**, 680-687.

Leonard G. D., Fojo T., and Bates S. E. (2003). The role of ABC transporters in clinical practice. *Oncologist* **8**, 411-424.

Letrent S. P., Pollack G. M., Brouwer K. R., and Brouwer K. L. R. (1999). Effects of a potent and specific P-glycoprotein inhibitor on the blood-brain barrier distribution and antinociceptive effect of morphine in the rat. *Drug Metab Dispos* **27**, 827-834.

Liedtke C. M. (1988). Differentiated properties of rabbit tracheal epithelial cells in primary culture. *Am J Physiol* **255**, C760-C770.

Lin Y. J., and Schanker L. S. (1981). Pulmonary absorption of amino-acids in the rat-evidence of carrier tranport. *Am J Physiol* **240**, C215-C221.

Lin H., Li H., Cho H.-J., Bian S., Roh H.-J., Lee M.-K., Kim J. S., Chung S.-J., Shim C.-K., and Kim D.-D. (2006). Air-liquid interface (ALI) culture of human bronchial epithelial cell monolayers as model for airway drug transport studies. *J Pharm Sci* **96**, 341-350.

Ling V. (1995). P-glycoprotein: its role in drug resistance. *Am J Med* **99**, 31S-34S.

Liu Z., Lheureux F., Pouliot J. F., Heckel A., Bamberger U., and Georges E. (1996). BIBW22BS, potent multidrug resistance-reversing agent, binds directly to P-glycoprotein and accumulates in drug-resistant cells. *Mol Pharmacol* **50**, 482-492.

Lipworth B. J. (1996). Pharmacokinetics of inhaled drugs. *Br J Clin Pharmacol* **42**, 697-705.

Lisanti M. P., Scherer P. E., Tang Z., and Sargiacomo M. (1994). Caveolae, caveolin and caveolin-rich membrane domains: a signaling hypothesis. *Trend Cell Biol* **4**, 321-235.

Longmore W. J. (1982). The isolated perfused lung as a model for studies of lung metabolism, in: *Lung Development: Biological and Clinical Perspectives* (Farrel P. M., ed), 101-110, Academic Press Inc.

Loo T. W., and Clarke D. M. (1997). Correction of defective protein kinesis of human P-glycoprotein mutants by substrates and modulators. *J Biol Chem* **272**, 709-712.

Lowes S., Cavet M. E., and Simmons N. L. (2003). Evidence for a non-MDR1 component in digoxin secretion by human intestinal Caco-2 epithelial layers. *Eur J Pharmacol* **458**, 49-56.

Ma J., Bhat M., and Rojanasakul Y. (1996). Drug metabolism and enzyme kinterics in the lung, in: *Inhalation Aerosols: Physical and Biological Basis for Therapy* (Hickey A. J., ed), 155-196, Marcel Dekker, New York.

Manford F., Tronde A., Jeppsson A.-B., Patel N., Johansson F., and Forbes B. (2005). Drug permeability in 16HBE14o- airway cell layers correlates with absorption from the isolated perfused rat lung. *Eur J Pharm Sci* **26**, 414-420.

Mason G. R., Peters A. M., Bagdades E., Myers M. J., Snooks D., and Hughes J. M. B. (2001). Evaluation of pulmonary alveolar epithelial integrity by the detection of restriction to diffusion of hydrophilic solutes of different molecular sizes. *Clin Sci* **100**, 231-236.

Mason R. J., and Crystal R. G. (1998). Pulmonary cell biology. *Am J Respir Crit Care Med* **157**, S72-S81.

Masood A. R., and Thomas S. H. L. (1996). Systemic absorption of nebulized morphine compared with oral morphine in healthy subjects. *Br J Clin Pharmacol* **41**, 250–252.

Materna V., Pleger J., Hoffmann U., and Lage H. (2004). RNA expression of MDR1/P-glycoprotein, DNA-topoisomerase I, and MRP2 in ovarian carcinoma patients: correlation with chemotherapeutic response. *Gynecol Oncol* **94**, 152-60.

Mathias N. R., Timoszyk J., Stetsko P. I., Megill J. R., Smith R. L., and Wall D. A. (2002). Pemeability characteristics of Calu-3 human bronchial epithelial cells: *In vitro-in vivo* correlation to predict absorption in rats. *J Drug Target* **10**, 31-40.

Mathias N. R., Yamashita F., and Lee V. H. L. (1996). Respiratory epithelial cell culture models for evaluation of ion and drug transport. *Adv Drug Deliv Rev* **22**, 215-249.

Matsukawa Y., Lee V. H. L., Crandall E. D., and Kim K.-J. (1997). Size-dependent dextran transport across rat alveolar epithelial cell monolayers. *J Pharm Sci* **86**, 305-309.

Mehendale H. M., and El Bassiouni E. A. (1975). Uptake and disposition of aldrin and dieldrin by isolated perfused rabbit lung. *Drug Metab Dispos* **3**, 543-556.

Mette S. A., Pilewski J., Buck C. A., and Albelda S. M. (1993). Distribution of integrin cell adhesion receptors on normal bronchial epithelial cells and lung cancer cells *in vitro* and *in vivo*. *Am J Respir Cell Mol Biol* **8**, 562-572.

Moscow J. A., Schneider E., Ivy S. P., and Cowan K. H. (1997). Multidrug resistance. *Cancer Chemother Biol Response Modif* **17**, 139-177.

Moseley R. H., Smit H., van Solkema B. G., Wang W., and Meijer D. K. (1996). Mechanisms for the hepatic uptake and biliary excretion of tributylmethylammonium: studies with rat liver plasma membrane vesicles. *J Pharmacol Exp Ther* **276**, 561-567.

Niemeier R. W., and Bingham E. (1972). An isolated perfused lung preparation for metabolic studies. *Life Sci* **11**, 807-820.

Niven R. W., and Byron P. R. (1988). Solute absorption from the airways of the isolated rat lung. I. The use of absorption data to quantify drug dissolution or release in the respiratory tract. *Pharm Res* **5**, 574-579.

Niven R. W., and Byron P. R. (1990). Solute absorption from the airways of the isolated rat lung. II. Effect of surfactants in absorption of fluorescein. *Pharm Res* **7**, 8-13.

Niven R. W. (1992). Modulated drug therapy with inhalation aerosols, in *Pharmaceutical inhalation aerosol technology* (Hickey A. J., ed.), 321-359, Marcel Dekker, Chicago.

Noe B., Hagenbuch B., Stieger B., and Meier P. J. (1997). Isolation of a multispecific organic anion and cardiac glycoside from rat brain. *Proc Natl Acad Sci USA* **94**, 10346-10350.

Okuda S., Fukuda Y., Takahashi K., Fujita T., Yamamoto A., and Muranishi S. (1996). Transport of drugs across the Xenopus pulmonary membrane and their absorption enhancement by various absorption enhancers. *Pharm Res* **13**, 1247-1251.

Ott R. J., Hui A. C., Yuan G., and Giacomini K. M. (1991). Organic cation transport in human renal brush-border membrane vesicles. *Am J Physiol* **261**, F443-F451.

Pal D., Udata C., and Mitra A. K. (2000). Transport of cosolane – a highly lipophilic novel anti-HIV agent – across Caco-2 cell monolayers. *J Pharm Sci* **89**, 826-833.

Patel J., Pal D., Vangala V., Gandhi M., and Mitra A. K. (2002). Transport of HIV-protease inhibitors across 1α,25di-hydroxy vitamin D3-treated Calu-3 cell monolayers: modulation of P-glycoprotein activity. *Pharm Res* **19**, 1696 -1703.

Patton J. S. (1996). Mechanisms of macromolecule absorption by the lungs. *Adv Drug Deliv Rev* **19**, 3-36.

Patton J. S., Bukar J., Nagarajan S. (1999). Inhaled insulin. *Adv Drug Deliv Rev* **35**, 235–247.

Pavelic Z. P., Reising J., Pavelic L., Kelley D. J., Stambrook P. J., and Gluckman J. L. (1993). Detection of P-glycoprotein with four monoclonal antibodies in normal and tumor tissues. *Arch Otolaryngol Head Neck Surg* **119**, 753-757.

Pennock G. D., Dalton W. S., Roeske R. W., Appleton P. C., Mosley K., Plezia P., Miller T. P., and Salmon S. E. (1991). Systemic toxic effects associated with high-dose verapamil infusion and chemotherapy administration. *J Natl Cancer Inst* **83**, 105-110.

Pezron I., Mitra R., Pal D., and Mitra A. K. (2002). Insulin aggregation and assymetric transport across human bronchial epithelial cell monolayers (Calu-3). *J Pharm Sci* **91**, 1135-1146.

Planes C., Escoubet B., Blot-Chabaud M., Friedlander G., Farman N., and Clerici C. (1997). Hypoxia downregulates expression and activity of epithelial sodium channels in rat alveolar epithelial cells. *Am J Respir Cell Mol Biol* **17**, 508–518.

Plopper C. G. (1996). Structure and function of the lung, in: *Respiratory system* (Jones T. C., Dungworth D. L., and Mohr U., eds.), 135-150, Springer Verlag, Berlin.

Predescu S. A., Predescu D. N., and Palade G. E. (1997). Plasmalemmal vesicles function as transcytotic carriers for small proteins in the continuous endothelium. *Am J Physiol* **272**, H937-H949.

Puchelle E., de Bentzmann G. S., and Higenbottam T. (1995). Airway secretions and lung liquids, in: *Respiratory Medicine* (Brewis R. A. L., Corrin B., Geddes D. M., and Gibson G. J., eds.), 97-111, W. B. Saunders Company Ltd, London.

Reignier J., Mazmanian M., Chapelier A., Alberici G., Menasche P., Wiess M., and Herve P. (1995). Evaluation of a new presevation solution-Celsior in the isolated rat lung. *J Heart Lung Transplant* **14**, 601-604.

Robert J., and Jarry C. (2003). Multidrug resistance reversal agents. *J Med Chem* **46**, 4805–4817.

Roepe P. D. (1995). The role of the MDR protein in altered drug translocation across tumour cell membranes. *Biochem Biophys Acta* **1241**, 385-406.

Romaldson P., Bendayan M., Gingras D., Piquette-Miller M., and Bendayan R. (2004). Cellular localization and functional expression of P-glycoprotein in rat astrocyte cultures. *J Neurochem* **89**, 788-800.

Rosenberg M. F., Kamis A. B., Callaghan R., Higgins C. F., and Ford R. C. (2003). Three-dimensional structures of the mammalian multidrug resistance P-glycoprotein demonstrate major conformational changes in the transmembrane domains upon nucleotide binding. *J Biol Biochem* **278**, 8294-8299.

Roth L. A., and Wiersman D. A. (1979). Role of the lung in total body clearance of circulating drugs. *Clin Pharmacokinet* **4**, 355-367.

Rubin B. K. (1996). Therapeutic aerosols and airway secretions. *J Aerosol Med* **9**, 123-130.

Ryrfeldt A., and Nilsson E. (1978). Uptake and biotransformation of irbuterol and terbutaline in isolated perfused rat and guinea pig lungs. *Biochem Pharmacol* **27**, 301-305.

Ryrfeldt A., Persson G., and Nilsson E. (1989). Pulmonary disposition of the potent glucocorticoid budesonid, evaluated in an isolated perfused rat lung model. *Biochem Phamacol* **38**, 17-22.

Sabattini E., Bisgaard K., Ascani S., Poggi S., Piccioli M., Ceccarelli C., Pieri F., Fraternali–Orcioni G., and Pileri S. A. (1998). The EnVision ™ system: a new immunohistochemical method for diagnostics and research. Critical comparison with the APAAP, ChemMate™, CSA, LABC, and SABC techniques. *J Clin Pathol* **51**, 506–511.

Sakagami M., Omidi Y., Campbell L., Kandalaft L. E., Barar J., and Gumbleton M. (2004). Molecular evidence for the expression of MHC class I-like IGG receptor, FcRn, within intact rat alveolar epithelium and in primary alveolar cell cultures. *Respir Drug Deliv* **9**, 885-888.

Sauna Z. E., Smith M. M., Muller M., Kerr K. M., and Ambudkar S. V. (2001). The mechanism of action of multi-drug-resistance-linked P-glycoprotein. *J Bioenerg Biomembr* **33**, 481-491.

Sawada G. A., Barsuhn C. L., Lutzke B. S., Houghton M. E., Padbury G. E., Ho N. F., and Raub T. J. (1999). Increased lipophilicity and subsequent cell partitioning decrease passive transcellular diffusion of novel, highly lipophilic antioxidants. *J Pharm Exp Ther* **288**, 1317-1326.

Saeki T., Ueda K., Tanigawara Y., Hori R., and Komano T. (1993). Human P-glycoprotein transports cyclosporine A and FK506. *J Biol Chem* **268**, 6077-6080.

Sakagami M. (2006). *In vivo, in vitro* and *ex vivo* models to assess pulmonary absorption and disposition of inhaled therapeutics for systemic delivery. *Adv Drug Deliv Rev* **58**, 1030-1060.

Sakagami M., Byron P. R., and Rypacek F. (2002). Biochemical evidence for transcytotic absorption of polyaspartamide from the rat lung: Effects of temperature and metabolic inhibitors. *J Pharm Sci* **91**, 1958-1968.

Salathé M., O'Riordan T. G., and Wanner A. (1997). Mucociliary clearance, in: *The Lung: Scientific Foundations* (Crystal R. G., and West J. B., eds.), 2295-2308, Lippincott-Raven Publishers, Philadelphia.

Samet J. M., and Cheng P. W. (1994). The role of airway mucus in pulmonary toxicology. *Environ Health Perspect* **102 Suppl 2**, 89-103.

Schanker L. S. (1978). Drug absorption from the lung. *Biochem Pharmacol* **27**, 381–385.

Schanker L. S., and Hemberger J. A. (1983). Relation between molecular weight and pulmonary absorption rate of lipid - insoluble compounds in neonatal and adult rats. *Biochem Pharmacol* **32**, 2599-2601.

Schanker L. S., Mitchell E. W., and Brown R. A., Jr. (1986). Species comparison of drug absorption from the lung after aerosol inhalation or intratracheal injection. *Drug Metab Dispos* **14**, 79-88.

Scheffer A., Pinjeborg A., Smit E., Mueller M., Postma D., Timens W., van der Walk P., de Vries E., and Scheper R. (2002). Multidrug resistance related molecules in human and murine lung. *J Clin Pathol* **55**, 332-339.

Schinkel A. (1997). The physiological function of drug-transporting P-glycoproteins. *Sem Cancer Biol* **8**, 161-170.

Schinkel A. (1999). P-glycoprotein, a gatekeeper in the blood-brain barrier. *Adv Drug Deliv Rev* **36**, 179-194.

Schinkel A. H., Wagenaar E., van Deemter L., Mol C. A. A. M., and Borst P. (1995). Absence of the mdr1a P-glycoprotein in mice affects tissue distribution and pharmacokinetics of dexamethasone, digoxin, and cyclosporin A. *J Clin Invest* **96**, 1698–1705.

Schneeberger E. E. (1978). Structural basis for some permeability properties of the air-blood barrier. *Fed Proc* **37**, 2471-2478.

Schneeberger E. E. (1991). Airway and alveolar epithelial cell junctions, in: *The Lung: Scientific Foundations* (Crystal R. G., and West J. B., eds), 205-214, Raven Press, New York.

Schnitzer J. E., Oh P., Pinney E., and Allard J. (1994). Filipin-sensitive caveolae-mediated transport in endothelium: reduced transcytosis, scavenger endocytosis, and capillary permeability of selected macromolecules. *J Cell Biol* **127**, 1217-1232.

Schnitzer J. E. (2001). Caveolae: from basic trafficking mechanisms to targeting transcytosis for tissue-specific drug and gene delivery *in vivo*. *Adv Drug Deliv Rev* **49**, 265-280.

Schuetz E., Schinkel A., Relling M., and Schuetz J. (1996). P-glycoprotein: a major determinant of rifampicin-inducible expression of cytochrome P4503A in mice and humans. *Proc Natl Acad Sci USA* **93**, 4001-4005.

Serikov V. B. (1985). Importance of changes in pulmonary circulation perfusion and lymphodynamics during pulmonary edema formation. *Pathol Physiol* **14**, 1-19.

Shapiro A. B., and Ling V. (1995). Reconstitution of drug transport by purified P-glycoprotein. *J Biol Chem* **270**, 16167-16175.

Shaul P. W., and Anderson R. G. (1998). Role of plasmalemmal caveolae in signal transduction. *Am J Physiol* **275**, L843-L851.

Shen J., Elbert K. J., Yamashita F., Lehr C. M., Kim K. J., and Lee V. H. (1999). Organic cation transport in rabbit alveolar epithelial cell monolayers. *Pharm Res* **16**, 1280-1287.

Sikic B. I., Fisher G. A., Lum B. L., Halsey J., Beketic-Oreskovic L., and Chen G. (1997). Modulation and prevention of multidrug resistance by inhibitors of P-glycoprotein. *Cancer Chemother Pharmacol* **40**, S13-S19.

Singh M., Krouse M., Moon S., and Wine J. J. (1997). Most basal I-sc in Calu-3 himan airway cells is bicarbonate-dependent Cl^- secretion. *Am J Physiol Lung Cell Mol Physiol* **16**, L690-L698.

Simionescu M. (1991). Lung endothelium: Structure-function correlates, in: *The Lung: Scientific foundations* (Crystal R. G., and West J. B., eds.), 301-312, Raven Press Ltd, New York.

Skach W. R. (2000). Defects in processing and trafficking of the cystic fibrosis transmembrane conductance regulator. *Kidney Int* **57**, 825-831.

Smith A. J., van Helvoort A., van Meer G., Szabo K., Welker E., Szakacs G., Varadi A., Sakardi B., and Borst P. (2000). MDR3 P-glycoprotein, a phosphatidylcholine translocase, transports several cytotoxic drugs and directly interacts with drugs as judged by interference with nucleotide trapping. *J Biol Chem* **275**, 23530-23539.

Staub N. C. (1991). *Basic Respiratory Physiology*, Churchill Livingstone Inc, New York.

Staud F., and Pavek P. (2005). Breast cancer resistance protein (BCRP/ABCG2). *Int J Biochem Cell Biol* **37**, 720-725.

Stouch T. R., and Gudmundsson O. (2002). Progress in understanding the structure–activity relationships of P-glycoprotein. *Adv Drug Deliv Rev* **54**, 315–328.

Stravrovskaya A. (2000). Cellular mechanisms of multidrug resistance of tumour cells. *Biochemistry (Moscow)* **65**, 95-106.

Sugawara I., Akiyama S., Scheper R. J., and Itoyama S. (1997). Lung resistance protein (LRP) expression in human normal tissues in comparison with that of MDR1 and MRP. *Cancer Lett* **112**, 23-31.

Sweeney T. D., and Brain J. D. (1991). Pulmonary deposition: determinants and measurement techniques. *Toxicol Pathol* **19**, 384-397.

Takano M., Yumoto R., and Murakami T. (2006). Expression and function of efflux drug transporters in the intestine. *Pharmacol Ther* **109**, 137-161.

Tamai I., and Safa A. (1991). Azidopine noncompetitively interacts with vinblastine and cyclosporine A binding to P-glycoprotein in multidrug resistant cells. *J Biol Chem* **266**, 16796-16800.

Tanigawara Y., Okamura N., Hirai M., Yashura M., Ueda K., Kioka N., Komano T., and Hori R. (1992). Transport of digoxin by human P-glycoprotein expressed in porcine kidney epithelial cell line (LLC-PK1). *J Pharmacol Exp Ther* **263**, 840-845.

Tang F., Horie K., and Borchardt R. T. (2002). Are MDCK cells transfected with the human MDR1 gene a good model of the human intestinal mucosa? *Pharm Res* **19**, 765-772.

Taylor G. (1990). The absorption and metabolism of xenobiotics in the lung. *Adv Drug Deliv Rev* **5**, 37-61.

Taylor A. M., Storm J., Soceneantu L., Linton K. J., Gabriel M., Martin C., Woodhouse J., Blott E., Higgins C. F., and Callaghan R. (2001). Detailed characterisation of cysteine-less P-glycoprotein reveals subtle pharmacological differences in function from wild-type protein. *Br J Pharmacol* **134**, 1609-1618.

Taylor G., and Kelleway I. (2001). Pulmonary drug delivery, in *Drug Delivery and Targeting* (Hillery A. M., Lloyd A. W., and Swarbrick J. eds), 269-300, Taylor & Francis, London.

Thiebaut F., Tsuruo T., Hamada H., Gottesman M., Pastan I., and Willingham M. (1987). Cellular localisation of the multidrug resistance gene product in normal human tissue. *Proc Natl Acad Sci USA* **84**, 7735-7738.

Tian Q., Zhang J., Chan E., Duan W., and Zhou S. (2005). Multidrug resistance proteins (MRPs) and implication in drug development. *Drug Dev Res* **64**, 1-18.

Theodore J., Robin E. D., Gaudio R., and Acevedo J. (1975). Transalveolar transport of large polar solutes (sucrose, inulin, dextran). *Am J Physiol* **229**, 989-996.

Tronde[a] A., Baran G., Eirefelt S., Lennernas H., and Bengtsson U. H. (2002). Miniaturized nebulization cathethers: A new approach for delivery of defined aerosol doses to the rat lung. *J Aerosol Med* **15**, 283-296.

Tronde[b] A., Krondahla E., Chelpin H. E., Brunmark P., Bengtsson U. H., Ekstroeme G., and Lennernaesa H. (2002). High airway-to-blood transport of an opioid tetrapeptide in the rat lung after aerosol delivery. *Peptides* **23**, 469-478.

Tronde[a] A., Nordén B., Jeppsson A-B., Brunmark P., Nilsson E., Lennernäs H., and Hultkvist Bengtsson U. (2003). Drug absorption from the rat lung - correlations with drug physicochemical properties and epithelial permeability. *J Drug Target* **11**, 61–74.

Tronde[b] A., Nordén B., Marchner H., Wendel A-K., Lennernäs H., and Bengtsson U. H. (2003). Pulmonary absorption rate and bioavailability of drugs *in vivo* in rats: Structure-absorption relationships and physicochemical profiling of inhaled drugs. *J Pharm Sci* **92**, 1216-1233.

Troutmant M. D., and Thakker D. R. (2003). Rhodamine 123 requires carrier-mediated influx for its activity as a P-glycoprotein substrate in Caco-2 cells. *Pharm Res* **20**, 1192-1199.

Trussardi A., Poitevin G., Gorisse M. C., Faroux M. J., Bobichon H., Delvincourt C., and Jardillier J. C. (1998). Sequential overexpression of LRP and MRP but not P-gp 170 in VP16-selected A549 adenocarcinoma cells. *Int J Oncol* **13**, 543-548.

Tsuji A. (1999). Tissue selective drug delivery utilizing carrier-mediated transport systems. *J Control Release* **62**, 239-244.

Tsuro T., Iida H., and Sakurai Y. (1981). Overcoming of vincristine resistance in P388 leukemia *in vivo* and *in vitro* through enhanced cytotoxicity of vincristine and vinblastine by verapamil. *Cancer Res* **41**, 1967-1972.

Tsuro T., Iida H., Yamashiro M., Tsukagoshi S., and Sakurai Y. (1982). Enhancement of vincristine- and adriamycin-induced cytotoxicity by verapamil in P388 leukemia and its sublines resistant to vincristine and adriamycin. *Biochem Pharmacol* **31**, 3138-3140.

Tyler N. K., Hyde D. M., Hendickx A. G., and Plopper C. G. (1989). Cytodifferentiation of two epithelial populations of the respiratory bronchiole during fetal lung development in the rhesus monkey. *Anat Rec* **225**, 297-309.

Ueda K., Cornwell M. M., Gottesman M. M., Dean M., Hamon Y., and Chimini G. (2001). The human ATP-binding cassette (ABC) transporter superfamily. *J Lipid Res* **42**, 1007-1017.

Valodia P., and Syce J. A. (2000). The effect of fenfluramine on the pulmonary disposition of 5-hydroxytryptamine in the isolated perfused rat lung: a comparison with chlorphentermine. *J Pharm Pharmacol* **52**, 53-58.

Valverde M., Duaz M., Sepulveda F., Gill D., Hyde S., and Higgins C. (1992). Volume regulated chloride channels associated with the human multidrug-resistance P-glycoprotein. *Nature* **355**, 830-833.

van den Bosch J. M. M., Westermann C. J. J., Aumann J., Edsbäcker S., Tönnesson M., and Selroos O. (1993). Relationship between lung tissue and blood plasma concentrations of inhaled budesonide. *Biopharm Drug Dispos* **14**, 455-459.

van Putte B. P., Hendricks J. M. H., Romijn S., Guetens G., de Boeck G., de Bruijn E. A., and van Schil P. E. Y. (2002). Single-pass isolated lung perfusion versus recirculating isolated lung perfusion with mephalan in rat model. *Ann Thorac Surg* **74**, 893-898.

van der Sandt C. J., Blom-Roosemalen M. C. M., de Boer A. G., and Breimer D. D. (2000). Specificity of doxorubicin versus rhodamine-123 in assessing P-glycoprotein functionality in the LLC-PK1, LLC-PK1:MDR1 and Caco-2 cell lines. *Eur J Pharm Sci* **11**, 207-214.

van der Valk P., van Kalken C. K., Ketelaars H., Broxterman H. J., Scheffer G., Kuiper C. M., Tsuruo T., Lankelma J., Meijer C. J., Pinedo H. M., *et al* (1990). Distribution of multi-drug resistance-associated P-glycoprotein in normal and neoplastic human tissues: Analysis with 3 monoclonal antibodies recognizing different epitopes of the P-glycoprotein molecule. *Ann Oncol* **1**, 56-64.

van Montfoort J. E., Schmid T. E., Adler I. D., Meier P. J., and Hagenbuch B. (2002). Functional characterisation of the mouse organic-anion-transporting polypeptide 2. *Biochim Biophys Acta* **19**, 183-188.

Vanbever R., Ben-Jebria A., Mintzes J. D., Lange R., and Edwards, D. A. (1999). Sustained release of insulin from insoluble inhaled particles. *Drug Dev Res* **48**, 178-185.

van Scott M. R., Lee N. P., Yankaskas J. R., and Boucher R. C. (1988). Effect of hormones on growth and function of cultured canine tracheal epithelial cells. *Am J Physiol* **255**, C237-C245.

van Scott M. R., Yankaskas J. R., and Boucher R. C. (1986). Culture of airway epithelial cells: research techniques. *Exp Lung Res* **11**, 75-94.

Verschraagen M., Koks C. H., Schellens J. H., and Beijnen J. H. (1999). P-glycoprotein system as a determinant of drug interactions: the case of digoxin-verapamil. *Pharmacol Res* **40**, 301-306.

von Wichert P., and Seifart C. (2005). The lung, an organ for absorption? *Respiration* **72**, 552–558.

Walker B. L., and Kummerow F. A. (1964). Erythrocyte fatty acid composition + apparent permeability to non-electrolytes. *Proc Soc Exp Biol Med* **115**, 1099.

Wan H., Winton H. L., Soeller C., Stewart G. A., Thompson P. J., Gruenert D. C., Cannel M. B., Garrod D. R., and Robinson C. (2000). Tight junction properties of the immortalized human brochial epithelial cell lines Calu-3 and 16HBE14o-. *Eur Respir J* **15**, 1058-1068.

Waters C., Krejcie T., and Avram M. (2000). Facilitated uptake of fentanyl, but not alfentanil, by human pulmonary endothelial cells. *Anesthesiology* **93**, 825-831.

Weibel E. R. (1991). Design of airways and blood vessels considered as branching trees, in: *The Lung: Scientific Foundations* (Crystal R. G., and West J. B., eds), 711-720, Raven Press Ltd, New York.

Weksler B., Ng B., Lenert J. T., and Burt M. E. (1995). Isolated single-lung perfusion-a study of the optimal perfusate and other pharmacokinetics factors. *Ann Thorac Surg* **60**, 624-629.

Wiesel J. M., Gamiel H., Vlodavsky I., Gay I., and Ben-Basset H. (1983). Cell attachment, growth characteristics and surface morphology of human upper-respiratory tract epithelium cultured on extra cellular matrix. *Eur J Clin Invest* **13**, 57-63.

Willey J. C., Lechner J. F., and Harris C. C. (1984). Bombesin and C-terminal tetradecapeptide of gastrin releasing peptide are growth factors for normal human bronchial epithelial cells. *Exp Cell Res* **153**, 245-248.

Wills[a] P., Warnery A., Phung-Ba V., Legrain S., and Scherman D. (1994). High lipophilicity decreases drug transport across intestinal epithelial cells. *J Pharmacol Exp Ther* **269**, 654-658.

Wills[b] P., Phung-Ba V., Warnery A., Lechardeur D., Raeissi S., Hidalgo I. J., and Scherman D. (1994). Polarised transport of docetaxel and vinblastine mediated by P-glycoprotein in human intestinal epithelial cell monolayers. *Biochem Pharmacol* **48**, 1528-1530.

Wioland M.-A., Fleury-Feith J., Corlieu P., Commo F., Monceaux G., Lacau-St-Guily J., and Bernaudin J.-F. (2000). CFTR, MDR1, and MRP1 immunolocalization in normal human nasal respiratory mucosa. *J Histochem Cytochem* **48**, 1215-1222.

Witherspoon S. M., Emerson D. L., Kerr B. M., Lloyd T. L., Dalton W. S., and Wissel P. S. (1996). Flow cytometric assay of modulation of P-glycoprotein function in whole blood by the multidrug resistance inhibitor GG918. *Clin Cancer Res* **2**, 7–12.

Wright S. R., Boag A. H.,Valdimarsson G., Hipfner D. R., Campling B. G., Cole S. P., and Deeley R. G. (1998). Immunohistochemical detection of multidrug resistance protein in human lung cancer and normal lung. *Clin Cancer Res* **4**, 2279-2289.

Xiong L., Legagneuxa J., Wassef M., Oubenaissa A., Detruit H., Mouas C., and Menasche P. (1999). Protective effects of Celsior in lung transplantation. *J Heart Lung Transplant* **18**, 320-327.

Yamaya M., Finkbeiner W. E., and Widdicombe J. H. (1991). Ion transport by cultures of human tracheobronchial submucosal glands. *Am J Physiol* **261** (*Lung Cell Mol Physiol* **5**), L485-L490.

Yamaya M., Finkbeiner W. E., Chun S. Y., and Widdicombe J. H. (1992). Differentiated structure and function of cultures from human tracheal epithelium. *Am J Physiol Lung Cell Mol Physiol* **262**, L713-L724.

Yoshida H., Okumura K., Kamiya A., and Hori R. (1989). Accumulation mechanism of basic drugs in the isolated perfused rat lung. *Chem Pharm Bull* **37**, 450-453.

Zhou S. Y., Piyapolrungroj N., Pao L.-H., Li C., Liu G., Zimmermann E., and Fleisher D. (1999). Regulation of paracellular absorption of cimetidine and 5-aminosalicylate in rat intestine. *Pharm Res* **16**, 1781-1785.

8 LIST OF PAPERS

Bosquillon C., Clear N., Bennett J., and Forbes B. (2008). A simple isolated perfused lung technique for measurement of pulmonary absorption. *J Pharm Pharmacol*. Submitted.

Holas T., Zbytovska J., Vavrova K., Berka P., Madlova M., Klimentova J., and Hrabalek A. (2006). Thermotropic phase behavior of long-chain alkylammonium-alkylcarbamates. *Therm Acta* **441**, 116-123.

Madlova M., Bosquillon C., and Forbes B. (2008). P-gp activity in continuous and primary airway epithelial cells and the isolated perfused lung. *Eur J Pharm Biopharm*. Accepted.

9 SOUHRN

P-glycoprotein (P-gp) je membránový transportní protein přítomný v cytoplazmatické membráně buněk hlavních fyziologických bariér, například v mozku, ledvinách, plicích a placentě. Přestože popisu tohoto proteinu bylo věnováno již mnoho studií, jeho přesná lokalizace a funkce v plicích není doposud plně objasněna. Ke studiu pulmonární absorbce léčiv *in vitro* se s výhodou používají buněčné modely, například linie bronchiálních buněk Calu-3. Předchozí studie zabývající se výzkumem P-gp v Calu-3 prokázaly nesrovnalosti v rámci aktivity a lokalizace tohoto proteinu. Účelem předkládané disertační práce bylo systematické studium vlivu P-gp na absorbci léčiv v buňkách Calu-3, primárních kulturách lidských bronchiálních buněk (NHBE) a isolovaných krysích plicích (IPL). Intestinální buněčná linie Caco-2, která vykazuje nadměrnou expresi P-gp byla ve studii použita jako pozitivní kontrola. Aktivita a lokalizace P-gp v buňkách byla studována pomocí permeačních experimentů s využitím P-gp substrátu digoxinu a inhibitorů verapamilu a GF120918A. Za účelem studia P-gp v buněčných systémech byly buňky pěstovány na polyesterových filtrech (Transwell®) na rozhraní vzduch-medium (Calu-3, NHBE) nebo medium-medium (Caco-2). Integrita buněčných vrstev byla doložena hodnotou fluxu [^{14}C]-mannitolu. Transport digoxinu v Calu-3 linii se lišil v závislosti na použité pasáži buněk, době kultivování buněk a použitém inhibitoru. Eflux digoxinu, který bylo možné ovlivnit přítomností GF120918A byl pozorován pouze u buněk pasáže vyšší než 53. Zdánlivá permeabilita digoxinu v Calu-3 a Caco-2 buňkách byla statisticky významně větší ($p > 0.05$) ve směru z apikální k basální buněčné straně jak bylo doloženo hodnotou effluxu 2.08 a 8.58 v 21 den v kultuře. Efflux v Calu-3 a Caco-2 byl snížen o 40.0 %, respektive 50.9 % v přítomnosti GF120918A. V NHBE byl transport digoxinu v basálním směru 2.58-krát vyšší než v apikálním a nebyl ovlivněn přítomností GF120918A. V podobném smyslu inhibitor GF120918A neovlivnil absorbci digoxinu v modelu izolovaných krysích plic, přestože přítomnost P-gp v plicní tkáni byla potvrzena pomocí immunohistochemie. Nicméně hodnota absorbce digoxinu v tomto modelu byla významně zvýšena ($p > 0.05$) z 28.7 ± 9.9 % ($t = 90$ min, bez přítomnosti inhibitoru) na 43.5 ± 6.7 % za použití verapamilu obsaženém v perfusním roztoku, což naznačuje přítomnost aktivního transportního mechanismu v IPL modelu.